1-1-2012

The Role of Snail Homolog 1 in Embryonic Stem Cell Differentiation

Jennifer Gill
Washington University in St. Louis

WASHINGTON UNIVERSITY IN ST. LOUIS

Division of Biology and Biomedical Sciences

Immunology

Dissertation Examination Committee:

Kenneth M. Murphy, Chair
Deepta Bhattacharya
Brian Edelson
Raphael Kopan
Gregory Longmore
Wojciech Swat

The Role of Snail Homolog 1 in Embryonic Stem Cell Differentiation

by

Jennifer Gibson Gill

A dissertation presented to the
Graduate School of Arts and Sciences
of Washington University in
partial fulfillment of the
requirements for the degree
of Doctor of Philosophy

May 2012

Saint Louis, Missouri

ABSTRACT OF THE DISSERTATION

The Role of Snail Homolog 1 in Embryonic Stem Cell Differentiation

by

Jennifer Gibson Gill

Doctor of Philosophy in Biology and Biomedical Sciences

Immunology

Washington University in St. Louis, 2012

Professor Kenneth M. Murphy, Chairperson

During gastrulation, epiblast cells undergo an epithelial-to-mesenchymal transition (EMT) as they ingress through the primitive streak and form mesoderm. To better understand the molecular pathways of EMT during this developmental transition, we developed a model system utilizing mouse embryonic stem (ES) cells. We show that EMT occurs during ES cell differentiation and is dependent on the Wnt signaling pathway. We further show that the Wnt-dependent transcription factor Snail homolog 1 (Snail) is expressed and capable of inducing EMT in differentiating ES cells. In addition to EMT, Snail accelerates differentiation, promotes mesoderm commitment, and restricts markers of primitive ectoderm and epiblast.

Snail's impact on differentiation can be partly explained through its repression of ES cell-associated microRNAs, including the miR-200 family. The miR-200 family is down-regulated in a Wnt-dependent manner during ES cell differentiation. We find that maintenance of miR-200 expression prevents EMT and stalls differentiating ES cells at

an epiblast-like stem cell (EpiSC) stage. Consistent with a role for Activin in EpiSC maintenance, we show that miR-200 requires Activin to efficiently maintain cells at the epiblast stage. Together, these findings demonstrate that Snail and miR-200 act in opposition to regulate EMT and exit from the EpiSC stage towards induction of germ layer fates. By modulating expression levels of Snail, Activin, and miR-200, we are able to control the timing of EMT and transition out of the EpiSC state.

Beyond a role in gastrulation, Snail has also been demonstrated to be important in vasculogenesis. Snail-deficient mice display early vascular defects while Snail-overexpressing tumors are associated with increased angiogenesis. We utilized our ES cell model as a means to better understand Snail's relationship with vasculogenesis. We find that unlike other types of mesoderm, Snail's induction of Flk1+ endothelial cells is cell-intrinsic and independent of Wnt, BMP, and Activin signaling pathways. Based on the transcriptional profile of Flk+ sorted cells, we hypothesize that Snail selectively induces endothelium in a subset of ES cells that resemble primitive endoderm. We further demonstrate that Snail's induction of endothelium requires the down-regulation of the miR-200 family, which directly target the 3'UTRs of Flk1 and Ets1.

ACKNOWLEDGMENTS

This body of work would not have been possible without the contributions of many people. I would first like to thank Ken Murphy for the privilege of working in his laboratory for the last five and a half years. Ken is a trailblazer and a world-class scientist, and I feel incredibly lucky to have had him as a teacher and mentor. He has profoundly shaped the way I approach science, life, and obstacles. I would also like to thank Theresa Murphy, who has been a second mentor to me over the course of my training. She has been an endless source of knowledge, both technical and otherwise, and I am forever grateful for her help, support, and friendship over these years.

I owe a great deal of gratitude to the members of the Murphy lab, who have been vital in making these last years intellectually stimulating, fun, and always full of laughter. I had the pleasure and privilege of working closely with Coleman Lindsley, an exceptional graduate student who graciously welcomed me to the ES cell project. He was a terrific person to work with, and he was a patient teacher when the learning curve was steep. I am also grateful for Ellen Langer, a post-doctoral associate and excellent collaborator that provided a great deal of insight and support to the project. I would also like to thank those that provided financial support for my training and work: the NIH, the Washington University School of Medicine MSTP Training Grant, and the Howard Hughes Medical Institute.

I owe endless thanks to a number of people outside of the lab. I am forever thankful to my Mom and Dad. They always fostered my curiosity, believed in me, and selflessly supported me in all of life's endeavors. Their love and devotion has served as

my foundation, and I can only hope to pass forward this gift to my own children. I am also grateful for my brother Stephen and the Gill, Mahoney, and Warden families, who bring me so much happiness, encouragement, and support.

I thank my children, Clark and Kate, who have filled my life with endless joy. What a gift to watch them face the world with enthusiasm, fearlessness, and the purest of wonder. Throughout my time in graduate school, they always reminded me of what brought me to science in the first place and the child-like eyes needed to face new observations and problems.

Finally, I am forever indebted to my husband, Corey, whose unconditional love and unwavering support have given me a strength I could never have imagined. He has patiently listened to me talk about science and every-other-topic-in-the-world for the last eleven and a half years. He is nothing short of the best.

TABLE OF CONTENTS

LIST OF FIGURES

LIST OF ABBREVIATIONS

BMP	Bone morphogenetic protein
DKK1	Dickkopf 1
DOX	Doxycycline
EMT	Epithelial to mesenchymal transition
EB	Embryoid body
EGF	Epidermal growth factor
EMT	Epithelial mesenchymal transition
EpiSC	Epiblast-like stem cell
ES	Embryonic stem
ESD-EpiSC	Embryonic stem cell derived epiblast-like stem cell
FACS	Fluorescence activated cell sorting
FCS	Fetal calf serum
FGF	Fibroblast growth factor
FLK1	Fetal liver kinase 1
GSK3β	Glycogen synthase kinase 3β
ICM	Inner cell mass
iPS	Inducible pluripotent stem
LIF	Leukemia inhibitory factor
MEF	Mouse embryonic fibroblast
MESP1	Mesoderm posterior 1
miR	MicroRNA
NT	No treatment

PECAM1	Platelet/endothelial cell adhesion molecule
PDGFRα	Platelet derived growth factor receptor, α-chain
RT-PCR	Reverse transcription polymerase chain reaction
SCM	Serum containing medium
Snail	Snail homolog 1
Slug	Snail homolog 2
SNAG	Snail/Gfi1 repressor domain
SRM	Serum replacement medium
TGFβ	Transforming Growth Factor β
TIE2	Endothelial-specific receptor tyrosine kinase
Twist	Twist homolog 1
UTR	Untranslated region
VE-CADHERIN	Vascular endothelial cadherin
WNT	Wingless-related MMTV integration site
Zeb1	Zinc finger homeobox 1a
Zeb2	Zinc finger homeobox 1b; SIP1

CHAPTER 1

Introduction

Epithelial Mesenchymal Transition

Epithelial to mesenchymal transition (EMT) is a morphogenetic process in which polarized epithelial cells convert to motile, mesenchymal cells. Epithelial cells are characterized by their polarity and intercellular junction proteins, while mesenchymal cells are characterized by their limited intercellular associations, enhanced migratory capacity, and secretion of extracellular matrix components (Figure 1). These two distinct cellular phenotypes were initially described more than one hundred years ago, and the ability of cells to interconvert between these states was described by Frank Lillie in 1908(Lillie, 1908) during his studies of chick embryogenesis. Despite these early findings, EMT was not extensively studied as a process until the early 1980s, when *in vitro* work allowed for the characterization and manipulation of EMT in epithelia and MDCK cells(Greenburg and Hay, 1982; Stoker and Perryman, 1985).

Since its initial description in the developing chick, EMT has been documented to occur in primarily three types of biological processes: embryogenesis and development, wound healing, and metastasis. While clearly different, these processes nevertheless share similarities in regulation, transcriptional networks, and functional morphology. Despite EMT's prevalence in numerous biological settings and models, many aspects of its molecular circuitry remain unclear.

Gastrulation and Germ Layer Fate Commitment

The first EMT to take place during embryogenesis is gastrulation, when cells acquire the ability to migrate concomitant with the specification of the three primary germ layers (ectoderm, endoderm, and mesoderm). Ectoderm-derived tissues eventually go on to make up the nervous system and the epidermis of the skin. While endoderm gives rise to the endocrine, gastrointestinal, and respiratory systems, mesoderm derivatives include the musculoskeletal and cardiovascular systems.

Prior to mouse gastrulation, the day 4 implanting blastocyst consists of a vesicular structure containing the inner cell mass (ICM) surrounded by trophectoderm (Figure 2). The trophectoderm generates the ectoplacental cone and extraembryonic ectoderm which later form the placenta(Tam and Loebel, 2007)). In a process regulated by FGF signaling, the ICM then gives rise to primitive endoderm (Gata6+ cells) and the epiblast (Nanog+ cells)(Chazaud et al., 2006; Yamanaka et al., 2010). The primitive endoderm delineates into parietal endoderm, visceral endoderm, and extraembryonic mesoderm. The latter two are important in later patterning of the embryo and generation of the yolk sac, respectively. The epiblast gives rise to the embryo proper, including the three primary germ layers.

During gastrulation, cells of the epiblast undergo an EMT and migrate through the primitive streak to form mesoderm and definitive endoderm. The cells located in the most posterior aspect of the primitive streak are the first to migrate and go on to become extraembryonic mesoderm. Subsequently, cells continue to migrate through the primitive streak in a temporal wave from posterior (going the earliest) to anterior (going the latest), generating lateral plate mesoderm, paraxial mesoderm, and axial mesoderm (the notochord). The remaining cells of the epiblast that do not migrate form the ectoderm.

While a number of transcription factors have been associated with controlling EMT, including Snail (*Snai1*) (Cano et al., 2000; Ikenouchi et al., 2003), Zeb1 (Eger et al., 2005), Zeb2 (Comijn et al., 2001), Twist(Yang et al., 2004), and Slug (*Snai2*) (Bolos et al., 2003), Snail has been associated with the EMT of mouse gastrulation. Expression of Snail in the epiblast acts to repress E-cadherin (*Cdh1*), claudins, and occludin (*Ocln*) directly, which promote disassociation of epithelial cells to allow subsequent migration through the primitive streak. Embryos lacking Snail fail to undergo gastrulation and form minimal amounts of mesoderm(Carver et al., 2001). Snail also acts subsequently to gastrulation, since conditional deletion of Snail under control of a Meox2-Cre leads to gastrulation followed by abnormal development of mesoderm and defects in left-right asymmetry (Murray and Gridley, 2006). In *Drosophila*, Snail has also been suggested to act in fate determination, repressing neuroectoderm (Nambu et al., 1990), although it is unclear whether Snail similarly influences fate choices in vertebrates.

During gastrulation, the simultaneous coordination of tissue morphogenesis, germ layer specification, and axis development clearly involves a complex system of signaling pathways and transcriptional programs. While knockout mice and embryo studies have helped elucidate some of the key players in this process, *in vitro* systems are useful for performing a deeper analysis of the molecular network.

The Embryonic Stem Cell Model System

The derivation of pluripotent cell lines from the inner cell mass (ICM) of the murine blastocyst was first described thirty years ago(Evans and Kaufman, 1981; Martin, 1981). These embryonic stem (ES) cells are defined by their ability to contribute to all

somatic and germ cell lineages upon injection into morula or blastocyst stage embryos. By culturing these cells in the presence of serum and LIF or BMP and LIF, ES cells can be passaged indefinitely while still maintaining their pluripotency(Evans and Kaufman, 1981; Smith et al., 1988; Ying et al., 2003). LIF maintains ES cell pluripotency primarily through the JAK-Stat3 signaling pathway but also through a parallel PI(3)K/Akt pathway (Niwa et al., 2009). Each of these pathways downstream of LIF lead to the induction of the quintessential ES cell transcription factors Klf4, Sox2, Nanog, and Oct4.

When LIF is removed, ES cells undergo spontaneous differentiation as embryoid bodies (EBs). Depending on the *in vitro* culture conditions, ES cells can generate a wide range of cell types derived from all three primary germ layers. Included in this list are cardiomyocytes(Doetschman et al., 1985), neurons(Tropepe et al., 2001), insulin-secreting cells(Lumelsky et al., 2001), chondrocytes (Kramer et al., 2000), and others.

Differentiating embryonic stem (ES) cells, which have been shown to model the gastrulating embryo(Kramer et al., 2000), spontaneously undergo an EMT. While this has been documented by us and others (Eastham et al., 2007; Lindsley et al., 2006), little is known regarding the regulation or functional significance of EMT in differentiating ES cells. Because of their developmental relevance, their inherent propensity to undergo this process, and the relative ease of *in vitro* culture systems, ES cells serve as an ideal model system to study and better understand the genetic regulatory networks surrounding developmental EMT.

In addition to gastrulation, ES cell differentiation has been shown to parallel earlier stages of embryo development. Recent studies have found that upon differentiation, murine ES cells transition from an inner cell mass-like cell (ICM-like) to

an ES cell-derived epiblast-like stem cell (ESD-EpiSC) around day 2 of differentiation (Zhang et al., 2010). Cells at the latter stage maintained their pluripotency after passage in culture with Activin and FGF. ESD-EpiSCs had similar transcriptional profiles as traditional EpiSCs, which are derived from the epithelialized mouse egg cylinder (a later stage than the blastocyst inner cell mass)(Brons et al., 2007; Tesar et al., 2007). EpiSCs are characterized by a loss of full pluripotency markers such as *Rex1*, *Dppa3*, and *Pecam1*, the maintenance of select pluripotency markers like SSEA1 and *Nanog*, and the expression of epiblast markers such as *Sox17*, *Cerberus*, and *Nodal*. EpiSCs have been described to be very similar to human ES cells, which also require FGF/activin for pluripotent maintenance, have undergone X-inactivation, and share similar morphology(Brons et al., 2007; Tesar et al., 2007). The mechanisms surrounding maintenance and differentiation of the ESD-EpiSC state are currently unclear.

Signaling Pathways in Gastrulation and ES Cell Differentation

During gastrulation, three highly conserved pathways have emerged as key players in lineage specification and patterning of the primitive streak. These include the Wnt, BMP, and Activin signaling pathways. Experiments in both the embryo as well as embryonic stem cells have been important in clarifying each of their roles.

Canonical Wnt signaling is essential for generation of the primitive streak. Mice deficient in Wnt3, β-catenin, or LRP5/6 all fail to develop a primitive streak and mesoderm(Huelsken et al., 2000; Kelly et al., 2004; Liu et al., 1999). Studies in our lab examining the role of Wnt signaling during ES cell differentiation show that addition of DKK1, a soluble inhibitor of canonical Wnt signaling, inhibits all mesoderm and

endoderm formation(Lindsley et al., 2006). Interestingly, while Wnt signaling appears to be required for primitive streak formation, activated β-catenin is not sufficient on its own to induce formation of mesoderm or endoderm. Rather, Wnt activity appears to require other factors, such as BMPs, to induce primitive streak-associated gene programs.

Similar to the Wnt pathway, BMP signaling is also required for normal primitive streak formation. BMP activity is highest in the posterior streak and is necessary for posterior patterning and lineage specification during gastrulation. BMP4-/- embryos are deficient in posterior derivatives of the primitive streak, including extraembryonic and hematopoietic mesoderm (Winnier et al., 1995). Inhibition of BMP signaling through the addition of Noggin showed a skewing of differentiating human ES cells away from mesoderm and towards anterior primitive streak markers and endoderm(Sumi et al., 2008). Our studies in embryonic stem cells also show that BMP and Wnt function cooperatively to induce expression of the early mesoderm marker brachyury(Lindsley et al., 2006).

In contrast to the BMP pathway, Nodal/activin activity is greatest in the anterior streak/node region of the gastrulating embryo. While mice deficient in Nodal fail to form a primitive streak or mesoderm/endoderm, it has a preferential role in the development of the anterior primitive streak(Brennan et al., 2001; Camus et al., 2006; Mesnard et al., 2006). Studies in embryos and ES cells have demonstrated a dose-dependent relationship between activin and fate specficiation(Gadue et al., 2005). High levels of activin support the formation of endoderm and axial mesoderm (anterior streak) while low levels of activin are associated with posterior streak fates.

While Wnt, BMP, and activin pathways have been demonstrated to be important in affecting lineage determination and embryonic patterning, they also have roles in the maintenance of pluripotency. As aforementioned, BMP can act in combination with LIF to maintain ES cells in an undifferentiated state. Furthermore, activated SMAD2/3 downstream of activin/TGFβ signaling in human ES cells has been shown to directly activate the promoter of the pluripotency transcription factor Nanog(Xu et al., 2008). The role of Wnt signaling in maintenance of ES cell pluripotency has been more controversial, but studies using GSK3β inhibitors suggest that Wnt may also be important(Sato et al., 2004). The different roles of these three pathways in both ESC maintenance and promotion of differentiation suggest that their activity is highly dependent on the temporal window and context in which they are acting.

Snail and its Regulation

While Snail's role in gastrulation and early development has been characterized through knockout studies, much of what is known about Snail comes from studies in tumor and epithelial cell lines. Because Snail has been strongly correlated with promotion of EMT and metastasis in many types of cancer (Olmeda et al., 2007; Olmeda et al., 2008), this is a model system frequently used for studying Snail regulation and function.

Through many *in vitro* and some *in vivo* studies, the following pathways have been demonstrated to induce Snail expression: FGF, Wnt, TGFβ, BMP, EGF, Notch, and SCF among others (Figure 3, reviewed in (Barrallo-Gimeno and Nieto, 2005)). In contrast, the ES cell transcription factors Sox2 and Oct4 have been shown to repress

Snail transcription(Li et al., 2010). Interestingly, Snail has been found to bind and repress its own promoter, thereby limiting its own expression(Peiro et al., 2006). It has been hypothesized that Snail's expression may often be transient, where its role is to initiate EMT and repression of E-cadherin, while other EMT transcription factors such as Zeb1, Zeb2, and Slug may function to maintain E-cadherin repression and the mesenchymal phenotype(Peinado et al., 2007).

In addition to transcriptional regulation, Snail activity is also controlled through its stability and subcellular localization. GSK3β phosphorylates Snail to promote its nuclear export, ubiquitination, and subsequent degradation. Because Wnt signaling inhibits the activity of GSK3β, Wnt signaling has been shown to promote the stability and function of Snail(Yook et al., 2005). In addition to GSK3β, a number of other factors have been identified which regulate subcellular localization (LIV1, PAK1) and stability (LOXL2)(Peinado et al., 2005; Yamashita et al., 2004; Yang et al., 2005).

With numerous positive and negative regulators of transcription, stability, and localization, Snail function is tightly regulated. Maintenance of this balance is crucial in preventing pathogenesis from inappropriate Snail activity, as seen in various fibrotic(Boutet et al., 2006) and metastatic scenarios(Olmeda et al., 2007).

Snail Targets and its Downstream Functions

Snail induces EMT, at least in part, through the direct repression of a number of epithelial targets including E-cadherin(Cano et al., 2000), Claudins(Ikenouchi et al., 2003), Occludin(Ikenouchi et al., 2003), and Crumbs homolog 3(Whiteman et al., 2008). Snail has been shown to function as a repressor through its N-terminal SNAG domain,

which is required for binding to HDAC1/2, Sin3A, Ajuba, and polycomb repressor complex 2(Grimes et al., 1996; Herranz et al., 2008; Langer et al., 2008; Peinado et al., 2004a). Each of these has been described as a corepressor important for Snail's ability to down-regulate E-cadherin in various cell types and models.

Beyond direct repression of epithelial targets, Snail also induces several mesenchymal genes including members of the matrix metalloproteinase family, Zeb1/Zeb2, fibronectin, vimentin, and Rho GTPases (reviewed in(Barrallo-Gimeno and Nieto, 2005; Thiery et al., 2009)). Because Snail has never been demonstrated to be a direct activator, it is unclear how it is capable of inducing such a wide range of targets.

In addition to EMT, Snail has also been associated with additional biological functions. When expressed in MDCK cells, Snail was capable of decreasing proliferation and increasing resistance to apoptosis(Vega et al., 2004). This was partly explained by Snail's repression of the cell cycle protein CyclinD2. Snail has also been described to enhance tumor angiogenesis, which will be discussed further below. Understanding the mechanism by which Snail induces a wide range of targets and functions remains an important unanswered question in the field of EMT.

The microRNA-200 Family

In addition to the aforementioned transcription factors, EMT is also regulated by the microRNA-200 (miR-200) family (Figure 4). Forward genetic screens in tumor models and epithelial cell lines found that the five members of the miR-200 family, (mir-200c, -141, -200b, -200a, and -429), located in two genomic clusters, exert repressive actions on EMT by targeting the transcription factors Zeb1 and Zeb2 which themselves

repress E-cadherin(Bracken et al., 2008; Burk et al., 2008; Gregory et al., 2008; Korpal et al., 2008; Park et al., 2008). Although no functional role of miR-200 family microRNAs has been reported during early mouse development, examination of their effects in *in-vitro* model systems have shown that expression of miR-200 family members promote maintenance of the epithelial state and is associated with decreased tendency of tumors to metastasize (Gibbons et al., 2009; Olson et al., 2009). In addition, expression of the miR-200 family has been examined in the chick embryo, and was excluded from mesodermal tissues(Darnell et al., 2006), consistent with a proposed role in promoting non-mesenchymal cell phenotypes.

While the miR-200 family has been shown to have a clear role in EMT, controversy exists regarding its relationship with differentiation. One study reported that miR-200 inhibits the expression of Bmi1, a polycomb repressor that acts to promote "stemness" in embryonic stem cells (Wellner et al., 2009). While this study concluded that miR-200 members promoted differentiation, others have proposed that miR-200 family members attenuate differentiation through the direct inhibition of factors like Cadherin11 and Neuropilin1 (Lin et al., 2009). While each study supported its conclusion with specific markers, a global approach is needed to better clarify the effects of the miR-200 family on embryonic stem (ES) cell differentiation. Importantly, no one has examined the effects of miR-200 on EMT or fate restriction in the ES cell system.

Snail and the miR-200 Family

Interactions between Snail and miR-200 family members have recently been suggested by studies in the reprogramming of mouse embryonic fibroblasts (MEFs) to

inducible pluripotent stem (iPS) cells. First, the initiation of reprogramming of MEFs was associated with the reverse of EMT, in a process of mesenchymal to epithelial transition (MET) (Li et al., 2010; Samavarchi-Tehrani et al., 2010). A signature of MET is the induction of E-cadherin and other epithelial markers. Importantly, ectopic expression of Snail in MEFs undergoing reprogramming was associated with decreased efficiency of iPS cell generation (Li et al., 2010). In contrast, forced expression of E-cadherin or miR-200 family members augmented the efficiency of reprogramming (Chen et al., 2010; Samavarchi-Tehrani et al., 2010). While these studies did not examine the potentially direct interactions of Snail and miR-200, these results showed that Snail and miR-200 families exert opposite effects during MET.

Snail and Vasculogenesis

In Meox2-Cre/Snail$^{loxp/loxp}$ mice, where Snail is selectively deleted in the embryo proper, gastrulation occurs, but the mice die from extraembryonic vascular defects including failure of chorionic-allantoic fusion and a severe reduction in blood vessels in the embryo proper as detected by VE-cadherin staining(Lomeli et al., 2009; Murray and Gridley, 2006). These findings suggest that in addition to its general function in gastrulation, Snail has a specific role in vasculogenesis in both the embryo proper as well as extraembryonic tissues.

In addition to its expression in the primitive streak, Snail is also expressed in extraembryonic tissues such as extraembryonic mesoderm, the allantois (derived from extraembryonic mesoderm) and parietal and visceral endoderm (derived from primitive endoderm), which is adjacent to the yolk sac (Nieto et al., 1992; Smith et al., 1992;

Veltmaat et al., 2000). Snail's role in these extraembryonic tissues has not been well-characterized and remains unclear. However, an ex vivo analysis of allantoic explants from Meox2-Cre/Snail$^{loxp/loxp}$ mice showed clusters of PECAM+ cells that were highly disorganized relative to control explants(Lomeli et al., 2009). It was unclear whether or not the requirement for Snail was cell-autonomous or non-cell-autonomous manner in these cells.

Beyond the embryo, Snail has also been linked to endothelial formation in the setting of tumors. Non-small cell lung carcinomas overexpressing Snail as well as MDCK-Snail xenograft tumors displayed increased concentrations of blood vessels, which were thought primarily to be a result of cell-extrinsic effects(Peinado et al., 2004b; Yanagawa et al., 2009). In contrast, expression studies have suggested that Snail may have a cell-intrinsic role in endothelial formation. In addition to being upregulated after VEGFA stimulation(Wanami et al., 2008), Snail has been found to be highly expressed in endothelial cells of invasive breast cancer vasculature(Parker et al., 2004), spindle cell carcinoma(Zidar et al., 2008), and oral squamous cell carcinoma(Schwock et al., 2010). The latter study noted the expression of Snail in endothelial cells was greater in blood vessels close to the tumor, suggesting that the blood vessels of tumors uniquely express Snail as compared to the endothelium of normal tissue. Recently, a subset of glioblastoma tumor-derived stem-like cells were found to differentiate directly into endothelial cells(Ricci-Vitiani et al., 2010; Wang et al., 2010). While the precursors of these cells were clearly of tumor origin, a mechanism which links both tumorigenesis and the specification of endothelial cells has yet to be characterized.

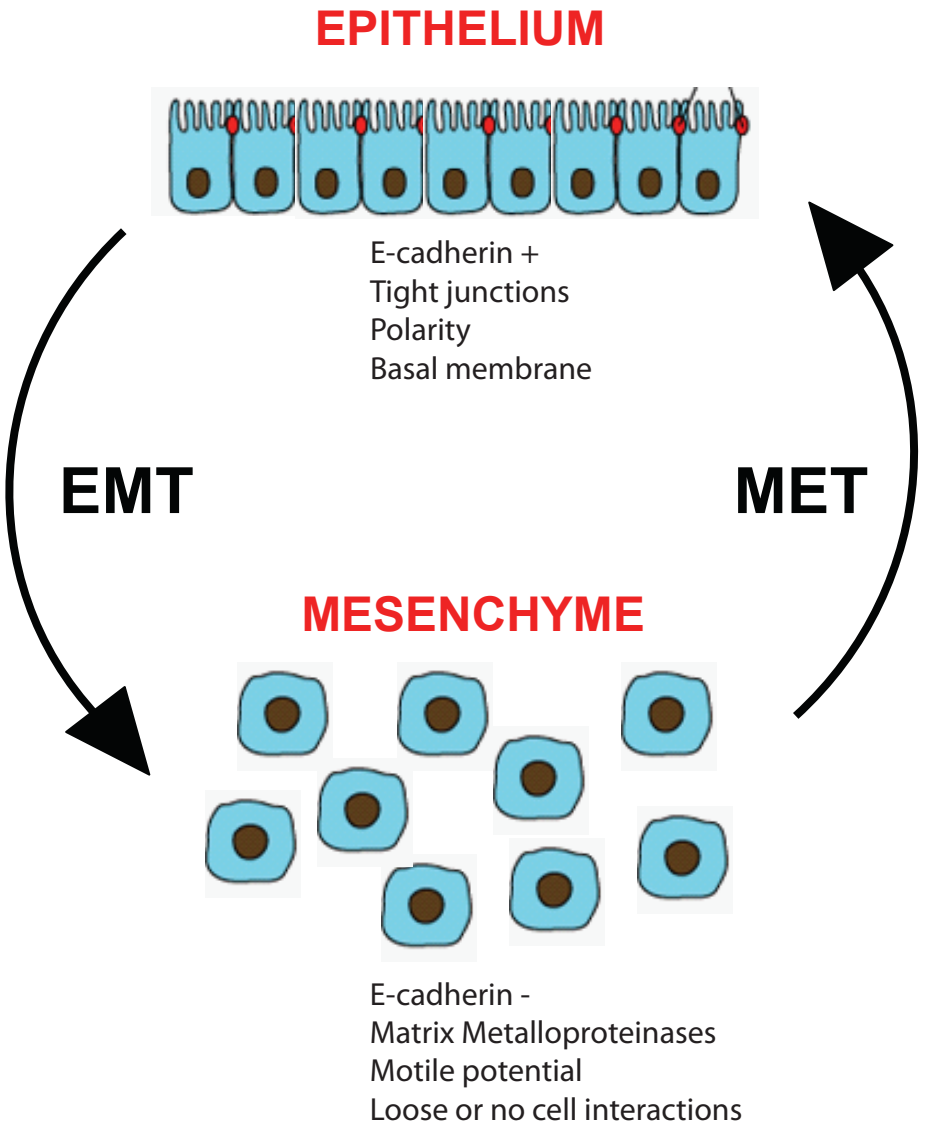

Figure 1: Diagram of Epithelial to Mesenchymal Transition.

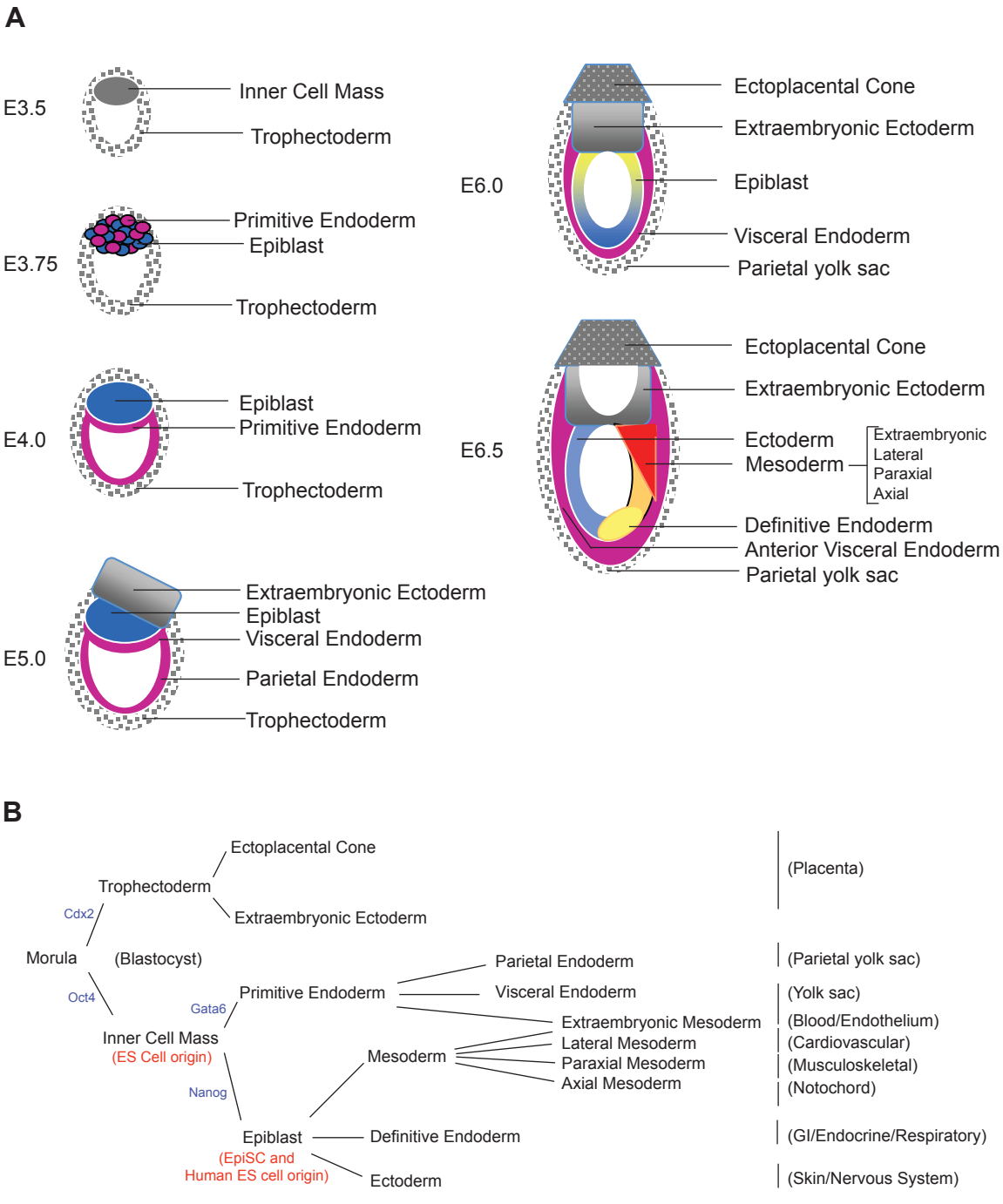

Figure 2: Patterning of the mouse embryo through early gastrulation. (A) Stages of embryo development from blastocyst to the early primitive streak stage. (B) Lineage development from morula to germ layer derivatives.

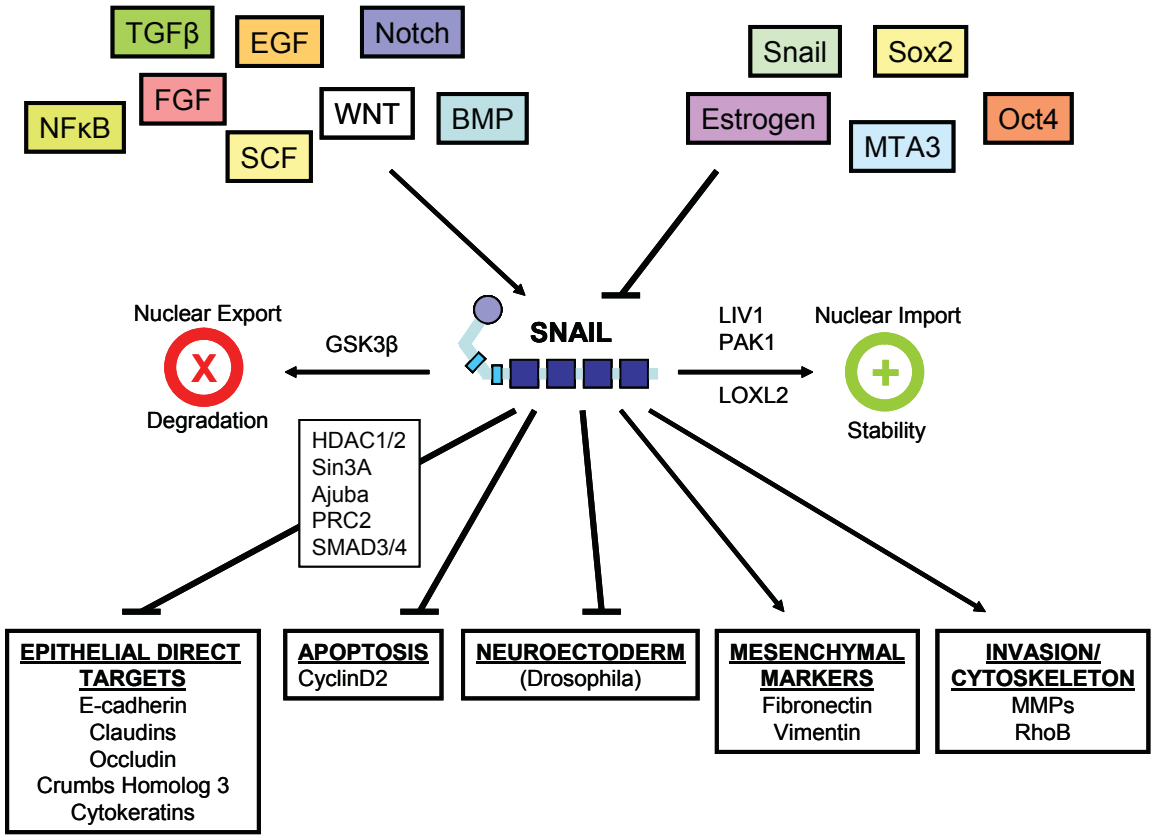

Figure 3: Signaling and molecular networks surrounding Snail homolog 1.

A

Mouse Chromosome 4:

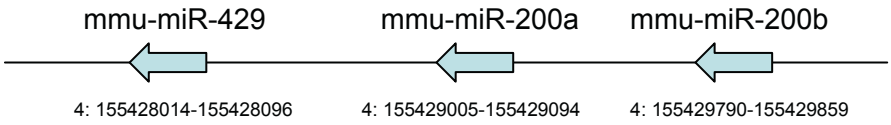

(Note: Located in intron 1 of Ttll10 tubulin tyrosine ligase-like family, member 10; however, this microRNA family in humans is intergenic)

Mouse Chromosome 6:

(Note: Located in intron 1 of processed transcript: RP24-297C1.9-001; however, this microRNA family in humans is intergenic)

B

Sequence Alignment of the miR-200 Family

Mmu-miR-200a:	U**AACACUG**UCUGGUAACGAUGU
Mmu-miR-141:	U**AACACUG**UCUGGUAAAGAUGG
Mmu-miR-200b:	U**AAUACUG**CCUGGUAAUGAUGA
Mmu-miR-200c:	U**AAUACUG**CCGGGUAAUGAUGGA
Mmu-miR-429:	U**AAUACUG**UCUGGUAAUGCCGU

Figure 4: The microRNA 200 Family. (A) Depiction of the genomic locations for the miR-200 family. (B) Sequence alignment of the miR-200 family. The seed sequences are shown in bold and red.

CHAPTER 2

Experimental Procedures

ESC Maintenance and Differentiation

MC50 (a gift from Dr. Robert Schreiber) and modified A2lox cells (Iacovino et al., 2009) were maintained on feeder layers of irradiated mouse embryonic fibroblasts in IMDM with 15% FCS, NEAA (0.1 mM each), L-glutamine (2 mM), sodium pyruvate (1 mM), Pen/Strep (1000 U/ml), 2- mercaptoethanol (55 μM), and LIF (EsGro, Chemicon International; 1000 U/ml). Using gene-specific primers (Table 1), individual cDNAs were cloned from embryoid body RNA or genomic DNA and inserted into the p2lox targeting vector (Figure 5). To generate inducible cell lines, A2lox cells were co-transfected with gene-specific p2lox vectors and Cre recombinase as previously described (Lindsley et al., 2006).

Prior to differentiation, ES cells were passaged once in the absence of feeder layers (still in the presence of LIF). To initiate differentiation, ES cells were plated in petri dishes in suspension at 1.5×10^4 cells/ml in IMDM with 10% FCS, NEAA (0.1mM each), L-glutamine (2 mM), sodium pyruvate (1 mM), Pen/Strep (1000 U/ml), and 2-mercaptoethanol (55 μM) and supplemented where indicated with DKK-his as described (Lindsley et al., 2006), SB-431542 (10 μM, Sigma), rm-Noggin (500ng/mL, R&D Systems), or SU5402 (10uM, Tocris Bioscience). Gene expression was induced by addition of doxycycline (250-1000 ng/ml, unless otherwise indicated).

Generation of recombinant DKK1-his

Recombinant DKK1 was either purchased from R&D Systems or prepared by transient transfection of 293F/T cells with calcium phosphate precipitation of pcDNA-DKK1-his. Supernatant was collected daily for 3 days, adjusted to pH 8.0 by the addition of 1/3 volume of 1X Ni-NTA binding buffer, and purified over a nickel-NTA binding resin (Qiagen). Purified DKK-his was dialyzed in PBS and detected by Western blot using an antibody to penta-His (Qiagen). Except where indicated, recombinant Dkk1-His was added to differentiation cultures at 1×, defined as the concentration required to inhibit generation of Flk1-expressing cells in SCM through day 5 (~160-200 ng/ml, depending on the batch.)

Flow Cytometry

Cells were disassociated with trypsin/EDTA for 5 minutes at 37°C and stained with antibodies. Primary antibodies: biotin α-mE-cadherin (R&D Systems, 1.25ug/ml, 1:200), PE α-Flk1 (eBioscience, Avas12a1, 1:200), biotin α-Flk1 (eBioscience, Avas12a1, 1:200), APC α-PDGFRα (eBioscience, APA5, 1:200), α-SSEA1 (DSHB, MC-480, 1:200), αVE-cadherin, (eBioscience, eBioBV13, 1:200), αTie-2 (eBioscience, TEK4, 1:200), biotin α-c-kit (BD Pharmingen, 2B8, 1:200), APC α-CD34 (eBioscience, RAM34, 1:200). Secondary detection reagents: SA-APC (BD Pharmingen, 1:400), SA-PE-Cy7 (BD Pharmingen, 1:400), and PE α-mouse IgM (BD Pharmingen, R6-60.2, 1:200). Data were acquired on a FACS Caliber (Becton Dickinson) or the FACS Canto II (Becton Dickinson) and analyzed on FlowJo (Tree Star).

A2.Snail DKK and DKK+dox samples were sorted as described in the text based on Flk1 expression using a MoFlo cytometer (Cytomation).

Gene Expression Analysis

To evaluate expression of individual genes, RNA was isolated with RNeasy kits (Qiagen), cDNA was synthesized using Superscript III (Invitrogen), and PCR was performed using Taq Polymerase (Promega). Non-quantitative RT-PCR was performed using intron-spanning, gene-specific primers (Table 1) and cycle number varied from 25-28 cycles. Quantitative RT-PCR was performed using SYBR Green PCR Master Mix (Applied Biosystems) and the StepOne Plus Real-Time PCR System (Applied Biosystems). Large-scale gene expression analysis was done using Affymetrix MOE430_2.0 arrays as described (Lindsley et al., 2008). Data were normalized and modeled using DNA-Chip Analyzer/dChip (Li and Wong, 2001a; Li and Wong, 2001b). CEL Files and accompanying data were deposited in the NCBI GEO database under accession numbers GSE24289 (*A2.miR200c* data), GSE24291 (*A2.snail* data, 6/12/24h DKK +/- doxycycline chips), and GSE26524 (*A2.snail* Flk1+ sort).

Immunofluorescent Microscopy

Cells were differentiated as described and placed at day 2 on Type I Collagen-coated 4-well chamber slides (BD Bioscience). On day 4, cells were fixed with 2% formaldehyde in PBS, blocked with 1% BSA, 0.5% saponin in PBS, and stained with antibody in blocking solution. Primary antibodies: biotin α-mE-cadherin (R&D Systems, 2.5μg/ml, 1:100), α-fibronectin (2.5 μg/ml, BD Transduction Laboratories), and N-cadherin (BD Biosciences, 2.5μg/ml, 1:100). Secondary antibodies: Streptavidin-

Alexa488 (Molecular Probes, 1:500) and Cy3 α-mIgG1 (Jackson Immunoresearch, 1:300). Nuclei were stained using Hoechst 33342 (1 μg/ml, Molecular Probes).

microRNA Expression Analysis

To analyze expression of individual microRNAs, total RNA was isolated using *mir*Vana miRNA Isolation kit (Ambion), and TaqMan microRNA assays (Applied Biosystems) were performed according to manufacture's instructions. Real-time PCR was performed on a StepOnePlus Real Time PCR system (Applied Biosystems). All individual microRNA data are expressed relative to a U6 snRNA TaqMan PCR performed on the same sample. Large scale microRNA expression data was analyzed using a microRNA Detection Microarray (LC Sciences).

Expression of microRNA Family Members

microRNA families were cloned from mouse genomic DNA using primers flanking the outermost family members (Table 1). This DNA was then cloned into the p2lox targeting vector such that the microRNA family members would be expressed from the doxycycline-inducible promoter or CAG promoter in the A2lox cells (Figures 18, 20, 49).

MicroRNA Knockdown Studies

FITC-labeled miRCURY LNA microRNA Power Inhibitors (Exiqon) were obtained to inhibit miR-141, miR-200c, or nothing (negative control with no known mouse sequence homology). A2lox ES cells were plated at a density of 200,000

cells/well of a 12-well plate and 50nM of the indicated LNA Power Inhibitor were transfected using Lipofectamine (LF2000, Invitrogen) and OptiMEM I reduced serum medium (GIBCO). Media was replaced 1 day later with normal ES cell media, and transfection was verified by microscopy and flow cytometry. The following day cells were harvested and set up for embryoid body differentiation as described above.

Epiblast-Stem Cell (EpiSC) Culture Conditions

A2.miR200c ES cells were differentiated as embryoid bodies (with and without doxycycline) for 5 days. On day 5, embryoid bodies were trypsinized and subsequently cultured and passaged in EpiSC conditions in the absence of MEFs or LIF similar to methods previously described (Brons et al., 2007; Chenoweth and Tesar, 2010). After trypsinization of the embryoid bodies, cells were plated at a density of 115,000 cells per well of a 6-well plate (pre-coated with fetal calf serum overnight and washed with PBS). Cells were cultured in IMDM with 20% Knockout Serum Replacement, NEAA (0.1 mM each), L-glutamine (2 mM), sodium pyruvate (1 mM), Pen/Strep (1000 U/ml), 2-mercaptoethanol (55 μM), 5ng/mL FGFb (GIBCO), and 20ng/mL rh-Activin A (GIBCO). Media was replenished daily. To passage, colonies were removed with a cell scraper, triturated into small clusters with a P200 pipette tip, and passaged every 2-3 days with typically a 1:3 split.

Blood/Endothelial Assays

For the methylcellulose hematopoietic assay, day 3 *A2.Snail* and *A2.Er71* embryoid bodies were trypsinized, passaged through a 20-gauge needle, and set up in

triplicate dishes in methylcellulose plus cytokines (Stem Cell Technologies, 03434) at a concentration of 50,000 cells/mL. BL-CFCs were counted in all samples on day 8. For the hemangioblast assay, the same *A2.Snail* and *A2.Er71* cells were plated at a density of 50,000 cells/mL in 24 well plates in 1% methylcellulose in differentiation media supplemented with D4T and kit-ligand conditioned media (gifts from KC Choi), and VEGF (5ng/mL, Peprotech). Images were recorded 4 days later using a Nikon Eclipse TS100 microscope and Optronics camera.

For the endothelial tube formation assay, 0.2mL of Matrigel (BD Biosciences) was added to each well of a 24-well plate and allowed to solidify at 37°C. Following solidification, 0.2mL of a cell suspension containing 5 x 10^4 *A2.Snail* cells on day 3 of embryoid body culture (after trypsinization and passage through a 20-gauge needle) were plated on top of the Matrigel in triplicate in differentiation media plus VEGF. The cultures were incubated at 37°C, 5% CO2 and observed at 24 hours for rearrangement of cells into tubular structures and networks. Images were recorded using a Nikon Eclipse TS100 microscope and Optronics camera.

Luciferase Assays

pMIR-Report Luciferase plasmids (Ambion) containing Luciferase with the indicated 3'UTRs, CMV-Renilla, and +/- 5uM miRNAs were cotransfected into 293T cells with Lipofectamine 2000 (Invitrogen). See Table 1 for a list of primers used to generate the 3' UTRs and mutations. Cells were harvested 24 hours later, and luciferase activity was measured using an Optocomp II automated luminometer (MGM Instruments,

Inc.). Firefly luciferase activity was normalized to Renilla luciferase activity to account for possible differences in cell density and transfection efficiency.

Western Analysis

A2.Snail.CAG.GFP, *A2.Snail.miR200A*, and *A2.Snail.miR200C* ES cell lines were plated in 10cm gelatinized dishes in ES cell media. Doxycyline was added in select dishes at 250ng/mL. Cells were harvested in RIPA buffer along with protease inhibitors 24 hours later. As a positive control for Snail expression, 10uM MG132 was added to a subset of the doxycycline dishes 4 hours prior to harvesting of the protein lysate. 30ug of protein lysate was added to each well of a 12% PAGE gel. Protein was transferred to a nitrocellulose membrane, blocked, and probed using an αSnail antibody (Abcam, ab17732 XX, 1:400) with HRP-anti-rabbit secondary (Jackson Immunoresearch, 1:20,000) or α-β-actin antibody (Santa Cruz Biotechnologies, sc-47778, 1:5000) with HRP-anti-mouse secondary (Jackson Immunoresearch, 1:20,000). ECL Plus Detection System (GE Healthcare) was used for detection following the manufacture instructions.

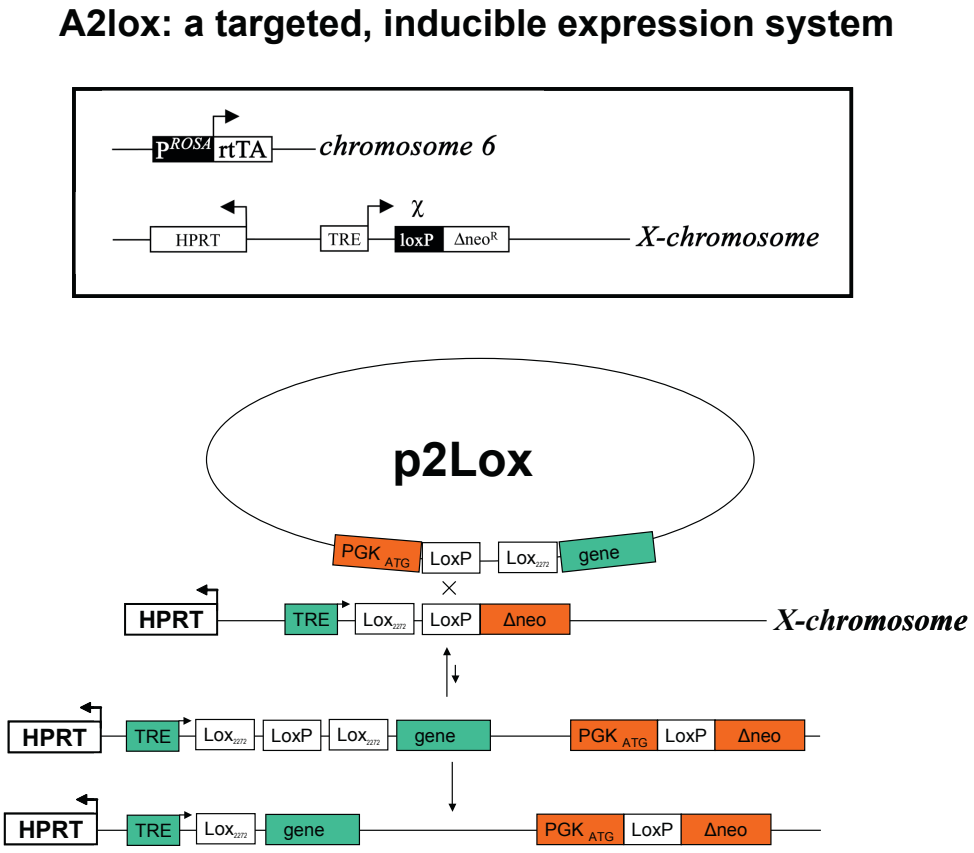

Figure 5: Schematic of p2lox targeting strategy. Plasmid and cells are from Michael Kyba; figure adapted from M. Kyba and R.C. Lindsley.

Table 1. Oligonucleotide primers used in this study.

	CLONING PRIMERS
Name	**Sequence**
C_mir200a/b/429 F (for A2.miR200a)	GCT**GGATCC**CTCCTTGGTTCCATGACCTGAGAA
C_mir200a/b/429 R (for A2.miR200a)	CTA**GATATC**GACTGGACCTGTTGTCTAGGCTATTCT G
C_mir200c/141 F (for A2.miR200c)	GCT**GGATCC**CCTTTCTTACGAAGACCGAGTCTCCA
C_mir200c/141 R (for A2.miR200c)	CTA**GATATC**CCTCAAGAGGAGGTGCCCAGG
C_mir335 F (for A2.miR335)	GAGAGAGTGGTGGGTCCAAGTAGGG
C_mir335 R (for A2.miR335)	GCAAGCTGACAGGACTTCAGGAGC
C_snail F	TAGGTCGCTCTGGCCAACATGC
C_snail R	AAGATGCCAGCGAGGATGGG
C_Flk1 3'UTR F	AATGGAAGTGGTCCTGTCCC
C_Flk1 3'UTR R	AACATAAGCACACAGGCAGAAACC
C_Ets1 3'UTR F	TCATGGACAGACGCGCAGAAG
C_Ets1 3'UTR R	TTATGAATGAATTTCTTTGTTTCTTTAATTTCAC
C_Gata2 3'UTR F	CAGGACTAGTGCAAGCCTCCCACTGGACAGACA
C_Gata2 3'UTR R	CAGGTTCGAACAACAGGCGACAGCATTCACAAAAA GTATT
	AROUND-THE-WORLD MUTATION PRIMERS
Name	**Sequence**
ATW ΔSNAG.Snail F	GGCCAACATGAAGCCGTCCGACCCCCGCCGG
ATW ΔSNAG.Snail R	GGACGGCTTCATGTTGGCCAGAGCGACCTA
ATW Flk1 3'UTR MUT F	CCAAGTCCT**ATCTGAA**TTAGCTTTGTGGCTTCCTGA TGGCAG
ATW Flk1 3'UTR MUT R	GCTAA**TTCAGAT**AGGACTTGGGGGCCTGACAGGAG TGGA
ATW Ets1 3'UTR MUT F1	GTGC**ATCTGAA**TTTTTTTCCTTAAAAAAATATCGTCT TAAGCTC
ATW Ets1 3'UTR MUT R1	TAAGGAAAAAAA**TTCAGAT**GCACAAAATTTAATAAAA TAAACTTCAACAT
ATW Ets1 3'UTR MUT F2	GGTCT**ATCTGAA**G**ATCTGAA**GTGAGTTTGTTGTTAT TTGCTGGC
ATW Ets1 3'UTR MUT R2	AC**TTCAGAT**C**TTCAGAT**AGACCACCTTAGAGCTTAA GACGATAT
ATW Gata2 3'UTR F	GAAGAATCGG**ATCTGAA**TTCTGTTTTTATGTTTTGG GCTTGTTTTA
ATW Gata2 3'UTR R	CAGAA**TTCAGAT**CCGATTCTTCTCTTATGCGGGTAC TAGCAC
	q-RT-PCR PRIMERS
Name	**Sequence**
FGF5 F	CACGAAGCCAGTGTGTTAAGTATTTTGG
FGF5 R	GCATCATCCAAAGCGAAACTTCAG
Fibronectin F	GGAATGGAAAGGGAGAATTCAAGTG
Fibronectin R	GGGGCAATTTACGTTAGTGTTTGTTC
Gapdh F	TGCCCCCATGTTTGTGATG
Gapdh R	TGTGGTCATGAGCCCTTCC
Nanog F	CTCTCCTCGCCCTTCCTCTGAAG

Nanog R	GGTGCTGAGCCCTTCTGAATCAG
N-cadherin F	ACAATCAACAATGAGACTGGGGACA
N-cadherin R	TCATTGACATCTGTCACCGTGATGA
Ncam1 F	TGCTGCGAACTAAGGATCTCATCTG
Ncam1 R	GCATTCTTGAACATGAGCTTCTGGA
Nodal F	GGATCATCTACCCCAAGCAGTACAATG
Nodal R	GCAAGCCAATTTCAGCACTCCC
Occludin F	CCTGGAGGTACTGGTCTCTACGTGG
Occludin R	TCTTTCCGCATAGTCAGATGGGG
Oct4 F	CAATGCCGTGAAGTTGGAGAAGG
Oct4 R	CGAAGCGACAGATGGTGGTCTG
Snail F	CGCTCTGAAGATGCACATCCGA
Snail R	TCACATCCGAGTGGGTTTGGAG
Sox2 F	CTCCATGACCAGCTCGCAG
Sox2 R	CCTTCTCCAGTTCGCAGTC
Zeb1 F	CCTACAGTCACTGCCCAGTTACCC
Zeb1 R	GCATACATTCCATTCTCTGTCTTCCG
Zeb2 F	CTGCCACTTTCATGCCACCAG
Zeb2 R	CGGAGTCTGTCATGTCATCTAGGC
	RT-PCR PRIMERS
Name	**Sequence**
E-cadherin F	GTCCTGCCAATCCTGATGAAATTG
E-cadherin R	CACTGATATAATTATTCTGCATCTCCCA
Fibronectin F	GGAATGGAAAGGGAGAATTCAAGTG
Fibronectin R	GGGGCAATTTACGTTAGTGTTTGTTC
Gapdh F	TGCCCCCATGTTTGTGATG
Gapdh R	TGTGGTCATGAGCCCTTCC
Snail F	CGCTCTGAAGATGCACATCCGA
Snail R	TCACATCCGAGTGGGTTTGGAG

CHAPTER 3

Snail promotes EMT and mesoderm differentiation

ES Cells Undergo a Wnt-Dependent EMT during Differentiation

In a previous study, we found that inhibition of canonical Wnt activity completely blocks expression of primitive streak and mesendoderm-associated genes during ES cell differentiation(Lindsley et al., 2006). This finding recapitulates *in vivo* findings demonstrating that primitive streak formation requires the canonical ligand Wnt3, Wnt co-receptors Lrp5/6, and β-catenin, the intracellular effector of canonical Wnt signaling(Huelsken et al., 2000; Kelly et al., 2004; Liu et al., 1999).

Because primitive streak formation in the embryo occurs concomitantly with EMT, we decided to study the expression of the epithelial marker E-cadherin during ES cell differentiation in the presence and absence of Wnt signaling. First, we performed a FACS analysis of E-cadherin expression on differentiating MC50 ES cells. E-cadherin is normally maintained for at least 3 days following withdrawal of LIF, but is increasingly lost on days 4, 5, and 6 in a Wnt-dependent manner (Figure 6A). When we analyzed gene expression patterns in NT and DKK-treated ES cell differentiation cultures from days 0 to 4, we found repression of additional epithelial markers (*Occludin*, *Claudin 6*, and *Epithelial V-like antigen 1*) as well as induction of mesenchymal markers (*Fibronectin*, *N-cadherin*, and *Snail*) (Figure 6B). The expression of Snail in differentiating ES cells closely corresponds to the loss of E-cadherin, showing a peak of expression on day 3.5 immediately preceding the onset of E-cadherin down-regulation (Figure 6C).

To further characterize EMT at the protein level, we examined expression of *E-cadherin* and *fibronectin* during ES cell differentiation. Undifferentiated ES cells express E-cadherin, but not fibronectin (data not shown). After 5 days of differentiation in serum-containing media, cells uniformly express fibronectin, but not E-cadherin, indicating that these cells have undergone EMT (Figure 7). In contrast, cells treated with DKK maintain E-cadherin expression and fail to induce fibronectin, reflecting their failure to undergo EMT. Additionally, cells differentiated in serum-containing media possess the capacity to adhere and spread on a gelatinized substrate, while DKK-treated cells remain in suspension (Figure 7). Together, these results indicated that Wnt signaling is required for the EMT of differentiating ES cells.

Snail promotes EMT in day 2 differentiating ES cells.

Snail homolog 1 (Snail) is required for the EMT of the gastrulating embryo (Carver et al., 2001). Given the expression pattern and Wnt-dependence of the EMT transcription factor Snail homolog 1 (Snail) during ES cell differentiation, we hypothesized Snail may play an important role in inducing EMT in ES cells.

Using an ES cell line with doxycycline-inducible Snail (*A2.snail*), we next sought to characterize how Snail affected E-cadherin levels in differentiating ES cells. We examined cultures treated with and without DKK, and with doxycycline added on day 0 or just prior to its normal endogenous expression on day 2. Interestingly, Snail was capable of down-regulating E-cadherin when induced on day 2, but not in day 0 cultures (Figure 8), suggesting that ES cells may lack factors required for Snail's function. In adherent differentiation cultures, induction of Snail on day 2 led to dramatic changes in

morphology, where Snail-induced cells acquired spindle-like morphologies and adhered as single cells (Figure 9B).

To further investigate EMT after Snail induction, we induced Snail on day 2, in the presence or absence of DKK (Figure 9A). RT-PCR showed that expression of E-cadherin is still evident on day 3 of differentiation in cultures without Snail induction, but is repressed by induction of Snail following doxycycline treatment (Figure 9C). Correspondingly, the mesenchymal marker fibronectin is induced by Snail in this system. Even though mesenchymal differentiation is normally blocked by inhibition of Wnt signaling, Snail is capable of powerful up-regulation of fibronectin expression (Figure 9C).

In addition, Snail induces a switch from E-cadherin expression to N-cadherin expression (Figure 10) in the majority of differentiating ES cells. The upregulation of N-cadherin is more robust in the presence of Wnt signaling, but also occurs in DKK cultures. These results show that Snail's actions in this differentiating ES cell culture system promote features of an EMT.

Snail accelerates the down-regulation of ES cell pluripotent markers

Because a number of pluripotency transcription factors including Sox2 and Oct4 have been found to repress Snail (Li et al., 2010), we wondered whether Snail may reciprocally play a role in limiting ES cell pluripotency. In order to examine potential actions of Snail on differentiation, we first examined the ability of Snail to regulate expression of the pluripotency marker SSEA1 (Figure 11). Normally, SSEA1 expression is gradually down-regulated during differentiation of ES cells in vitro. Interestingly, we

find that the loss of SSEA1 by differentiating ES cells is blocked by the addition of the Wnt inhibitor DKK. In contrast, induction of Snail in differentiating ES cells significantly accelerates the loss of SSEA1. Moreover, even in the presence of DKK, induction of Snail causes the down-regulation of SSEA1 in the majority of ES cells. Through a titration of doxycycline, we can confirm that this effect of Snail can be achieved at levels similar to endogenous and in a dose-dependent manner (Figure 12). In addition to SSEA1 down-regulation, we also show that Snail down-regulates expression of Sox2 and Oct4 transcripts, but not Nanog, by day 4 of differentiation (Figure 13). Thus, Snail promotes the loss of a pluripotency marker of ES cells, suggesting a potential role for Snail in promoting differentiation in addition to EMT.

Snail promotes mesoderm, but not ectoderm, differentiation

To refine this analysis and determine whether Snail-induced loss of pluripotency promoted fate determination, we examined two markers of mesodermal fate, Pdgfrα and Flk1 (Figure 14). Normal differentiating ES cells undergo EMT and begin to express these markers of mesodermal fates beginning on day 3 and continuing through day 5 (Figure 14, top row). Induction of Snail in differentiating ES cells accelerated the progression of Pdgfrα expression and Flk1 expression (Figure 14, 2nd row). Importantly, even when mesoderm differentiation was blocked through the addition of the Wnt signaling inhibitor DKK, the induction of Snail was still able to induce expression of these markers of mesoderm (Figure 14, bottom row).

To obtain a global view of the effects of Snail on ES cell differentiation we utilized microarrays of differentiating *A2.snail* ES cells under conditions of Wnt

signaling inhibition to prevent endogenous-promoted EMT and mesoderm differentiation (Figure 15). In the absence of Snail induction, these conditions lead to a pattern of differentiation that is strongly skewed towards an epithelial phenotype and ectodermal fates (Figure 15 and (Lindsley et al., 2006)). However, upon induction of Snail, expression of epithelial and ectodermal markers are inhibited (e.g. *Otx2*, *Zic5*, and *Cldn6*), while genes associated with mesenchymal and mesodermal fates are strongly induced (e.g. *Mmp2*, *Ncam1*, *Isl1*, and *Gata2*). These results establish a precedent for the ability of Snail to alter patterns of cell type differentiation and indicate that Snail expression favors mesodermal rather than ectodermal fate choices during ES cell differentiation.

(Acknowledgements: R.C. Lindsley generated the *A2.snail* line, performed the gene chip if Figure 6B, and performed the RT-PCR in Figure 9C)

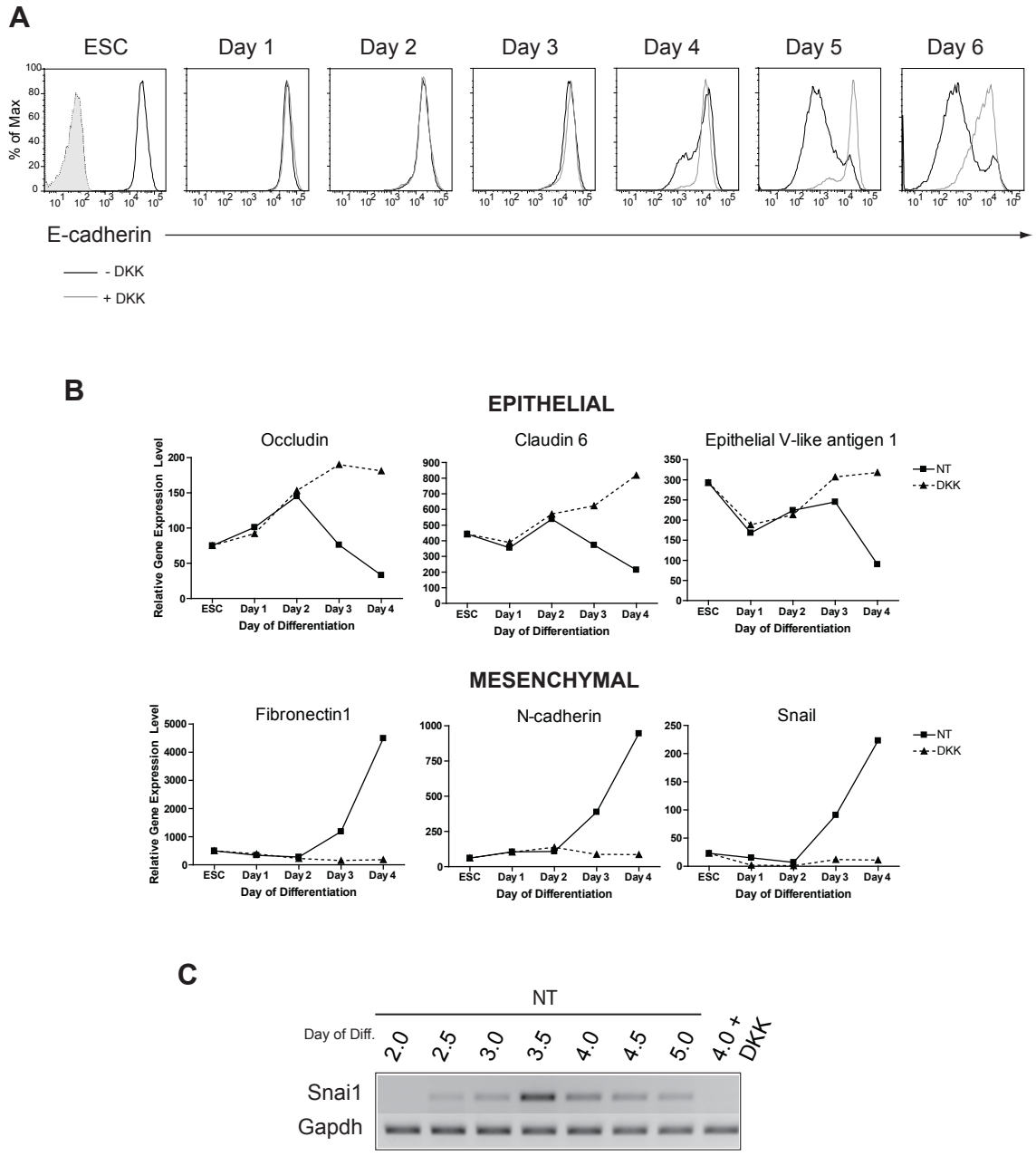

Figure 6: ES cells undergo a Wnt-dependent EMT during differentiation. (A) E-cadherin protein expression during MC50 ES cell differentiation was analyzed by flow cytometry in serum-containing differentiation conditions without (black line) or with (gray line) addition of the Wnt inhibitor DKK at day 0. A secondary antibody control is shown as a shaded plot in the ESC panel. (B) Gene expression analysis was performed by gene chip on days 0-4 of MC50 differentiation in the presence or absence of DKK from day 0-4. (C) RT-PCR of Snail and GAPDH during MC50 differentiation.

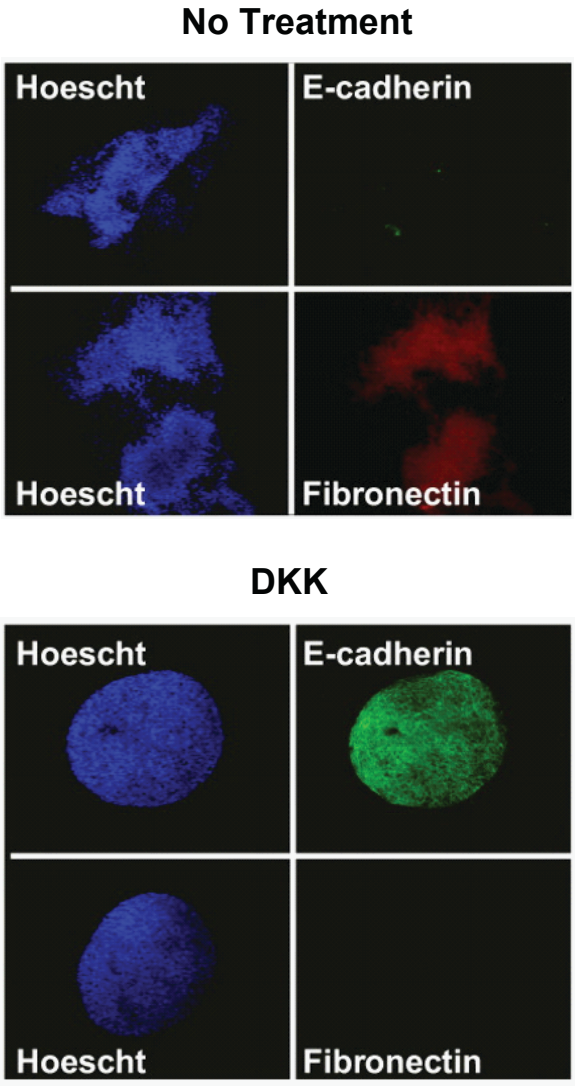

Figure 7: ES cells undergo a Wnt-dependent EMT during differentiation. Cells were differentiated in SCM alone (no treatment) or treated with Dkk1 for 4 days. On day 4, cells were washed and transferred to gelatinized plates in SRM without inhibitor and analyzed by fluorescence microscopy for expression of E-cadherin (green) or fibronectin (red) as described in the Materials and methods. Images of representative colonies, acquired using 10× objective magnification, are shown for unmanipulated (no treatment) and Dkk1-treated conditions.

Development 133(19):3787-96, 2006.

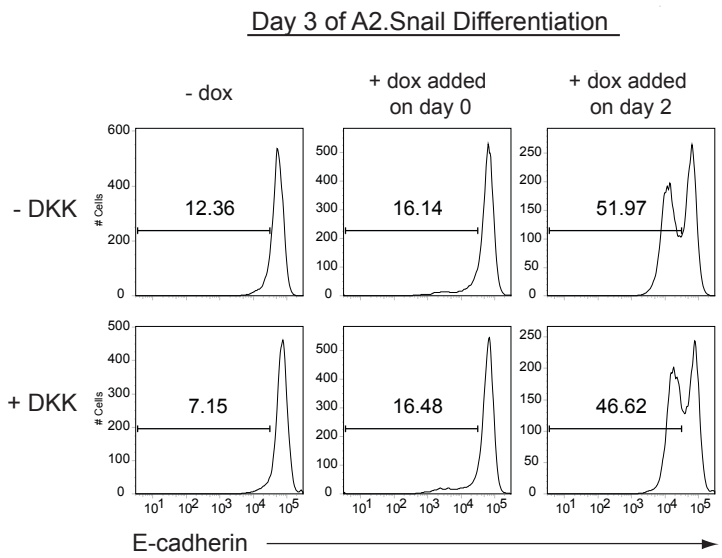

Figure 8: Induction of Snail on day 2 leads to the down-regulation of E-cadherin. FACS histogram of E-cadherin expression on day 3 of ES cell differentiation. *A2.Snail* ES cells were differentiated with or without DKK from day 0 and with or without addition of doxycycline at day 0 or day 2.

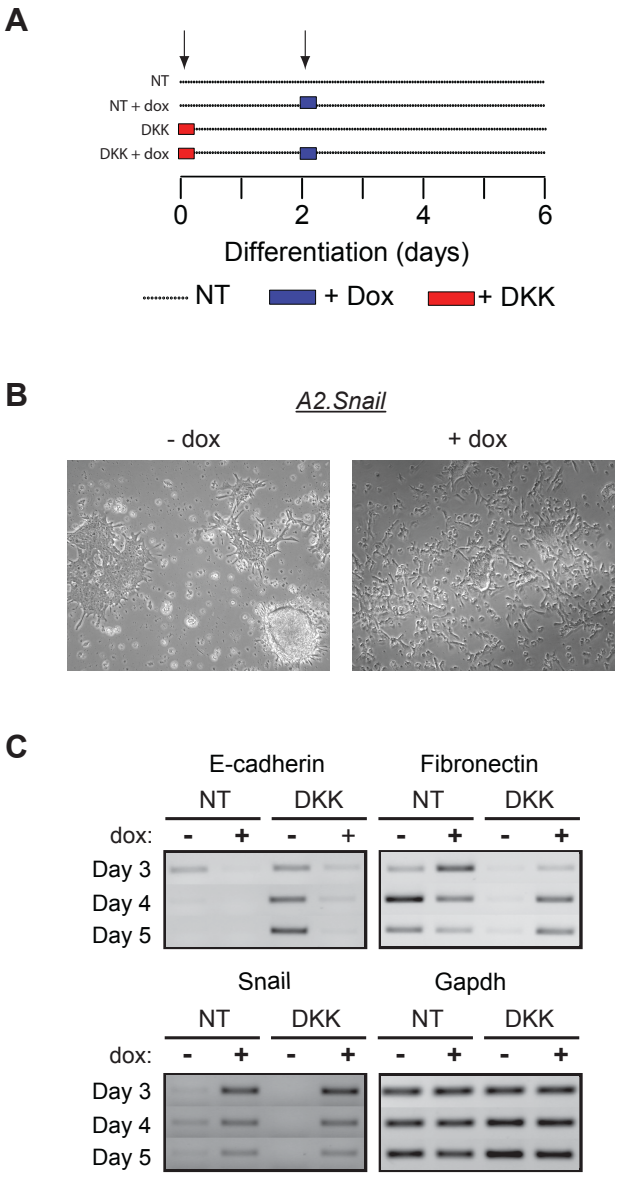

Figure 9: Snail induces an EMT in differentiating ES cells. (A) Outline of ES cell differentiation conditions. DKK is added at day 0, while doxycycline is added on day 2. (B) Light microscopy of *A2.Snail* cells on day 3.5 of differentiation in adherent cultures. Doxycycline was added on day 2. (C) *A2.Snail* cells were differentiated as described in (A). RNA was collected on days 3, 4, and 5, and RT-PCR was performed for the indicated genes.

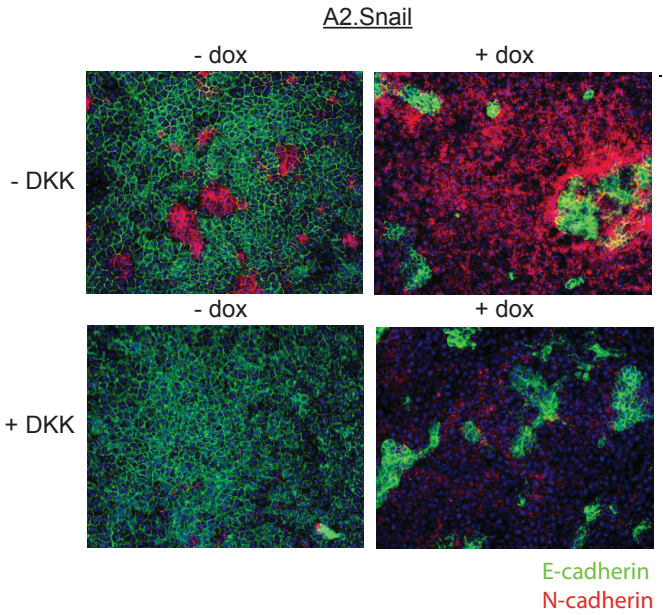

Figure 10: Immunofluorescence microscopy of Snail-induced EMT. *A2.Snail* ES cells were differentiated with or without DKK and doxycycline as outlined in Fig. 9A. Cells were placed on Type I Collagen-coated 4-well chamber slides on day 2 and fixed and stained on day 4. E-cadherin is shown in green and N-cadherin is shown in red.

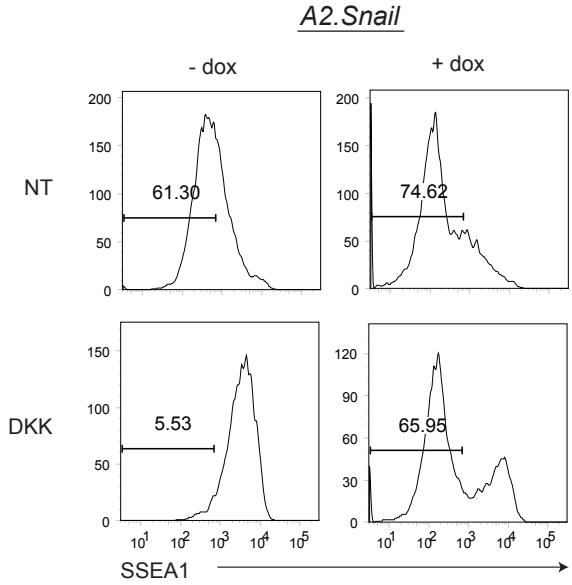

Figure 11: Snail induces the down-regulation of SSEA1. FACS analysis of SSEA-1 protein expression on day 4 of *A2.Snail* differentiation in the presence or absence of doxycycline added at day 2 and DKK added at day 0.

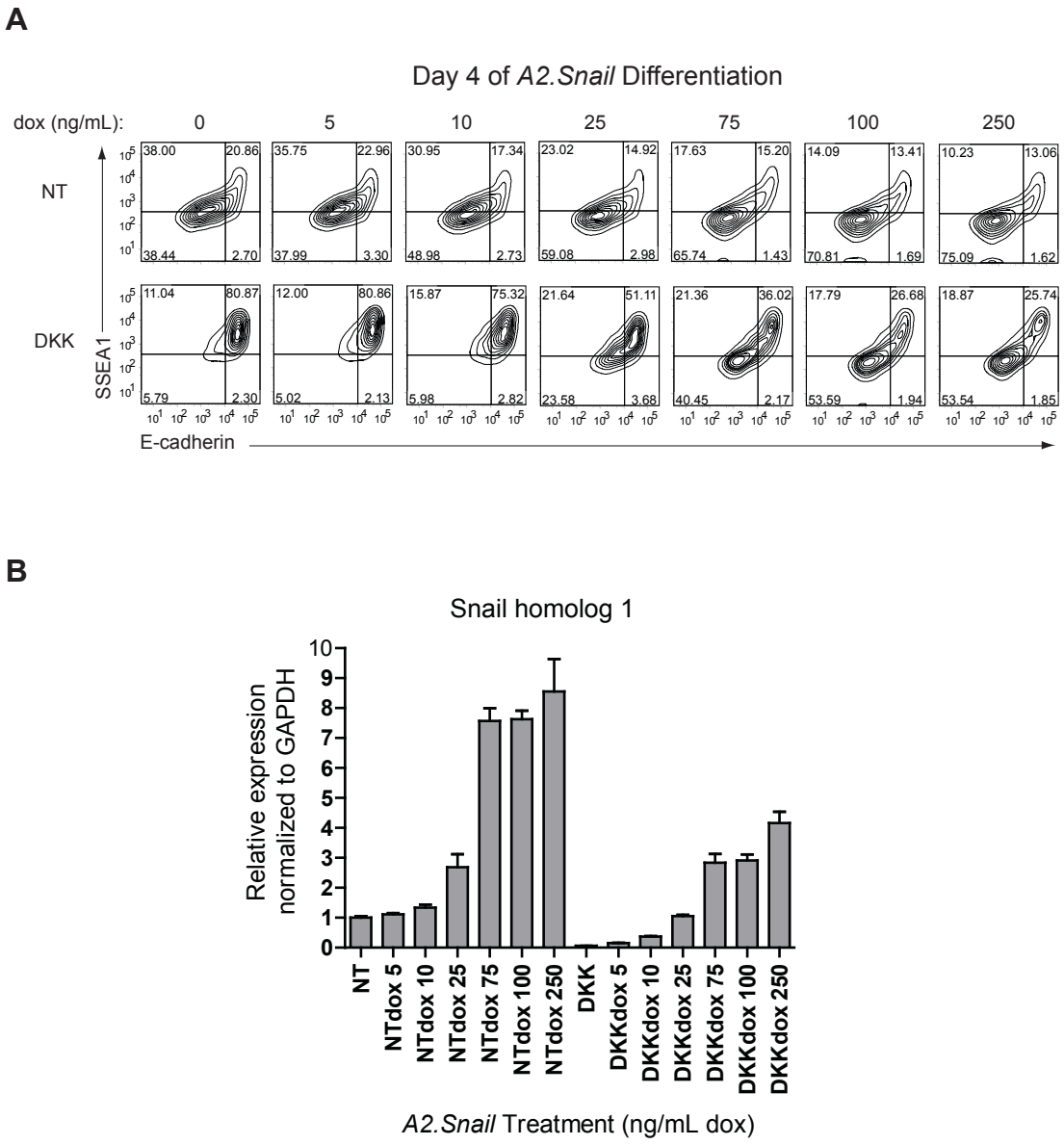

Figure 12: Snail down-regulates SSEA1/E-cadherin in a dose-dependent manner, even when Snail is induced at levels comparable to endogenous. (A) FACS plots of SSEA1 and E-cadherin in *A2.Snail* cells on day 4 of differentiation as described in Fig. 9A. Doxycycline concentration is indicated in ng/mL. (B) qRT-PCR of Snail expression levels on day 3 samples from (A). All samples were normalized to GAPDH and sample expression is listed relative to NT, which was set to 1.

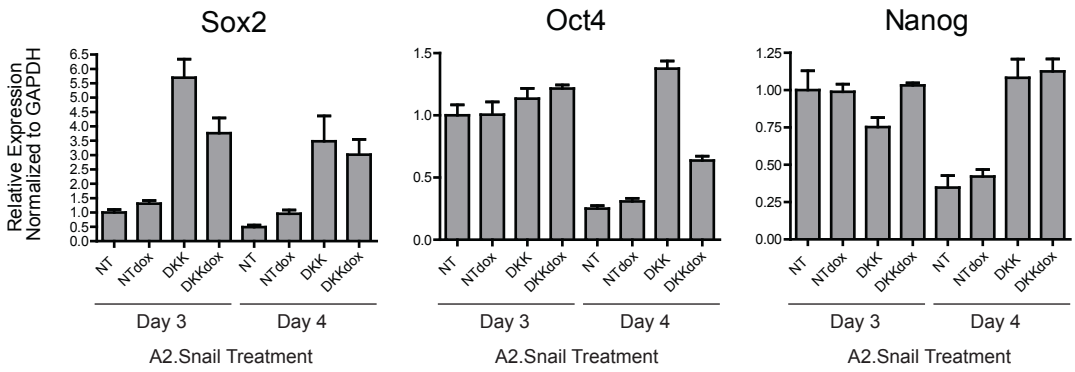

Figure 13: Snail down-regulates expression of Oct4 and Sox2, but not Nanog by day 4. qRT-PCR of Sox2, Oct4, and Nanog in *A2.Snai*l cells on day 3 and day 4 of differentiation as described in Supp. Fig. 1A. All samples were normalized to GAPDH and sample expression is listed relative to NT, which was set to 1.

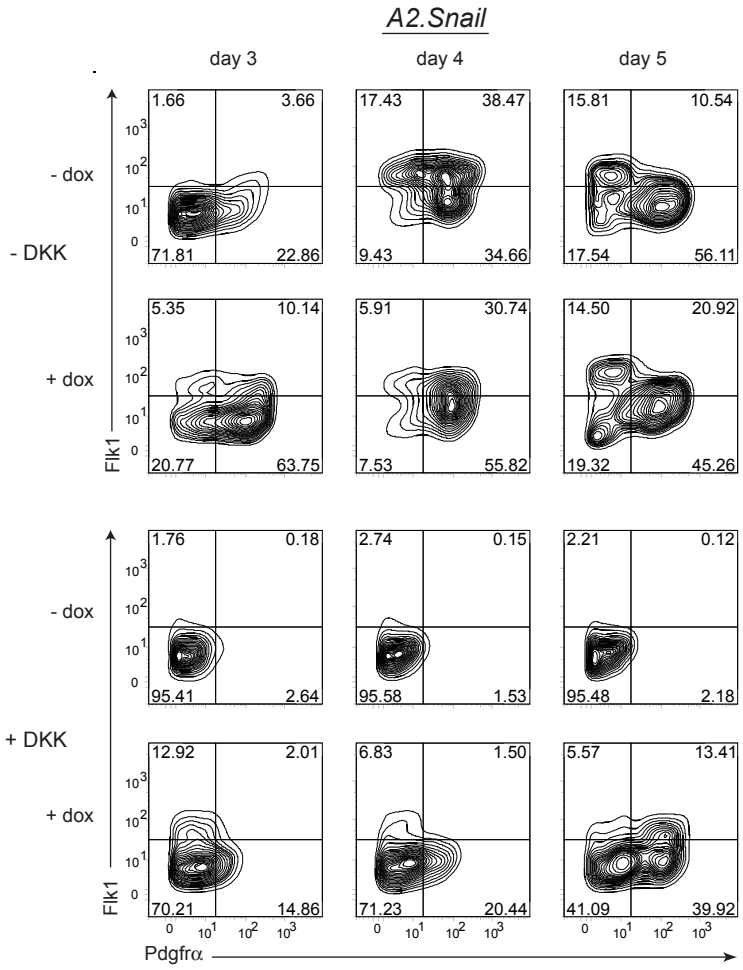

Figure 14: Snail accelerates the development of mesoderm. FACS analysis of Flk1 and PDGFRα protein expression on days 3, 4, and 5 of ES cell differentiation. *A2.Snail* cells were differentiated as outlined in Fig. 9A.

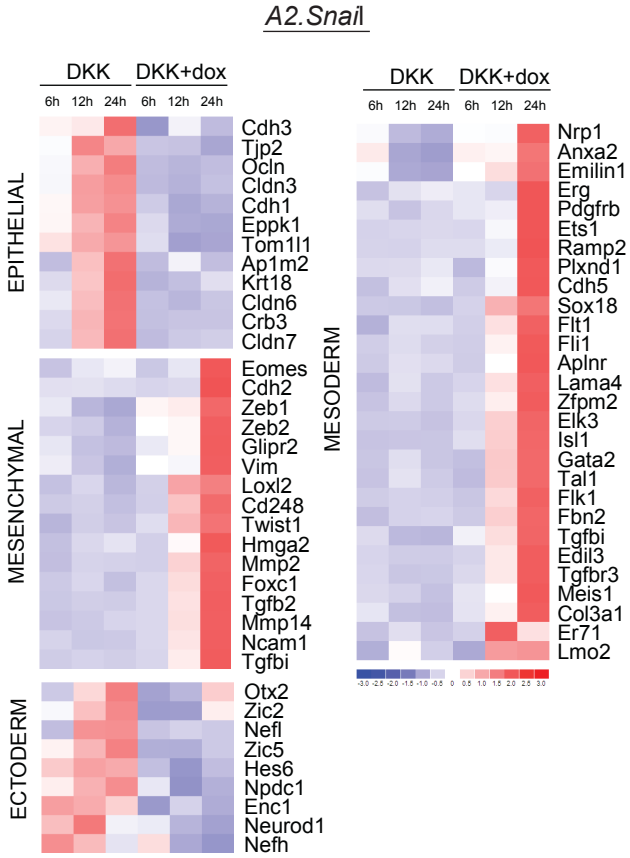

Figure 15: Snail promotes EMT and mesoderm commitment, while inhibiting ectoderm differentiation. Relative gene expression in *A2.Snail* ES cells differentiated with DKK in the absence or presence of doxyxycline. RNA was collected at 6, 12, and 24 hours after doxycycline addition (corresponding to day 2.25, 2.5, and 3 of differentiation). Red and blue indicate increased and decreased expression, respectively. Raw data can be found in the NCBI GEO database under accession number GSE24291.

CHAPTER 4

The miR-200 family prevents EMT and maintains differentiating ES cells as EpiSCs

Snail regulates multiple microRNAs, including the miR-200 Family

Snail reportedly acts as a transcriptional repressor, and yet some of its actions involve strong induction of target genes. We therefore wondered whether Snail might regulate the expression of miRNAs which could serve to repress indirectly induced targets of Snail. To address this, we carried out a global screen for miRNA expression under conditions of variable Snail expression (DKK and DKK+dox) (Figure 16A). Among the miRNAs that were significantly repressed by induction of Snail in ES cells were members of the miR-200 family (Figure 16B and Table 2). In addition, several miRNAs that have been associated with maintenance of pluripotency in ES cells were also inhibited by the induction of Snail. Notably, the miR-302 family, associated with differentiated mesoderm, was induced by Snail (Figure 16B).

Expression of the miR-200 family prevents EMT, differentiation, and mesoderm commitment

Since the miR-200 family has been associated with EMT through its targeted repression of Zeb1 and Zeb2, we wanted to more closely examine the expression pattern and relationship with Snail induction during ES cell differentiation (Figure 17). During normal ES cell differentiation (without inhibition of Wnt signaling), miR-200 family members are maintained until approximately day 3 of differentiation, and decreased by approximately 50% on day 4. Upon induction of Snail at day 2 of differentiation, miR-

200 family members are reduced by 50% after 24 hours and further reduced by day 4, indicating that Snail inhibits expression of each of the miR-200 family members examined. Furthermore, we observe that the expression of the miR-200 family members is strongly augmented under conditions that promote neuroectodermal fate and prevent EMT. In particular, the addition of the Wnt inhibitor DKK blocks mesoderm differentiation (Lindsley et al., 2006), and causes the gradual accumulation of higher levels of miR-200c, miR-200b, and miR-141 (Figure 17B). Importantly, even under these conditions in which high levels of miR-200 are normally expressed, the induction of Snail strongly represses the expression of endogenous miR-200 family miRNAs. These results indicate that Snail acts to repress the expression of the miR-200 family.

Given its expression pattern in ES cell differentiation and in response to Snail, we wanted to determine whether the miR-200 family could prevent EMT in ES cell differentiation as it has been shown to do in tumor models. We therefore generated ES cell lines harboring inducible expression of the miR-200c and miR-141 genomic cluster (*A2.miR200c*). In this cell line, miR-200c/141 are expressed downstream of a doxycycline-inducible transcriptional element (Figure 18A, B). Without induction of miR-200c/141, ES cells normally begin to lose expression of E-cadherin by day 4 of differentiation, with a majority of ES cells having lost E-cadherin on day 5 (Figure 19A). However, when miR-200c/141 is induced, differentiating ES cells maintain expression of E-cadherin at day 4 and day 5 opposite to the effects of Snail on E-cadherin expression (compare with Figure 8).

In addition to examining effects on EMT, we wanted to further understand how prevention of EMT by the miR-200 family might affect ES cell differentiation. We first

examined the effects of miR-200c/141 on the expression of mesodermal markers and pluripotency markers in differentiating ES cells (Figure 19B). Normal differentiating ES cells have induced the mesoderm markers Pdgfrα and Flk1 in a substantial number of cells by day 5 after differentiation (Figure 19B, first column, upper panel). However by maintaining expression of miR-200c/141 during ES cell differentiation, these mesodermal markers failed to be induced (Figure 19B 2nd and 3rd column, upper panel). Here, the level of expression of Flk1 and Pdgfrα in the presence of miR-200c expression is nearly as low as when mesoderm differentiation is blocked through the addition of the Wnt inhibitor DKK.

We also we examined the effect of miR-200c on the pluripotency marker SSEA1. Normally, by day 5 of ES cell differentiation, approximately 85% of ES cells have lost SSEA1 expression (i.e., 62%+16%) and have significantly down regulated E-cadherin expression. However, when miR-200c expression is maintained, SSEA1 expression is retained on the majority of ES cells with only 35% becoming SSEA1 negative. In addition, many fewer ES cells lose expression of E-cadherin when miR-200c expression is maintained. These results indicated that maintenance of miR-200c/141 expression during ES cell differentiation acts to prevent E-cadherin loss, inhibit induction of mesodermal markers, and prevent the down regulation of SSEA1. We found similar results when we generated an ES cell line with an inducible miR-200b/200a/429 cluster (Figure 20, 21). Furthermore, robust induction of a different microRNA (miR-335) failed to have the same effects as the miR-200 family, suggesting specificity (Figure 22). The effects of the miR-200 family are opposite to those of Snail shown above.

To determine whether loss of miR-200c/141 is sufficient for E-cadherin and SSEA1 down-regulation, we utilized LNA microRNA inhibitors (Exiqon) for loss-of-function studies. ES cells transfected with anti-miR-141 or anti-miR-200c, showed a slightly increased percentage of cells with down-regulated E-cadherin and SSEA1 on days 4 and 5 of differentiation as compared with a negative control inhibitor (Figure 23A, B). Because of the existing redundancy and target overlap in the miR-200 family, we hypothesize that the remaining uninhibited family members (miR-200a, miR-200b, and miR-429) may still be functioning to limit EMT and differentiation. Inhibition of miR-200c/141 alone was not sufficient to promote mesoderm induction (Figure 23C).

Expression of miR-200 family microRNAs promotes maintenance of the ESD-EpiSC state.

Because we observed that maintenance of miR-200c/141 inhibited expression of mesodermal markers while maintaining expression of SSEA1, we wondered whether the miR-200 family acted simply by preventing all differentiation of ES cells. To address this question, we carried out global gene expression analysis of ES cells at day 3, 4, and 5 of differentiation either in the presence or absence of miR-200c/141 expression from day 2. First, the induction of miR-200c and miR-141 did not simply prevent all changes associated with ES cell differentiation. Differentiating ES cells rapidly down-regulate the ES cell markers *Rex1*, *Dppa2*, and *Dppa4*, and the loss of these markers was not altered upon induction of miR-200c/141 (Figure 24A). The pluripotency markers Oct4, Nanog, and Sox2 are also down-regulated during normal ES cell differentiation, but induction of miR-200c and miR-141 led to only a partial loss of these genes (Figure 24B).

Consistent with our findings that miR-200c/141 inhibited Pdgfrα and Flk1 expression (Figure 19B), we found that mesoderm-associated genes were strongly blocked by miR-200c and miR-141. For example, *Er71*, a gene associated with blood and endothelium, and *Tal1* a gene associated with hemogenic endothelium, are normally strongly induced in differentiating ES cells, but their expression was virtually extinguished by miR-200c/141 (Figure 24C). In contrast, genes associated with primitive ectoderm (e.g. *Otx2*, *Fgf5*, and *Zic5*) were maintained by expression of miR-200c/141 (Figure 24D). Interestingly, when we looked for other genes strongly altered upon induction of miR-200c and miR-141, we identified a number of genes that have recently been associated with expression in EpiSCs and ESD-EpiSCs (Figure 24E). For example, *Nodal*, *Claudin6* (*Cldn6*), and *Cerberus 1* (*Cer1*) are genes associated with the EpiSC, and are substantially elevated upon expression of miR-200c/141. As EpiSCs have also been shown to maintain primitive ectoderm markers, these findings are consistent with the notion that maintenance of miR-200c/141 expression causes a failure of cells to progress past the EpiSC stage of ES cell differentiation.

Another feature associated with EpiSCs is in the nature of its morphology during culture. We find that a cell line harboring inducible expression of miR-200c/141 exhibits a phenotype that can be switched upon induction of expression by doxycycline. In the absence of induction, differentiating ES cells in adherent cultures grow as a round cluster of mostly spindle-shaped cells attached to each other. In contrast, induction of miR-200c/141 causes the morphology to switch to a homogenous flattened monolayer of cells tightly bound to the culture substrate (Figure 25A).

To better determine how similar miR200c/141-induced cultures were to EpiSCs, we examined the expression profile of a number of genes characterized as being mouse ES cell-specific, mouse EpiSC-specific, and genes shared between the two subsets (Tesar et al., 2007). In comparing day 5 miR200c/141-induced cultures to undifferentiated ES cells, we see that like EpiSCs, miR200c/141 induced cultures have down-regulated a number of ES cell-specific transcripts while partially maintaining other markers such as *Nanog* and *Nodal*. As seen in EpiSCs, *Cer1*, *Foxa2*, and other targets of nodal/Activin signaling were significantly upregulated (Figure 25B).

Because EpiSCs can be maintained through repeated passages in FGF and activin (in the absence of LIF), we wanted to determine whether *A2.miR200c* doxycycline-treated cells would also share this property with EpiSCs. To test this, we treated *A2.miR200c* ES cells with or without doxycycline from day 0 until day 5 of differentiation (Figure 26). On day 5, we performed a control FACs analysis (Figure 27B), trypsinized embryoid bodies, and transferred cells into FGF + Activin EpiSC culture conditions. Relative to untreated cultures, samples derived from day 5 doxycycline-treated cultures generated over 4-fold more colonies in EpiSC conditions (Figure 27B). In addition to generating more colonies, these colonies were notably larger and had a more flattened, EpiSC-like appearance (Figure 26, column under "Day 10"). Within a few passages, the fewer and smaller colonies derived from day 5 untreated embryoid body cultures differentiated and could not be sustainably cultured. In contrast, the colonies originally derived from day 5 doxycycline-treated cultures continued to grow and maintain EpiSC-like morphology in FGF and activin (Figure 26, column under "Day 55"). After 50 days in EpiSC culture (and nearly 20 passages), we isolated RNA from

these cells to determine whether they maintained markers of pluripotency and EpiSCs. As assessed by qRT-PCR these colonies continued to express pluripotency markers found in both ES cells and EpiSCs (Nanog and Oct4) as well as markers more specific to EpiSCs (FGF5 and Nodal) (Figure 28). The cultures that were consistently maintained in doxycycline had higher expression levels of both pluripotency and EpiSC markers, suggesting that doxycycline-induced miR-200c/141 expression may also assist in maintaining these cells as EpiSCs throughout long-term passaging.

In summary, gene expression and morphology suggest that the maintained expression of miR-200 family microRNAs allows the loss of several ES cell markers, but promotes maintenance of the EpiSC state, where cells fail to differentiate towards subsequent germ layer fates such as mesoderm.

A

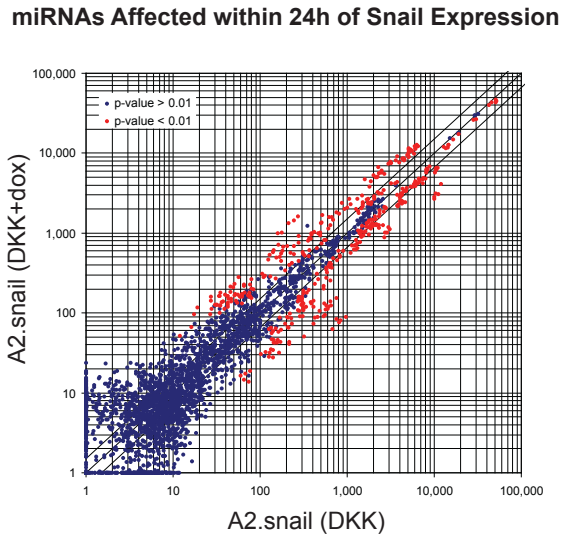

B

EPITHELIAL MAINTENANCE

miRNA	Fold Change
miR-200c	-3.29
miR-200b	-3.06
miR-429	-2.18

PLURIPOTENCY

miRNA	Fold Change
miR-295	-5.22
miR-291a-3p	-3.66
miR-294	-3.65
miR-292-3p	-2.84
miR-291a-5p	-2.06
miR-294*	-1.74
miR-292-5p	-1.51

MESODERM DIFFERENTIATION

miRNA	Fold Change
miR-302b	6.02
miR-302d	3.66

ES CELL/EMBRYO

miRNA	Fold Change
miR-669c	3.17
miR-468	2.85
miR-466h	2.53
miR-466g	2.52
miR-669f	2.33
miR-466f	2.27
miR-466f-3p	2.17
miR-466i	2.07
miR-467f	1.89

Figure 16: Snail alters the expression of several microRNA families within 24 hours. (A) Plotted are relative expression of 627 microRNAs in DKK and DKK+dox conditions on day 3 of *A2.Snail* ESC differentiation as described in Fig. 9A. Red dots represent microRNAs which were considered to be differentially expressed in the two samples with a p-value <0.01. (B) Table of microRNA families significantly altered within 24 hours of Snail expression. MicroRNAs in bold have been validated by an additional microRNA chip (biological replicate) and/or TaqMan microRNA q-PCR assays.

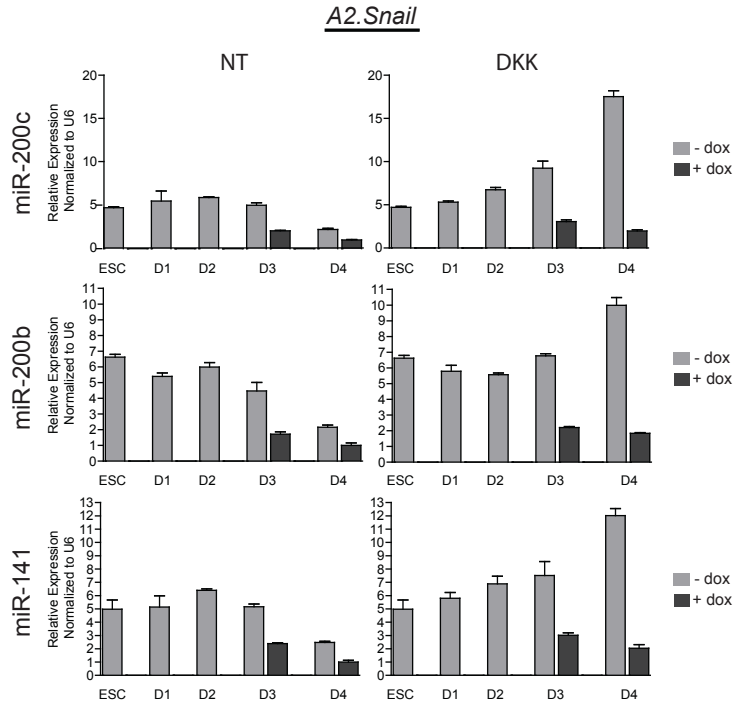

Figure 17: Snail represses expression of the miR-200 family. Real-time PCR of selected microRNAs using TaqMan microRNA assays. RNA samples were collected daily from ES cells differentiated as described in Fig. 9A. Doxycycline treatment is indicated by light gray bars (no dox) and dark gray bars (dox). Samples were normalized to U6 snRNA. Expression for each microRNA is shown relative to the condition with the lowest microRNA expression (D4 NT+dox), which was set at 1.

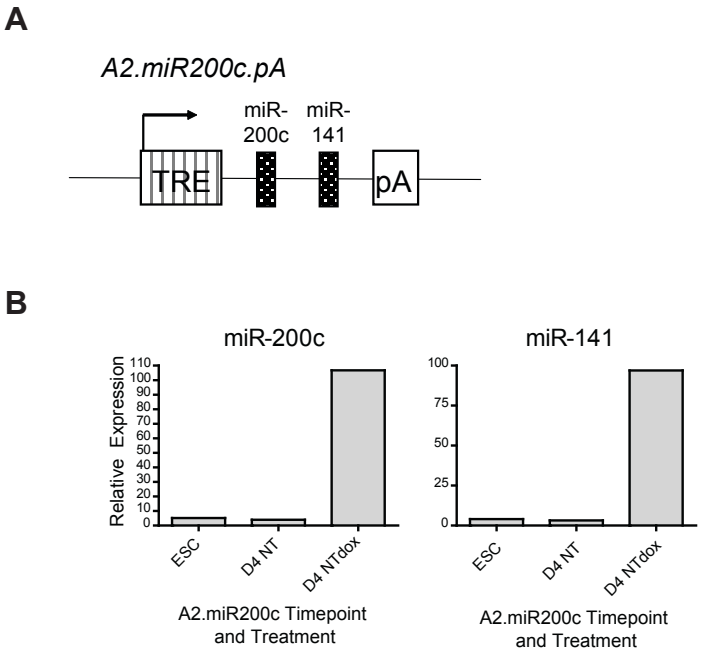

Figure 18: Generation of *A2.miR200c* cell line. (A) Diagram of the tetracycline-inducible locus for the *A2.miR200c* ES cell line. (B) TaqMan microRNA assays were performed for the indicated microRNAs in *A2.miR200c* lines as undifferentiated ES cells or after 4 days of differentiation +/- doxycycline addition at day 2**.**

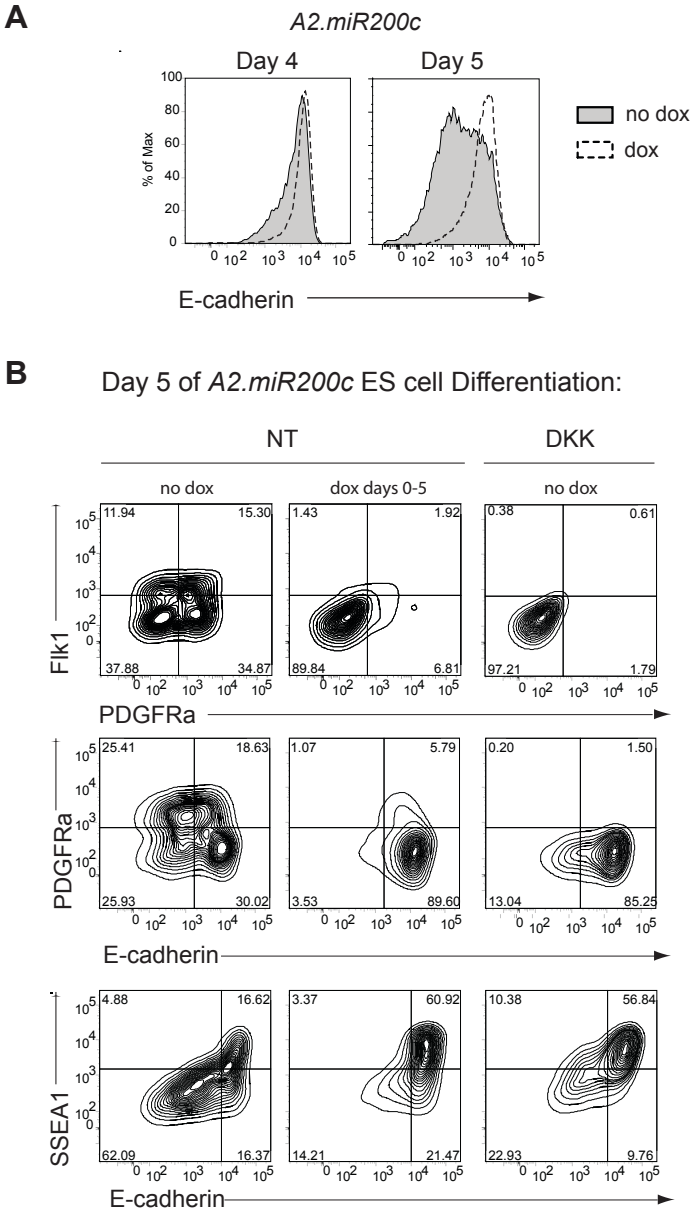

Figure 19: Expression of miR-200c/141 prevents EMT, differentiation, and mesoderm commitment in differentiating ES cells. (A) FACS analysis of E-cadherin on days 4 and 5 of *A2.miR200c* ES cell differentiation as described in Fig. 9A. Shown are conditions with and without the addition of doxycycline. Shown are gated live cells. (B) FACS analysis of Flk1, PDGFRα, E-cadherin, and SSEA1 on day 5 of *A2.miR200c* ES cell differentiation. Doxycycline was added beginning on Day 0 and replenished every other day. Shown are gated live cells.

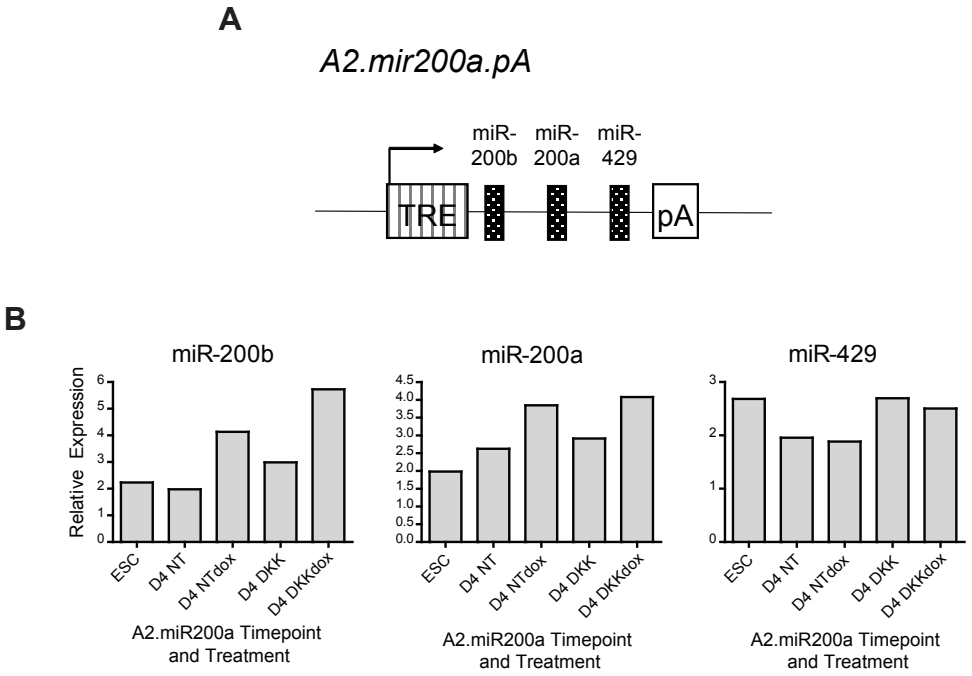

Figure 20: Generation of *A2.miR200a* ES cell line. (A) Schematic of the tetracycline-inducible locus for the *A2.miR200a* cell line. (B) TaqMan microRNA assays were performed for the indicated microRNAs in *A2.miR200a* lines as undifferentiated ES cells or after 4 days of differentiation +/- doxycycline addition at day 2.

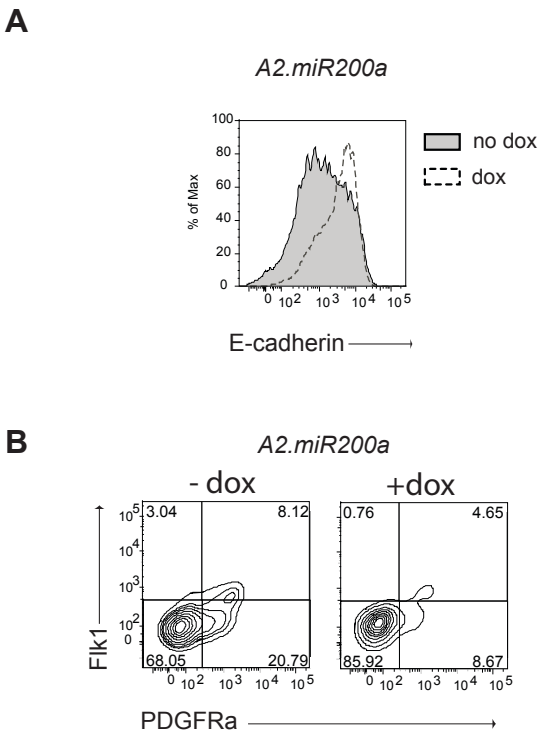

Figure 21: Expression of miR-200b/a/429 prevents EMT and mesoderm differentaition in differentiating ES cells. FACS analysis examining E-cadherin (A), Flk1 (B), and Pdgfrα (B) on day 5 of *A2.miR200a* ES cells differentiated in normal conditions +/- doxycycline addition on day 2 (and replenished on day 4). Shown are gated live cells.

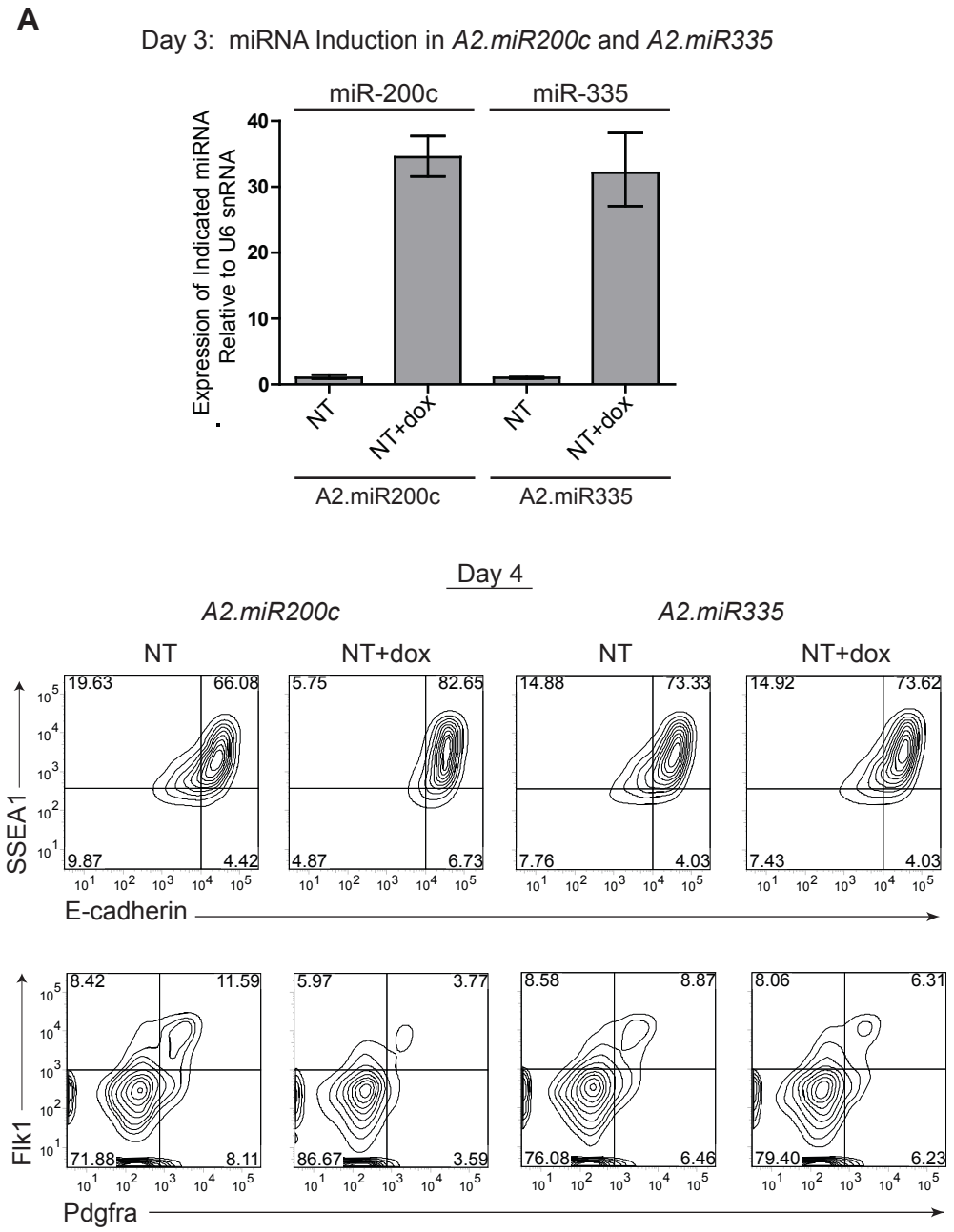

Figure 22: Expression of a different microRNA, miR-335 does not inhibit EMT or mesoderm commitment. (A) TaqMan microRNA assays were performed to detect levels of miR-200c (*A2.miR200c*) or miR-335 (*A2.miR335*) on day 3 of ES cell differentiation. Doxycycline was added at day 2 and RNA was collected on day 3. Expression levels were normalized to U6 snRNA levels. (B) FACS plots examining SSEA1/E-cadherin and Flk1/PDGFRα on day 4 of *A2.miR200c* and *A2.miR335* differentiation, with or without doxycycline addition on day 2.

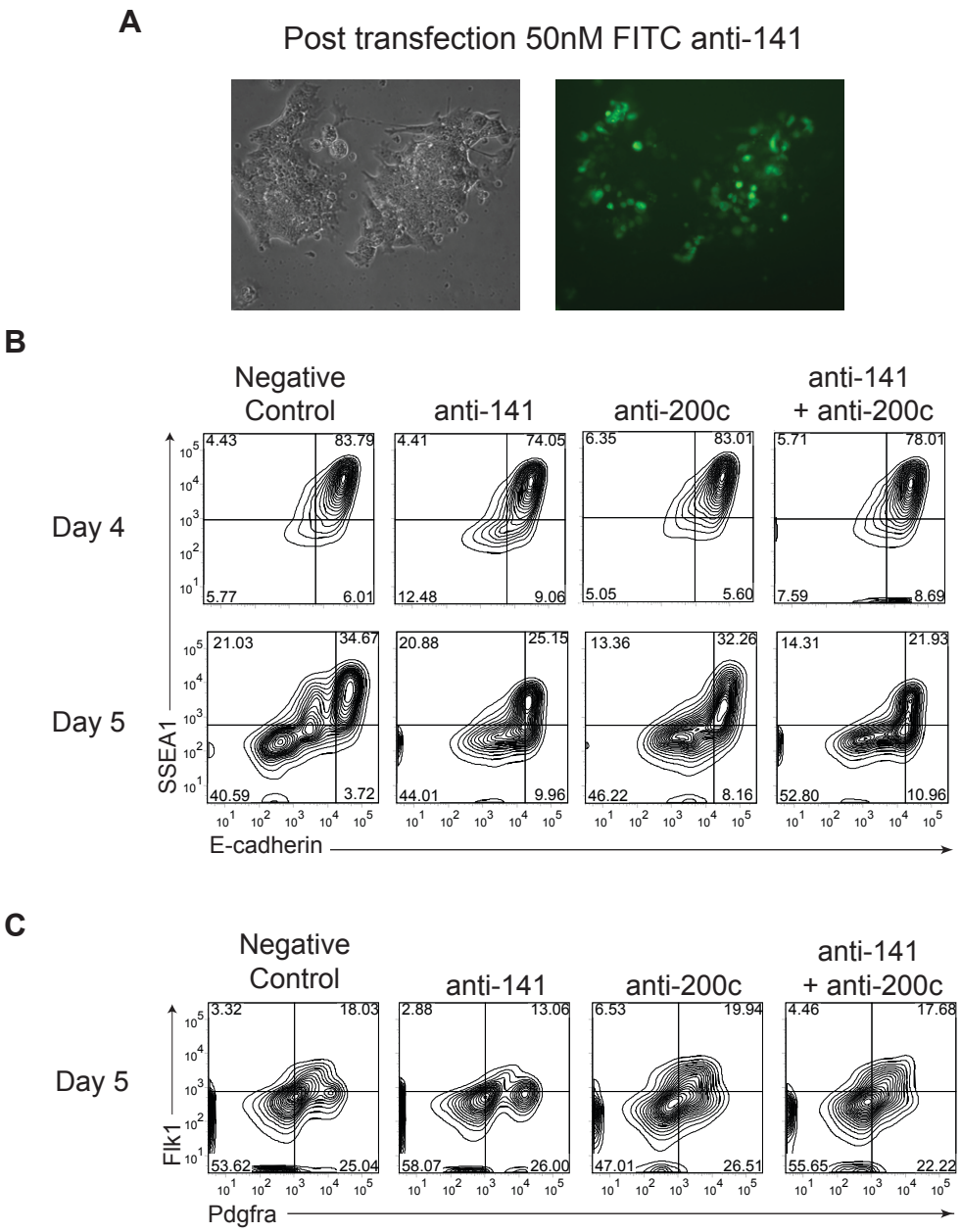

Figure 23: Inhibition of miR-200c/141 leads to modest induction of MET and differentiation, but not mesoderm commitment. (A) Representative image of *A2lox* ES cells 24 hours after transfection with 50nM of FITC-labeled miRCURY LNA miR-141 Power Inhibitor. (B) FACS plots of SSEA1 and E-cadherin on day 4 and 5 of differentiation of *A2lox* ES cells transfected with the indicated miRCURY LNA Power Inhibitors. (C) FACS plots of Flk1 and PDGFRα on day 5 of differentiation of *A2lox* ES cells described in (B).

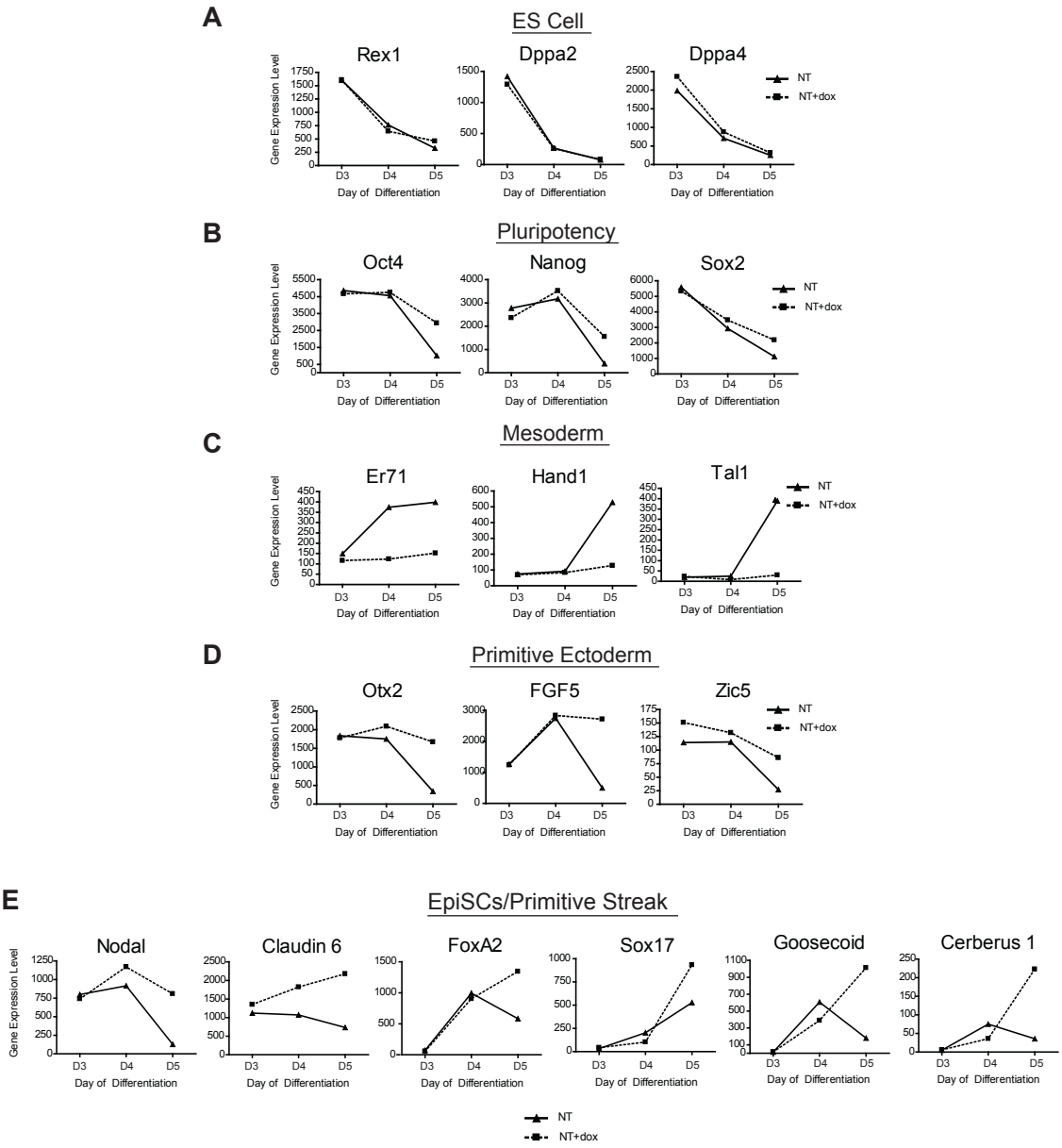

Figure 24: Gene expression profile of *A2.miR200c* ES cell differentiation with and without doxycycline. Relative gene expression in *A2.miR200c* ES cells differentiated in the absence or presence of doxycycline from day 2 and replenished on day 4. RNA was collected on day 3, 4, and 5 of ESC differentiation for microarray analysis. Raw data can be found in the NCBI GEO database under accession number GSE24289. (A-E) Shown are relative gene expression levels of the indicated ES cell markers over the timecourse of *A2.miR200c* differentiation with (dashed line) and without (filled line) doxycycline. Relative gene expression levels of markers of ES cells (A), pluripotency (B), mesoderm (C), primitive ectoderm (D), and EpiSCs/primitive streak (E).

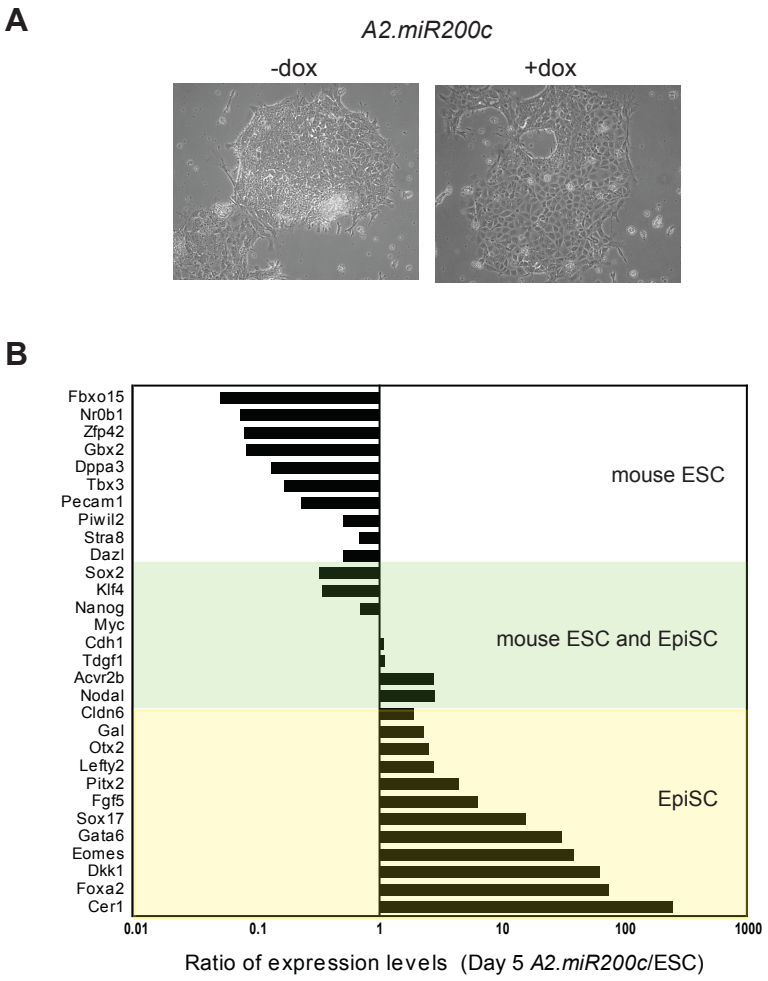

Figure 25: Maintenance of miR-200 expression generates cells with an EpiSC transcriptional profile. (A) Light microscopy of day 3.5 adherent ES cell differentiation of *A2.miR200c* cells with and without doxycycline addition on day 2. (B) Microarray data from day 5 *A2.miR200c* ES cells treated with doxycycline were normalized to MC50 ES cell microarray expression data. Ratios of selected genes were plotted on a log scale.

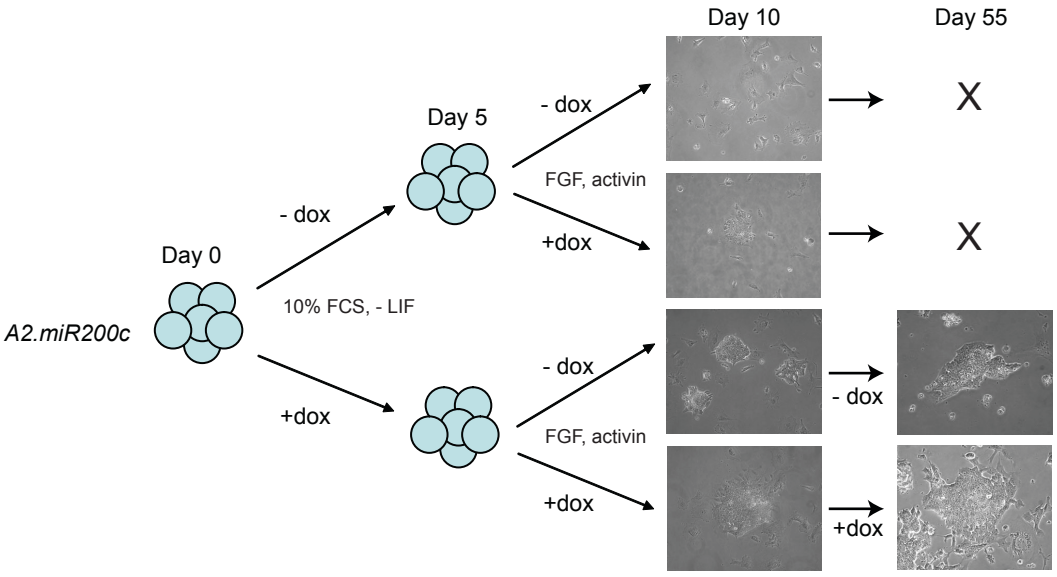

Figure 26: Experimental setup for generation of ESD-EpiSCs. Diagram of the setup of ES-cell derived EpiSC cultures from *A2.miR200c* cells. *A2.miR200c* cells were differentiated as embryoid bodies in 10% fetal calf serum in the absence of LIF for 5 days in the presence or absence of doxycycline. On day 5, embryoid bodies were trypsinized and plated in EpiSC culture conditions, with or without doxycycline (see Methods for details). Prior to passaging on day 10, colonies were counted in the various culture conditions. *A2.miR200c* cells that were not treated with doxycyline from days 0-5 failed to survive and proliferate more than a few passages. *A2.miR200c* cells that were treated with doxycycline from days 0-5 were passaged and maintained for an additional 45 days as ES-derived EpiSCs (for 50 days total), when they were harvested for RNA.

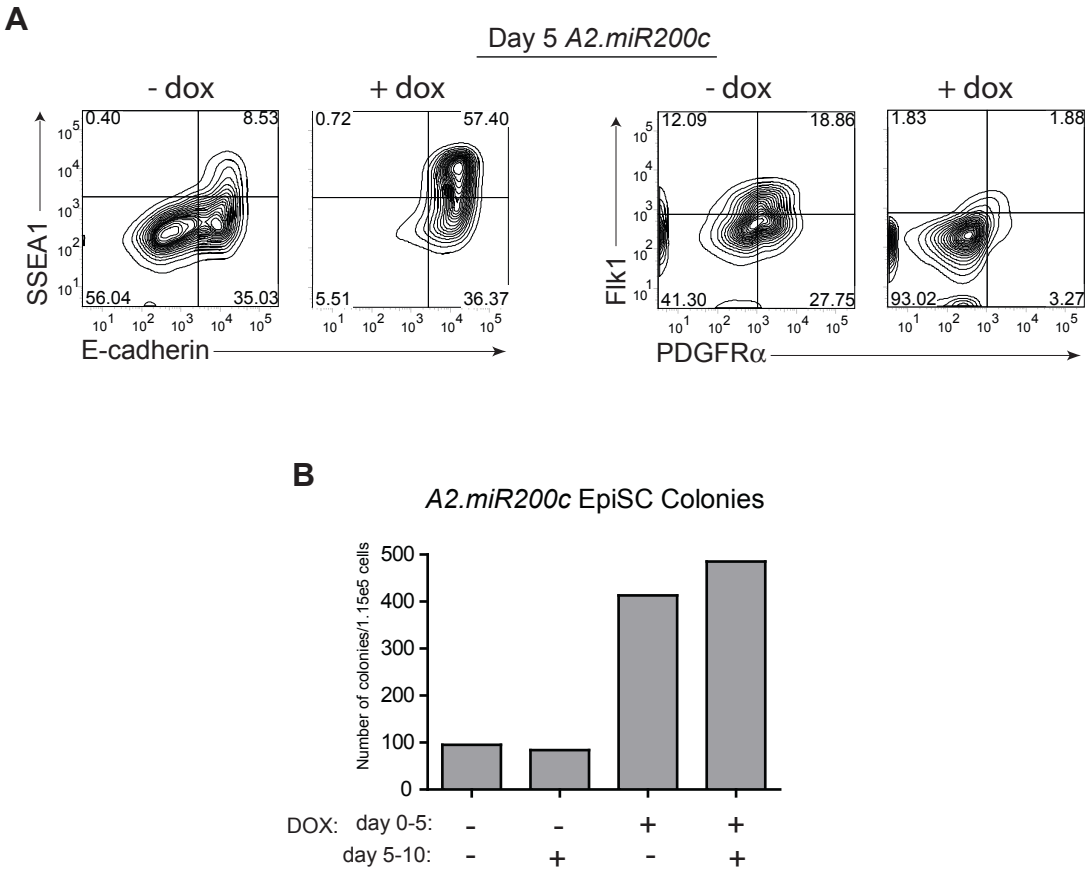

Figure 27: Generation of ESD-EpiSCs from *A2.miR200c* cells treated with and without doxycycline. (A) FACS for E-cadherin/SSEA1 and Flk1/PDGFRα expression on day 5 *A2.miR200c* cells treated with or without doxycycline (prior to plating in EpiSC conditions). (B) Day 5 *A2.miR200c* ES cells from (A) were trypsinized and replated in EpiSC culture conditions (see Methods and Fig. 26 for further details), with and without doxycycline maintenance. On day 10, the number of colonies per well were counted and documented.

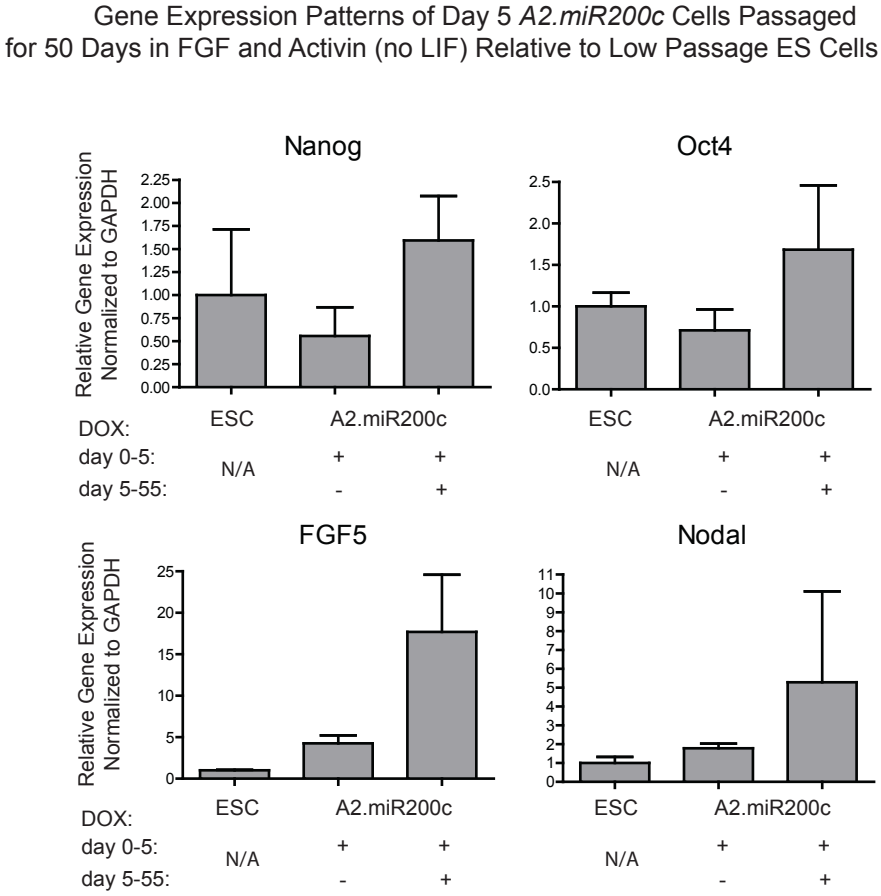

Figure 28: qRT-PCR of ES and EpiSC markers in ESD-EpiSCs passaged for 50 days. q-RT-PCR of Nanog, Oct4, FGF5, and Nodal in *A2.miR200c* ES-derived EpiSCs 50 days after passaging in FGF and activin. RNA from normal, low-passage ES cells grown in LIF was used to determine relative amounts of the indicated markers. All expression values were normalized to GAPDH.

Table 2: MicroRNA Screen for Snail-Regulated MicroRNAs
RNA samples were isolated on day 3 of ES cell differentiation, 24 hours after Snail induction

		DKK+ Snail	DKK	DKK+Snail/ DKK
Reporter Name	**p-value**	**Mean**	**Mean**	**Fold Change**
mmu-miR-21	1.05E-08	61	678	0.09
mmu-miR-295	4.56E-08	92	480	0.19
mmu-let-7c	5.72E-07	101	510	0.20
mmu-miR-494	1.12E-06	1,073	1,687	0.64
mmu-miR-292-3p	1.23E-06	849	2,409	0.35
mmu-miR-20b	1.40E-06	1,983	3,768	0.53
mmu-miR-106a	2.65E-06	1,937	3,563	0.54
mmu-miR-1187	2.99E-06	10,710	5,103	2.10
mmu-miR-293	4.22E-06	5,990	10,014	0.60
mmu-miR-669f	5.60E-06	4,408	1,894	2.33
mmu-miR-302b	6.54E-06	1,056	175	6.02
mmu-miR-574-5p	6.64E-06	11,250	5,323	2.11
mmu-miR-302d	6.98E-06	429	117	3.66
mmu-miR-690	7.01E-06	4,304	6,887	0.62
mmu-miR-574-3p	7.89E-06	6,013	2,328	2.58
mmu-miR-720	7.96E-06	985	1,999	0.49
mmu-miR-182	1.36E-05	558	1,009	0.55
mmu-miR-714	2.26E-05	2,750	3,887	0.71
mmu-miR-483	2.32E-05	682	296	2.30
mmu-miR-294	3.18E-05	2,809	10,250	0.27
mmu-miR-25	3.23E-05	827	1,349	0.61
mmu-miR-466f-3p	4.48E-05	8,627	3,981	2.17
mmu-miR-466i	4.88E-05	7,485	3,624	2.07
mmu-miR-672	5.13E-05	890	444	2.01
mmu-miR-23b	6.30E-05	619	1,022	0.61
mmu-miR-467f	6.84E-05	8,071	4,282	1.89
mmu-miR-466g	7.11E-05	4,255	1,685	2.52
mmu-miR-466f	7.69E-05	1,472	647	2.27
mmu-miR-466h	8.80E-05	411	163	2.53
mmu-miR-329	9.27E-05	1,188	1,788	0.66
mmu-miR-17	9.49E-05	3,669	5,359	0.68
mmu-miR-467a*	1.10E-04	1,474	516	2.86
mmu-miR-466j	1.11E-04	824	309	2.66
mmu-miR-1195	1.16E-04	631	457	1.38
mmu-miR-106b	1.22E-04	432	522	0.83
mmu-miR-18a	1.23E-04	311	505	0.62
mmu-miR-20a	1.25E-04	4,029	5,832	0.69

mmu-miR-134	1.26E-04	1,676	1,107	1.51
mmu-miR-23a	1.34E-04	252	478	0.53
mmu-miR-183	1.42E-04	1,578	2,251	0.70
mmu-miR-191	1.51E-04	336	514	0.66
mmu-let-7a	2.08E-04	148	412	0.36
mmu-miR-411*	4.15E-04	814	1,270	0.64
mmu-miR-290-5p	4.22E-04	6,011	7,782	0.77
mmu-miR-467b*	4.59E-04	2,371	1,069	2.22
mmu-miR-805	5.73E-04	2,120	1,469	1.44
mmu-miR-467g	5.82E-04	587	192	3.06
mmu-miR-292-5p	6.70E-04	2,395	3,623	0.66
mmu-miR-19b	7.91E-04	436	676	0.64
mmu-miR-376b	1.23E-03	1,869	1,414	1.32
mmu-miR-680	1.64E-03	2,635	1,994	1.32
mmu-miR-671-5p	1.79E-03	874	1,047	0.83
mmu-miR-379	2.44E-03	3,387	2,905	1.17
mmu-miR-107	2.47E-03	627	553	1.13
mmu-miR-689	2.81E-03	993	1,422	0.70
mmu-miR-92a	3.87E-03	2,916	3,919	0.74
mmu-miR-16	3.99E-03	1,132	1,502	0.75
mmu-miR-15b	5.21E-03	1,585	1,952	0.81
mmu-miR-130b	6.52E-03	642	561	1.15

The following transcripts are statistically significant but have low signals (signal < 500)

		DKK+ Snail	DKK	DKK+Snail/ DKK
Reporter Name	**p-value**	**Mean**	**Mean**	**Fold Change**
mmu-miR-27b	1.58E-08	89	253	0.35
mmu-miR-200c	3.19E-06	91	301	0.30
mmu-miR-674	4.22E-06	214	101	2.11
mmu-miR-874	6.92E-06	46	176	0.26
mmu-let-7b	9.45E-06	78	357	0.22
mmu-miR-200b	9.62E-06	35	108	0.33
mmu-miR-24	1.04E-05	104	249	0.42
mmu-miR-466d-3p	1.09E-05	133	43	3.12
mmu-miR-489	1.86E-05	63	137	0.46
mmu-let-7i	2.32E-05	41	131	0.31
mmu-let-7f	2.47E-05	83	215	0.39
mmu-miR-199a-3p	3.47E-05	53	95	0.56
mmu-miR-669c	3.99E-05	137	43	3.17
mmu-miR-712	4.49E-05	68	159	0.42
mmu-miR-294*	5.78E-05	60	104	0.57

mmu-miR-291a-5p	5.93E-05	106	218	0.49
mmu-miR-27a	7.37E-05	18	58	0.31
mmu-miR-206	7.65E-05	77	31	2.50
mmu-miR-877*	8.97E-05	129	67	1.91
mmu-miR-691	9.04E-05	136	72	1.91
mmu-miR-297a	1.03E-04	115	48	2.39
mmu-miR-207	1.09E-04	138	71	1.93
mmu-miR-669e	1.30E-04	160	63	2.53
mmu-miR-155	1.33E-04	36	76	0.48
mmu-miR-466f-5p	1.39E-04	164	67	2.45
mmu-miR-669h-3p	1.46E-04	265	71	3.74
mmu-miR-188-5p	2.38E-04	120	35	3.38
mmu-miR-322*	2.80E-04	48	17	2.88
mmu-miR-15a*	2.86E-04	143	66	2.16
mmu-miR-696	2.91E-04	150	77	1.95
mmu-miR-214	3.33E-04	218	154	1.42
mmu-miR-466a-3p	3.37E-04	74	23	3.16
mmu-miR-363	4.04E-04	109	225	0.48
mmu-miR-291a-3p	4.16E-04	21	78	0.27
mmu-miR-125b-5p	4.33E-04	133	194	0.69
mmu-miR-351	4.40E-04	124	38	3.24
mmu-miR-468	5.38E-04	170	59	2.85
mmu-miR-652	5.65E-04	61	35	1.76
mmu-miR-7a	5.92E-04	136	283	0.48
mmu-miR-327	5.98E-04	100	62	1.62
mmu-miR-29a	6.46E-04	45	139	0.32
mmu-miR-346	7.19E-04	419	234	1.79
mmu-miR-143	8.35E-04	25	46	0.53
mmu-miR-195	9.28E-04	172	118	1.46
mmu-miR-411	9.85E-04	121	168	0.72
mmu-let-7d	1.18E-03	74	155	0.48
mmu-miR-467e*	1.22E-03	178	56	3.20
mmu-miR-299*	1.26E-03	131	174	0.75
mmu-miR-669d	1.26E-03	102	39	2.61
mmu-miR-374	1.27E-03	119	226	0.52
mmu-miR-708	1.32E-03	57	79	0.72
mmu-miR-712*	1.41E-03	54	106	0.51
mmu-miR-466b-3-3p	1.55E-03	68	27	2.52
mmu-miR-31	2.30E-03	40	55	0.74
mmu-miR-183*	2.41E-03	53	77	0.69
mmu-miR-301a	2.45E-03	43	61	0.71
mmu-miR-485	2.46E-03	114	84	1.35
mmu-miR-429	2.52E-03	16	34	0.46
mmu-miR-221	2.58E-03	55	75	0.73
mmu-miR-150*	2.75E-03	84	46	1.82

mmu-miR-34c*	2.78E-03	96	59	1.63
mmu-miR-342-5p	3.27E-03	87	48	1.82
mmu-miR-713	3.67E-03	62	32	1.93
mmu-miR-501-3p	4.38E-03	39	23	1.65
mmu-miR-18b	4.43E-03	33	66	0.50
mmu-miR-295*	4.79E-03	53	78	0.68
mmu-miR-674*	5.06E-03	43	30	1.44
mmu-miR-328	5.29E-03	64	44	1.45
mmu-let-7g	6.75E-03	27	48	0.55
mmu-miR-19a	6.76E-03	14	24	0.58
mmu-let-7e	7.17E-03	324	225	1.44
mmu-miR-770-3p	8.17E-03	109	79	1.37
mmu-miR-467h	8.93E-03	61	24	2.55
mmu-miR-125a-5p	9.72E-03	345	236	1.46

CHAPTER 5

Snail, miR-200, and activin cooperate to regulate exit from the EpiSC stage

Inhibition of Activin promotes EMT and down-regulation of the miR-200 family concomitant with neuroectoderm differentiation

EpiSCs and ESD-EpiSCs are maintained through the actions of Activin (Brons et al., 2007; Tesar et al., 2007; Zhang et al., 2010), a TGFβ family member expressed throughout the anterior primitive streak in the developing embryo. It has previously been shown that removal of Activin from ES cell cultures promotes the differentiation of cells toward neuroectodermal lineages (Chambers et al., 2009). However, the role of microRNAs and EMT in this process has not been examined.

We hypothesized that inhibition of Activin with SB-431542, a small molecule inhibitor of ALK-4, -5, and -7, would prevent maintenance of the ESD-EpiSC in differentiating ES cell cultures and therefore lead to EMT and down-regulation of the miR-200 family. When we treated differentiating ES cell cultures with SB-431542 on day 2, we saw down-regulation of E-cadherin as well as SSEA1 in both the presence and absence of DKK (Figure 29, 30). Consistent with SB-431542 promoting neuroectoderm, we see a loss of the early mesoderm markers Flk1 and Pdgfrα (Figure 31).

Along with EMT, inhibition of Activin also led to the down-regulation of miR-200b and miR-141 (Figure 32), consistent with the role of these miRNAs in maintaining cells in an epithelial, EpiSC-like state. Therefore, both Snail and Activin inhibition are capable of inducing EMT and promoting exit from the epiblast as assessed by SSEA1

down-regulation. However, the germ layer induction differs in these two scenarios as Snail promotes mesoderm fates while SB-431542 biases towards neuroectoderm.

Snail and the miR-200 family cooperate with Activin to regulate exit from the ESD-EpiSC state

Because Activin appeared to be important in preventing EMT and differentiation in both NT and DKK-treated cultures, we wanted to know whether the miR-200 family required Activin for maintenance of cells in an SSEA1+/E-cadherin+ ESD-EpiSC state. We therefore examined differentiation of ES cells harboring inducible miR-200c/141 in the presence or absence of SB-431542 from day 2. In the absence of SB-431542, miR-200/141 was capable of retaining cells as E-cadherin+/SSEA1+ (Figure 33, bottom two plots). Importantly, when Activin signaling is inhibited by SB-431542, miR-200 is no longer capable of preventing cells from differentiating or undergoing EMT (Figure 33, 4^{th} and 6^{th} plots). This appears to be in part due to its inability to maintain sufficiently low levels of the transcription factors Zeb1 and Zeb2 (Figure 34). Furthermore, when Activin is inhibited in cultures expressing Snail, more cells undergo EMT and differentiation than in either condition alone (Figure 33, top three plots). Considering the expression pattern of these factors in the gastrulating embryo, a temporal order of migration and differentiation of cells from the epiblast through the primitive streak is apparent. Snail is expressed at highest levels in the posterior primitive streak, while nodal/Activin signaling is highest in the anterior streak. Our finding that miR-200 is excluded from mesoderm in differentiating ES cells corresponds with expression data in the chick (Darnell et al., 2006), indicating that miR-200 has an inverse expression pattern to Snail and is

correlated with Activin expression in the gastrulating embryo. By modulating expression levels of Snail, Activin, and miR-200, we are able to control the order in which cells undergo EMT and transition out of the ESD-EpiSC state. These findings correlate with the mouse embryo where cells of the posterior streak are the first to migrate, followed by a subsequent cascade of migration by cells positioned more anteriorly.

Taken together, we find that Snail, Activin, and the miR-200 family cooperate to regulate epiblast differentiation and progression through EMT and germ layer fate commitment (Figure 35).

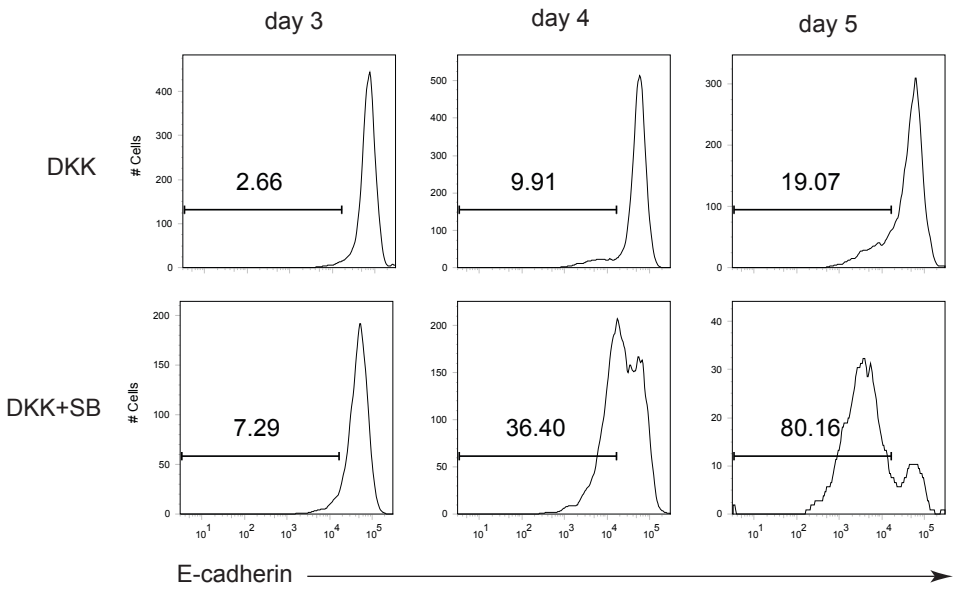

Figure 29: Inhibition of activin signaling promotes EMT in differentiating ES cells. *A2.Snail* ES cells were differentiated as described in Fig. 9A in the presence of DKK with or without the addition of 10μM SB-431542 on day 2. Live cells were gated and a histogram of E-cadherin expression on day 3, 4, and 5 of differentiation was plotted.

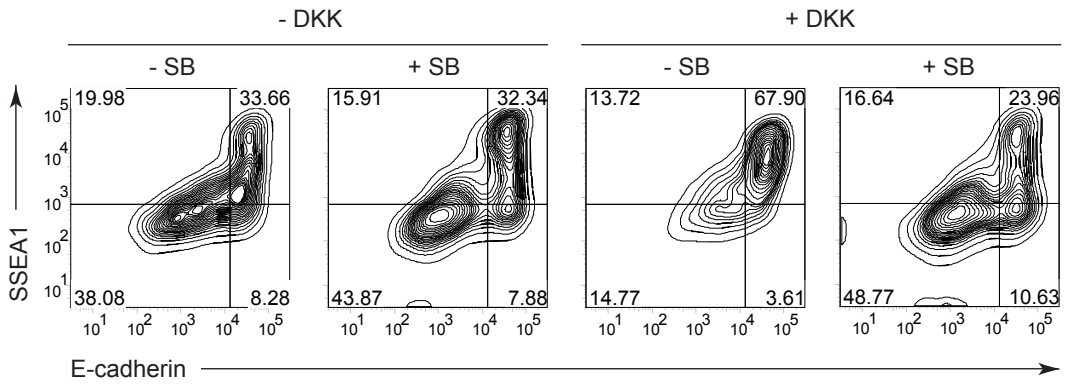

Figure 30: Inhibition of activin signalnig promotes down-regulation of SSEA1. FACS plots illustrating E-cadherin and SSEA1 expression on day 5 of ES cell differentiation as described in Fig. 29.

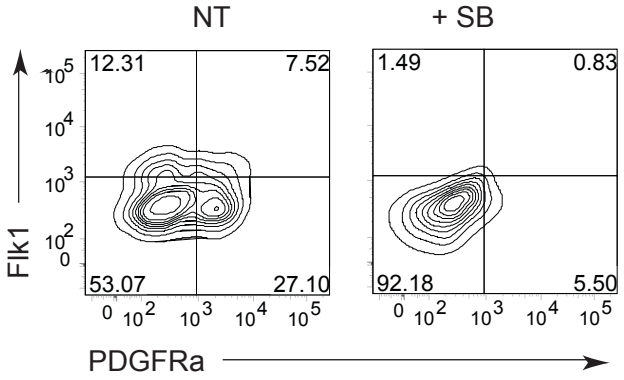

Figure 31: Activin signaling is required for the formation of mesoderm. FACS plots of Flk1-PE and PDGFRα-APC in day 5 ES cells treated with or without 10μM SB-431542 from day 2.

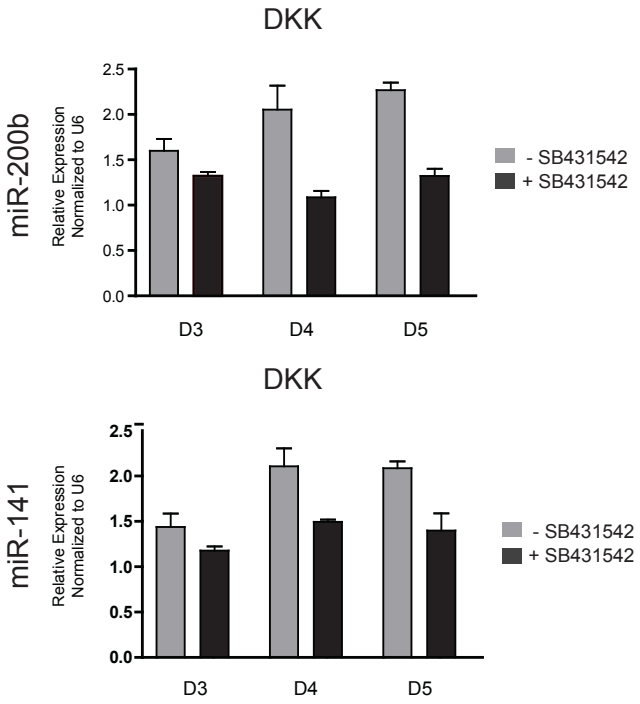

Figure 32: Activin signaling maintains expression of the miR-200 family. Real-time PCR of miR-200b and miR-141 microRNAs using TaqMan microRNA assays. RNA samples were collected daily from ES cells differentiated with DKK from day 0, with or without the addition of SB-431542. Samples were normalized to U6 snRNA.

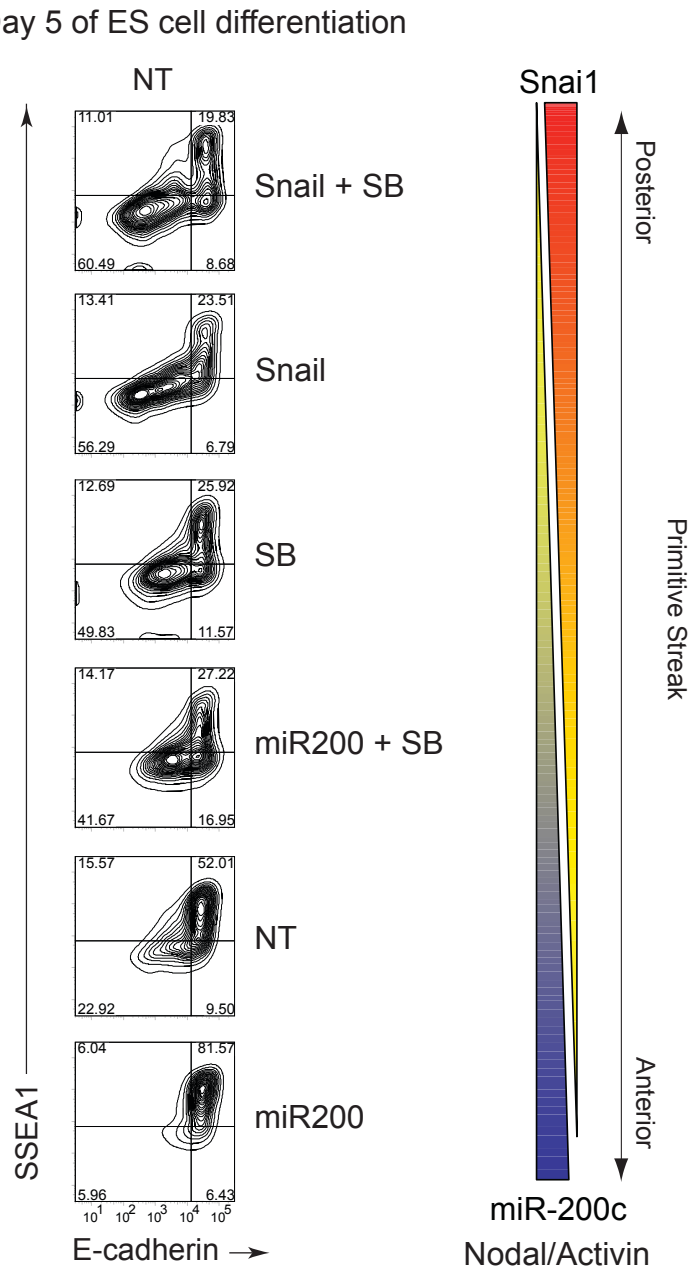

Figure 33: Snail, miR-200, and activin cooperate to regulate exit from the ESD-EpiSC state. *A2.miR200c* and *A2.Snail* cells were differentiated as described in Fig. 9A, with or without the addition of 10μM SB-431542, and with or without doxycycline on day 2 (replenished on day 4 for *A2.miR200c*). Shown is the FACS analysis for SSEA1 and E-cadherin on day 5 of differentiation. Unless indicated by Snail expression, all cell lines shown were *A2.miR200c*.

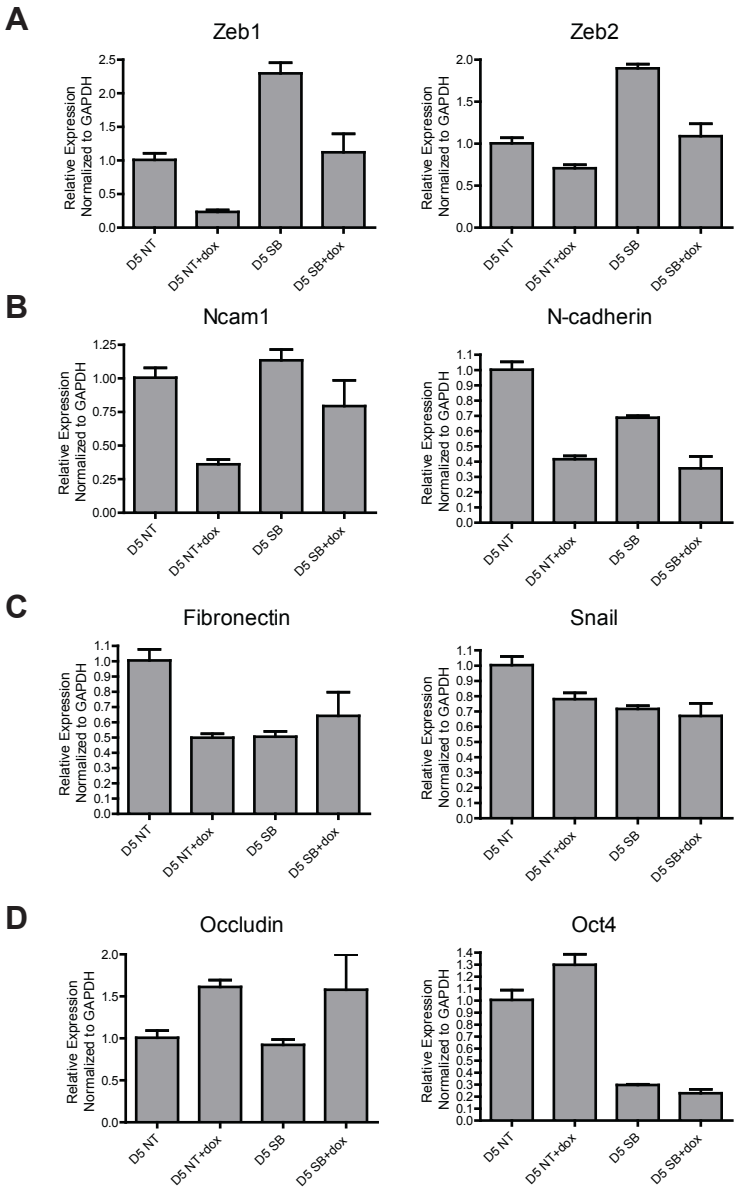

Figure 34: qRT-PCR of EMT and ES cell factors affected by miR-200 and activin activity. *A2.miR200c* ES cells were differentiated as described in Figure 33. RNA was isolated on day 5, and qRT-PCR was performed for the genes indicated. All samples were normalized to GAPDH and expression levels are given relative to day 5 NT condition, set to 1.

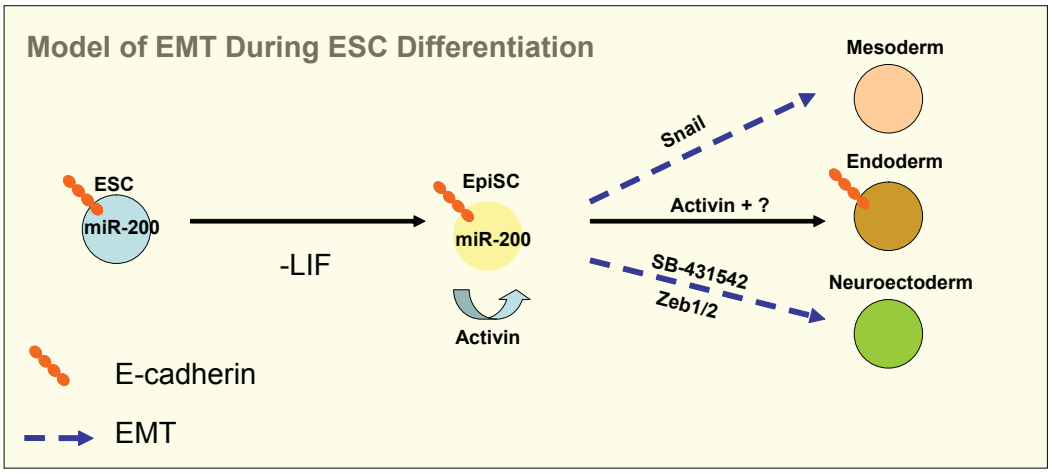

Figure 35: Working model for the role of Snail, miR-200, and activin in ES cell differentiation.

CHAPTER 6

Snail promotes the cell-autonomous generation of Flk1+ endothelial cells through the repression of the miR-200 family

Snail induces a Flk1+PDGFRα- population of endothelial cells independent of primitive streak signaling pathways

Using an ES cell line that inducibly expresses *Snail* upon addition of doxycycline (*A2.Snail*)(Lindsley et al., 2008), we previously found that *Snail* could induce EMT and accelerate mesoderm commitment in differentiating ES cells as assessed by the mesoderm markers Flk1 and PDGFRα (Figure 14). To evaluate how *Snail* induces $Flk1^+$ and $PDGFR\alpha^+$ cell populations, we analyzed the differentiation of *A2.Snail* ES cells while inhibiting Wnt, Activin, and BMP pathways, which are known to regulate primitive streak formation and patterning. Doxycycline-induction of *Snail* on day 1 generated populations expressing PDGFRα and Flk1, corresponding to early paraxial and lateral mesoderm respectively, by day 3 (Figure 36). Interestingly, when BMP, Activin or Wnt pathways were inhibited (by DKK, Noggin, or SB431542 respectively), the $PDGFR\alpha^-$ $Flk1^+$ population was selectively maintained (Figure 36). These results suggested that *Snail* induces the $Flk1^+$ single-positive population independently of cell-extrinsic cues important for primitive streak formation.

Since hemangioblasts express Flk1 and arise early in ES cell differentiation(Choi et al., 1998), we wondered whether *Snail*-induced Flk1+ cells might be progenitors of blood and endothelial lineages. We therefore assessed the Flk1+PDGFRα- cells induced by *Snail* for expression of other markers associated with endothelial and blood

progenitors. VE-cadherin, Tie-2, c-kit, and CD34 were expressed uniformly in the $Flk1^+$ population, similar to the normal population of $Flk1^+$ cells generated by *Snail* in the absence of DKK (Figure 37).

We next asked whether *Snail*-induced $Flk1^+$ cells had the potential to generate blood and endothelial lineages. To assess blood-forming potential, differentiating *A2.Snail* cells from untreated and doxycycline-treated cultures were plated in methylcellulose on day 3. *A2.Er71* cells, harboring a doxycycline-inducible transcription factor *Er71* that robustly induces hemangioblast differentiation(Lee et al., 2008), was used as a positive control. *Er71* strongly induced blast colonies as expected, but *Snail* was at least 100-fold less efficient in inducing blast colonies under all conditions (Figure 38A). Similar results were seen in additional hemangioblast assays (Figure 38B, bottom panel, and data not shown). No improvement in *Snail*'s ability to induce either primitive or definitive colonies was found by plating cells from day 6 (data not shown). In summary, *Snail* induces a $Flk1^+$ population that lacks significant potential to form blood lineages.

To examine the endothelial potential of *A2.Snail* cells, differentiating *A2.Snail* and *A2.Er71* cells were treated with or without doxycycline on day 1 and on day 3 were trypsinized and replated on Matrigel in the presence of VEGF. After 24 hours, doxycycline-treated *A2.Snail* cells formed networks of cells with a tubular, sprouting morphology characteristic of endothelial cell cultures (Figure 39), whereas untreated *A2.Snail* cells lacked these features, appearing instead as typical embryoid bodies. *A2.Snail* cells treated with DKK and *A2.Er71* cells showed similar morphological findings depending on the presence or absence of doxycycline (Figure 39).

Snail's induction of Flk1+ cells is cell-autonomous

Because *Snail* induced this endothelial-like Flk1^{+} population independently of BMP, Activin, and Wnt signaling, we asked whether it occurred by a cell-intrinsic or cell-extrinsic mechanism. We carried out a series of mixing experiments using various ratios of *A2.Snail* ES cells and *A2.CAG.GFP*, an ES cell line that constitutively expresses the GFP protein (Figure 40A). Without doxycycline treatment, neither cell line expressed significant Flk1 on day 4 at any ratio of cell mixing (Figure 40B, left panels). However, doxycycline treatment caused expression of Flk1 only in *A2.Snail* cells under all mixing ratios, while A2.GFP cells remained negative for Flk1 expression (Figure 40B, right panels). These results indicate that *Snail* promotes Flk1 expression through a cell-intrinsic mechanism.

Snail Flk1+ endothelial progenitors transcriptionally resemble primitive endoderm

Like cells of the embryo's inner cell mass, ES cells are heterogeneous with respect to their commitment to primitive endoderm or the epiblast, a process regulated by the transcription factors GATA6 and Nanog, respectively (Chazaud et al., 2006; Singh et al., 2007) . Conceivably, the mixed Flk1/PDGFRα expression pattern in *Snail*-expressing ES cells might be based upon differential actions of *Snail* in either GATA6-expressing or Nanog-expressing ES cells.

To reveal potential heterogeneity, we used flow cytometry to purify Flk1^{+} high and Flk1^{-} ES cells 24 hrs after induction of *Snail* in the presence or absence of DKK (Figure 41) and compared their transcriptional profiles using gene expression

microarrays. Consistent with our findings above, *Snail*-induced Flk1+ cells expressed numerous factors associated with endothelial progenitors (Figure 41). In addition, known targets of *Snail*, such as *Occludin*, *Claudin 3*, and *Crumbs homolog 3* were markedly inhibited by induction of *Snail* in both $Flk1^+$ and $Flk1^-$ population compared to cells in which *Snail* was not induced, indicating *Snail* was functional in both populations (Figure 42A). In contrast, other genes showed differential expression within these two subsets. In particular, the epiblast-specific genes Nanog and Oct4 were selectively in Flk1- cells (Figure 42B). In contrast, primitive endoderm-related genes such as GATA6, Sox7, and BMP2 were selectively expressed in the Flk1+ subset (Figure 42C). Interestingly, in addition to markers of primitive endoderm, $Flk1^+$ cells also shared a number of markers found to be upregulated in cancer stem cells, including CD105, CD34, CD44, Bmi1, and c-myc (Figure 42D, E). This could suggest that promotion of $Flk1^+$ cells by *Snail* may be mediated by actions selectively within the $GATA6^+$ subset of an initially heterogeneous ES cell population.

FGF receptor signaling is required for the formation of primitive endoderm(Yamanaka et al., 2010) and at least some cancer stem cells(Fillmore et al., 2010). To test if FGF signaling was required for *Snail*-induced Flk1 expression, we used the FGF signaling antagonist SU5402(Sun et al., 1999) . Treatment of ES cells with SU5402 from day 1 reduced the number of Flk1-expressing cells by approximately 3-fold (Figure 43A), and blocked *Snail*'s ability to down-regulate E-cadherin expression (Figure 43B). Consistent with these findings, FGFR1 knockout mice have defective *Snail* function and expression(Ciruna and Rossant, 2001), which suggests that the SU5402 findings are specific to FGF and not simply due to antagonizing Flk1 signaling itself.

Snail's induction of Flk1+ endothelial progenitors is indirect

Snail is thought to act primarily as a transcriptional repressor through its N-terminal SNAG domain(Grimes et al., 1996), and yet appeared to be promoting increased Flk1 expression. To test if Flk1 induction required the SNAG domain, we created the *A2.ΔSNAG.Snail* cell line, in which the SNAG repressor domain has been removed from the inducible *Snail* protein. As a control, we confirmed that deletion of this domain blocks *Snail*'s ability to inhibit expression of E-cadherin (Figure 44A, B), a known direct transcriptional target of *Snail*(Cano et al., 2000). In addition, this deletion also prevented the induction of Flk1 expression induced by *Snail* in differentiating ES cells (Figure 45A). A gene chip analysis of this cell line 24 hours after doxycycline addition confirmed that *ΔSNAG.Snail* was unable to repress epithelial or neuroectoderm markers (compared to wildtype Snail), nor was it able to induce mesenchymal or vascular mesoderm markers (Figure 45B). This result indicates that *Snail*'s induction of Flk1 is indirect, and may be mediated through *Snail* repressing a repressor of Flk1 expression.

The miR-200 family directly targets Flk1 and Ets1 3' UTRs

We previously found several miRNAs, including the miR-200b/c/429 family, that are inhibited by *Snail* during ES cell differentiation. We therefore wondered if *Snail*'s generation of $Flk1^+$ cells was mediated by repression of miRNAs that may repress Flk1 or other factors important for endothelial differentiation. Interestingly, we found that Flk1 itself is predicted to be a target of the miR-200b/c/429 family (Figure 46A). Consistent with this prediction, the induction of miR-200c in A2.miR200c/141 ES cells

reduces *Flk1* mRNA and protein expression (Figure 46B, 19B). This regulation of *Flk1* expression maps to the 3' UTR of the *Flk1* transcript, which contains a predicted miR-200c target at position 959 (Figure 46A). To test whether miR-200c directly targets *Flk1*, we generated luciferase reporter constructs containing a CMV-driven luciferase transcript upstream of the *Flk1* 3' UTR. We transfected these constructs into 293T cells with or without a miR-200c mimic. We found that miR-200c selectively repressed luciferase activity in constructs containing the native *Flk1* 3' UTR by 50%, but failed to reduce activity of a luciferase construct in which the target sequence at position 959-965 was scrambled (Figure 46C). Thus, miR-200c appears to directly down-regulate *Flk1* expression through the targeting of the *Flk1* 3' UTR.

We noted that two other genes *Ets1* and *Gata2*, which are known to be important in vasculogenesis(Lugus et al., 2007; Wei et al., 2009), were also induced by *Snail* (Figure 41). Interestingly, both *Ets1* and *Gata2* also contained predicted target sequences for miR-200c in their 3' UTR (Figure 47A, 48A). Similar to *Flk1*, *Ets1* and *Gata2* transcripts were both repressed by doxycycline induction of miR-200c/141in A2.miR200c/141 ES cells (Figure 47B, 48B). To test whether miR-200c directly targeted *Ets1* and *Gata2* 3' UTRs, we generated additional CMV-luciferase reporter constructs upstream of *Ets1* and *Gata2* 3' UTRs. Our data (Figure 47C) confirmed that the *Ets1* 3' UTR is responsive to miR-200c, as demonstrated by reduced luciferase activity in the presence of miR-200c, as recently reported(Chan et al., 2011). We further identified the location of these responsive sites to be at positions 574, 625, and 633 in the *Ets1* 3' UTR transcript. In contrast, miR-200c did not appear to directly repress the *Gata2* 3' UTR (Figure 48C). In addition to *Flk1* and *Ets1*, *Snail* strongly induced

expression of *Flt1* as well as *Neuropilin* 1 **(**Figure 41). Notably, these genes are also known to be targets of miR-200(Lin et al., 2009; Roybal et al., 2011). Together, these data support the hypothesis that miR-200 family microRNAs directly repress the level of several genes important or required for early vasculogenesis.

Snail requires the down-regulation of the miR-200 family to induce Flk1+ cells

To determine if repression of miR-200c/141 is required for *Snail*'s enhancement of Flk1 in differentiating ES cells, we generated *A2.Snail.miR200c* ES cell lines expressing doxycycline-inducible *Snail*, but constitutive expression of miR-200c/141 under the control of the chicken β-actin promoter (Figure 49A, B, C). We carried out a dose-response for doxycycline and examined the induction of Flk1 in these cell lines using flow cytometry (Figure 50). Without expression of miR-200c and miR-141, half-maximal induction of Flk1 occurred at 25ng/ml doxycycline, and maximal Flk1 was achieved at 100ng/ml (Figure 50, top row). In *A2.Snail.miR200c* cells constitutively expressing miR-200c and miR-141, there was a significant inhibition of Flk1 induction throughout the dose range of doxycycline (Figure 50, bottom row). Constitutive expression of miR-200a/b/429 family members in an additionally generated *A2.Snail.miR200a* line also reduced Flk1 induction in response to doxycycline, although not as strongly as seen with miR-200c and miR-141 (Figure 50, middle row**)**. Western analysis of protein expression verified that induction of *Snail* was similar across these cell lines (Figure 51B). Notably, *Snail*'s ability to down-regulate E-cadherin was compromised in the cell lines constitutively expressing the miR-200 family (Figure 51A). Since the miR-200 family directly targets Zeb1 and Zeb2 expression(Park et al., 2008),

this may suggest that *Snail* requires their function for efficient E-cadherin down-regulation. Overall, these data show that induction of Flk1 cells by *Snail* requires the down-regulation of the miR-200 family, which directly target the 3' UTRs of Flk1 itself, Ets1, and additional factors important in vasculogenesis.

(Acknowledgements: E.M. Langer performed the Flk1+ sort and gene chip; she also generated the pMir-Luciferase constructs for the endogenous Flk1 and Ets1 3' UTRs)

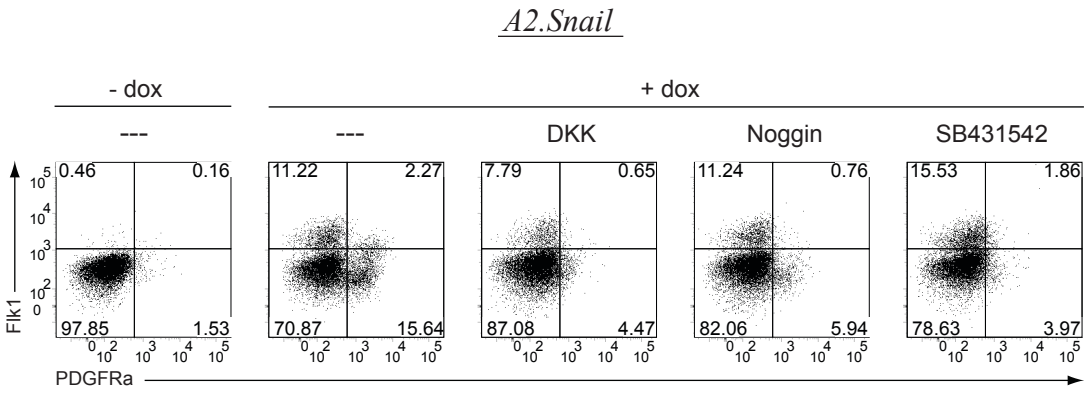

Figure 36: Snail induces a Flk1+PDGFRα- population independent of Wnt, BMP, and activin signaling. *A2.Snail* cells were differentiated with or without the addition of doxycycline and the indicated inhibitors on day 1 of differentiation. Shown is a FACS analysis for Flk1 and PDGFRα on day 3 of differentiation, where plots are gated on live cells.

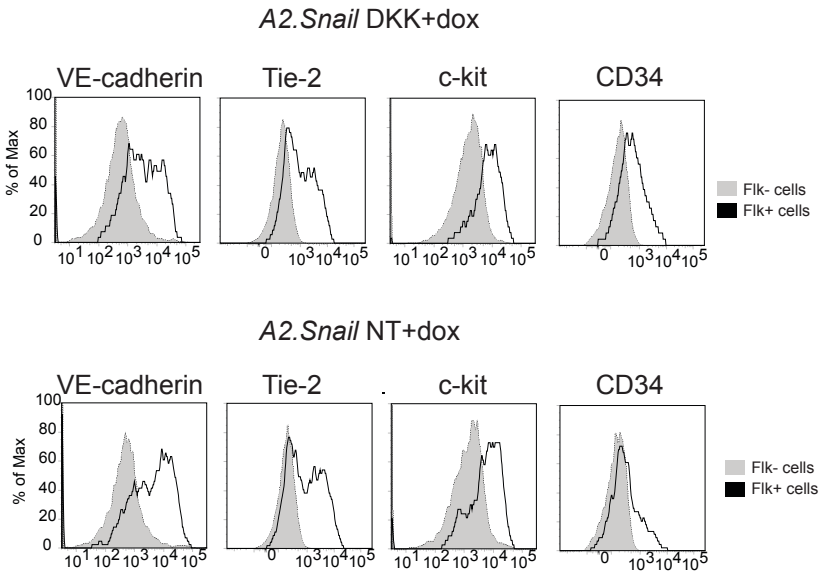

Figure 37: Snail-induced Flk1+ cells express hemangioblast markers. *A2.Snail* cells were differentiated and analyzed by FACS on day 3 of differentiation in the presence or absence of DKK +/- doxycycline on day 1. Histograms for VE-cadherin, Tie-2, c-kit, and CD34 are shown for Flk1+ and Flk1- gated populations.

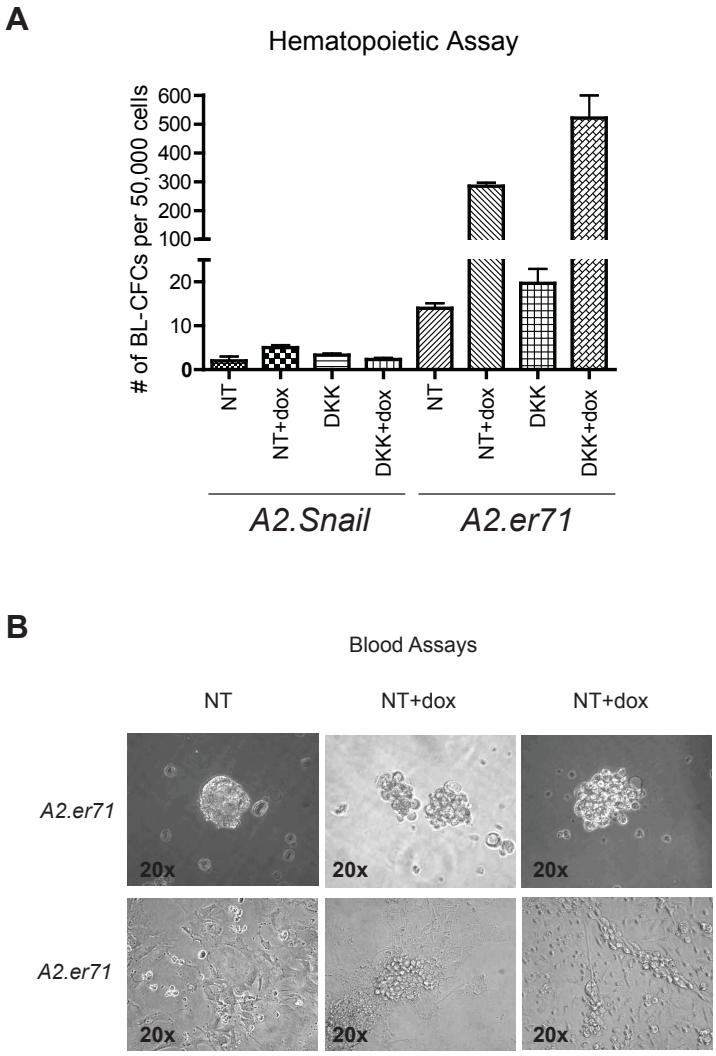

Figure 38: Snail does not promote hematopoietic or hemangioblast differentiation. (A) *A2.Snail* and *A2.Er71* cells were differentiated in the presence or absence of DKK with doxycycline addition on day 1. On day 3, cells were trypsinized and plated in triplicate methylcellulose dishes with defined cytokines. On day 8, BL-CFC colonies were counted for all conditions. Shown is the average # of BL-CFCs counted per 50,000 cells plated. (B) *A2.Er71* cells were differentiated with or without doxycycline addition on day 1. On day 3, cells were trypsinized and plated in triplicate methylcellulose dishes with defined cytokines for primitive and definitive hematopoiesis (top panel; quantitated in (A)) or hemangioblast formation (bottom panel). Shown are representative images for typical cell clusters of each condition. Snail showed only rare hemangioblast colonies in these assays that were of a similar frequency to control (see (A)).

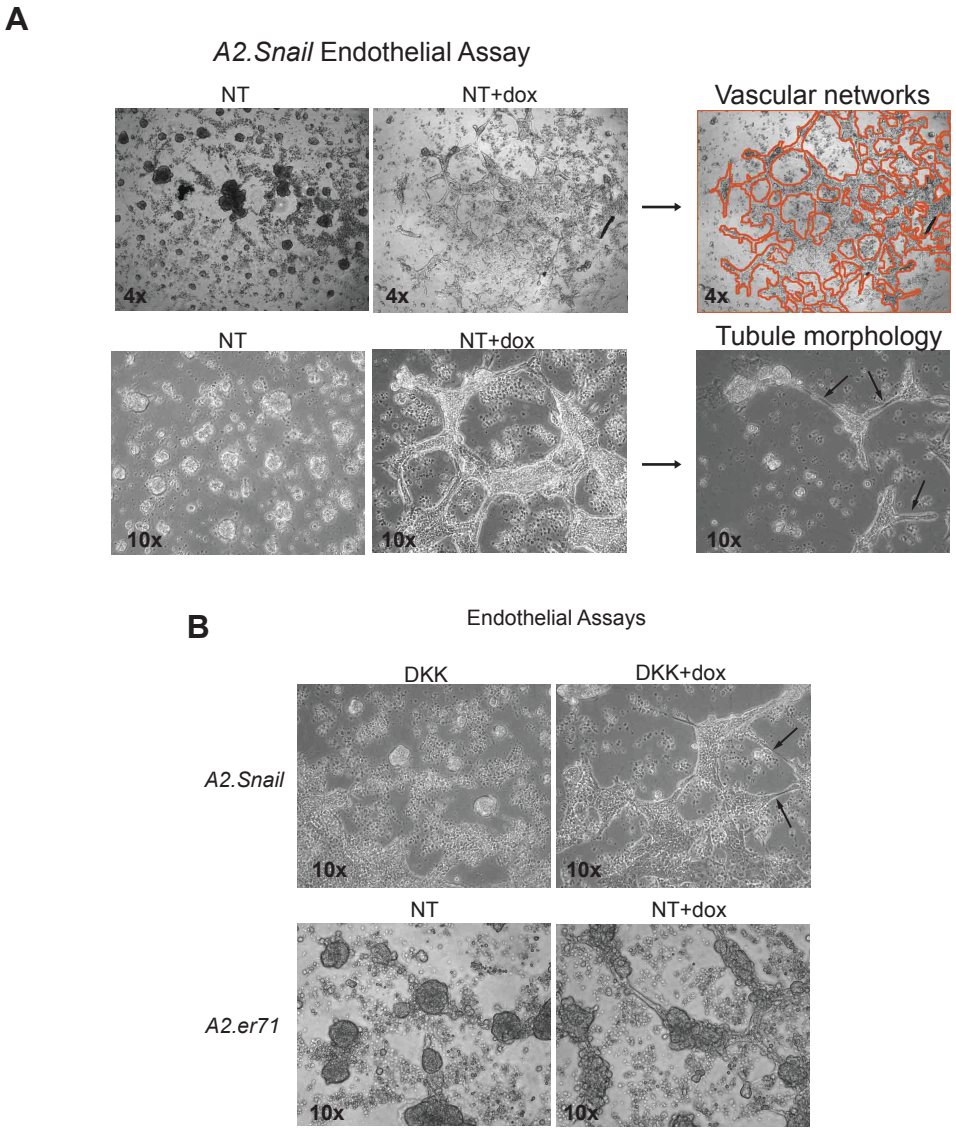

Figure 39: Snail promotes endothelial-like differentiation in a subset of differentiating ES cells. (A) Embryoid bodies from day 3 *A2.Snail* differentiation cultures (Fig. 38) were trypsinized and replated in Matrigel-coated 24-well plates with VEGF. On day 4, cultures were examined for the formation of networks and tubules. Red lines help delineate the outline of the vascular network while arrows show examples of tubules. (B) Embryoid bodies from day 3 *A2.Snail* and *A2.Er71* differentiation cultures were trypsinized and replated in Matrigel-coated 24-well plates with VEGF. On day 4, cultures were examined for the formation of networks and tubules.

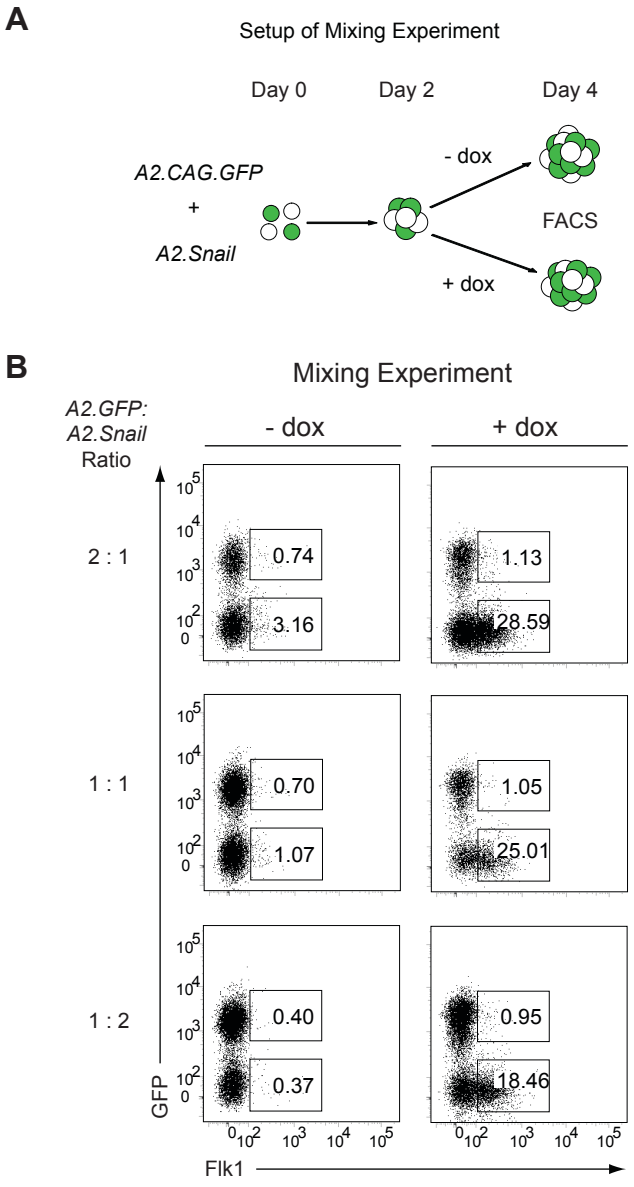

Figure 40: Snail's promotion of Flk1+ cells is cell-autonomous. (A) Diagram of mixing experiment setup. (B) *A2.CAG.GFP* and *A2.Snail* ES cells were mixed in ratios of 2:1, 1:1, and 1:2 at the onset of differentiation. Doxycycline was added on day 2 of differentiation and FACS analysis was performed on day 4. Shown is a FACS plot of live cells, examining GFP expression as well as Flk1.

A

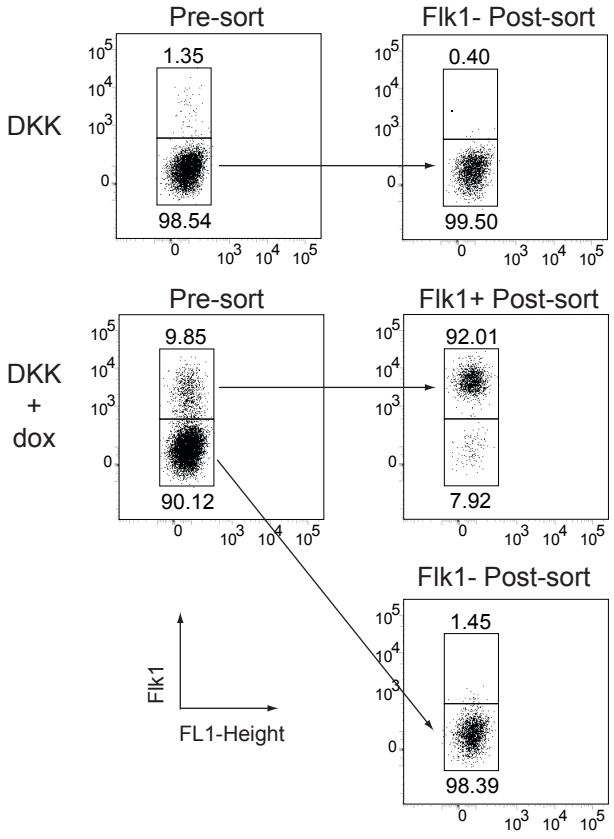

B

Gene	Flk1+/Flk1- Fold Induction
Igf1	294
Gata2	90
Lhx1	85
Neuropilin 2	77
Flk1	40
Sox18	36
Flt1	34
Lmo2	25
Fli1	24
Sox17	15
Tal1	14
VE-cadherin	13
Tie2	11
Neuropilin 1	11
Ets1	10
CD34	10
c-kit	6
Er71	3

Figure 41: Snail-induced Flk1+ cells express high levels of factors important for vasculogenesis. (A) *A2.Snail* cells were differentiated in DKK, with or without the addition of doxycycline on day 2. On day 3, Flk1+ high and Flk1- cells were sorted and RNA was isolated from each population. Total RNA was then submitted for gene chip analysis to characterize the separate populations. (B) Selected list of highly induced vascular genes induced in Flk1+ cells 24 hours after Snail induction.

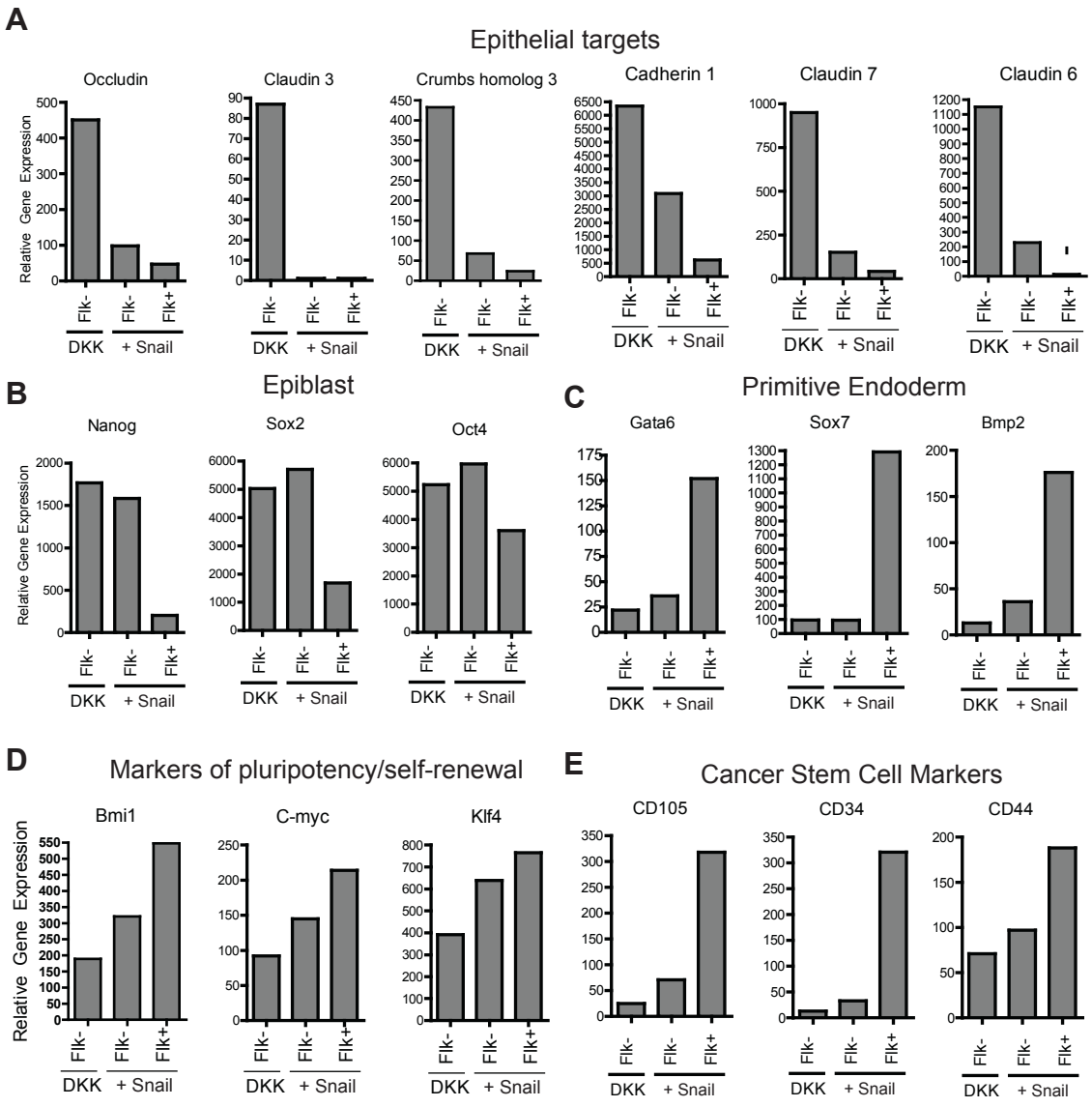

Figure 42: Snail Flk1+ cells appear to be derived from a primitive endoderm subset of ES cells and share common markers with cancer stem cells. Gene chip analysis described in Fig. 41. Relative gene expression of epithelial direct targets (A), epiblast markers (B), primitive endoderm (C), pluripotency (D), and cancer stem cell markers in the sorted populations.

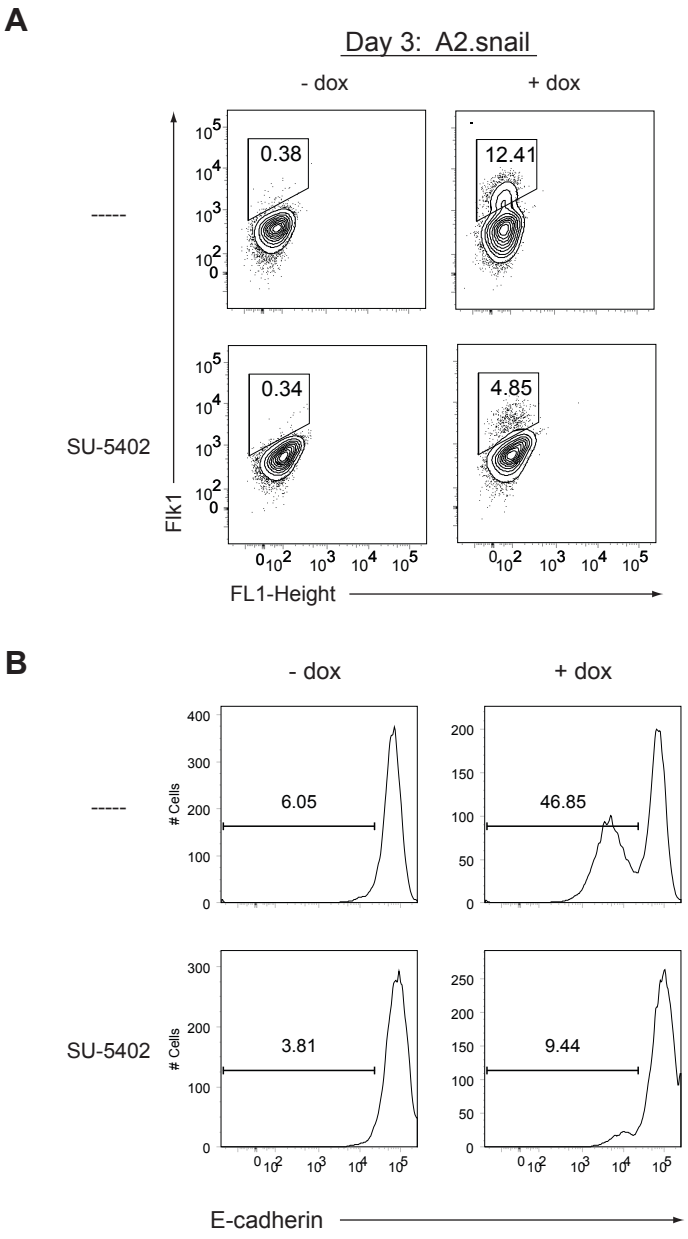

Figure 43: Snail induction of Flk1+ cells and EMT depends on FGF signaling. (A) *A2.Snail* ES cells were differentiated with and without the addition of doxycycline and the FGF-inhibitor SU-5402 on day 1. FACS analysis was performed on day 3 for Flk1. Shown are gated live cells. (B) *A2.Snail* ES cells were differentiated with and without the addition of doxycycline and the FGF-inhibitor SU-5402 on day 1. FACS analysis was performed on day 3 for E-cadherin. Shown are gated live cells.

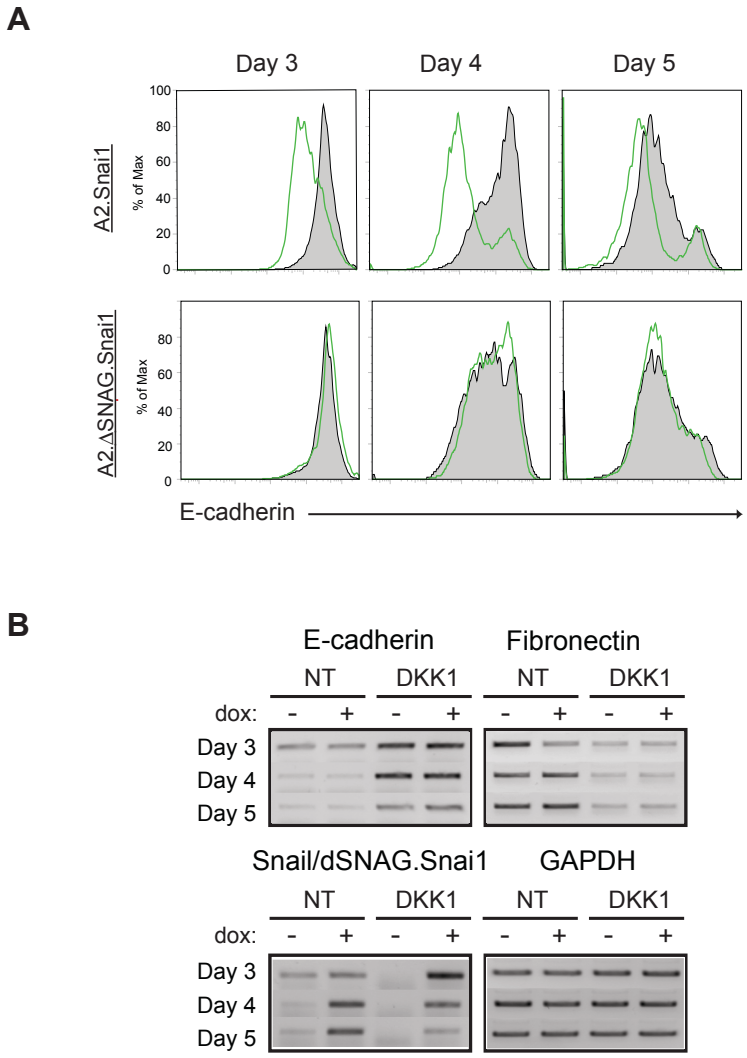

Figure 44: Generation of A2.ΔSNAG.Snail cell line. (A) *A2.Snail* and *A2.Δ SNAG.Snail* cells were differentiated as described in Fig. 9A. Doxycycline was added on day 2 of differentiation and FACS analysis was performed on day 4. Shown is a FACS plot of live cells, examining E-cadherin expression. (B) RNA was collected from cells differentiated as in (A) on days 3, 4, and 5, and RT-PCR was performed for the indicated markers. See Fig. 9 for *A2.Snail* comparison.

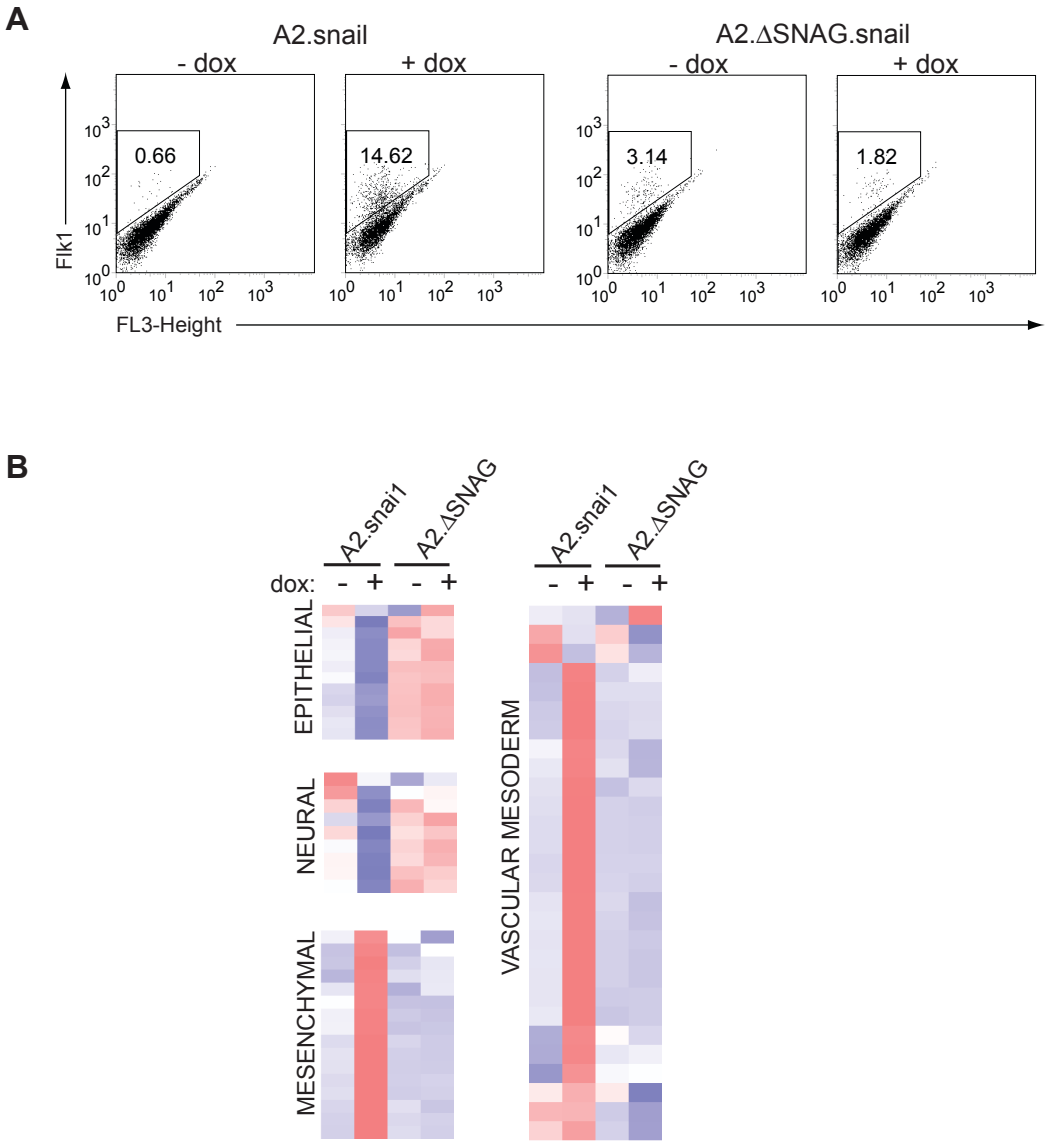

Figure 45: Snail depends on the SNAG repressor domain to induce Flk1+ cells. (A) *A2.Snail* and *A2.ΔSNAG.Snail* cells were differentiated as described in Figure 9A. Doxycycline was added on day 2 of differentiation and FACS analysis was performed on day 4. Shown is a FACS plot of live cells, examining Flk1 expression. (B) RNA was isolated from day 3 DKK +/- dox cultures for each cell line and submitted for gene chip analysis. Shown is a cluster analysis of various transcripts affected by Snail, including those related to vasculogenesis.

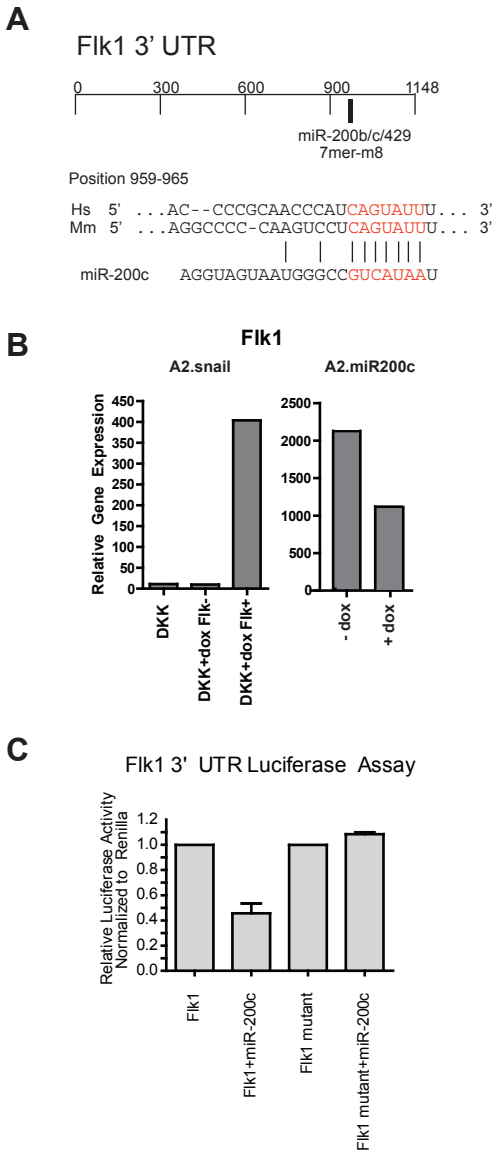

Figure 46: Snail directly targets the 3' UTR of Flk1. (A) Diagram of predicted miR-200c target sites in the 3' UTR of Flk1. (B) Relative expression of Flk1 in *A2.Snail* sorted populations from Fig. 41 as well as in day 5 *A2.miR200c* cells induced or not induced to express miR-200c/141 by doxycycline from day 2. (C) Relative luciferase activity of 293T cells transfected with a CMV-luciferase-Flk1 3'UTR construct, with or without addition of a miR-200c mimic, as well as 293T cells transfected with a CMV-luciferase-Flk1 MUTATED 3' UTR construct, with or without addition of a miR-200c mimic. Data was normalized to co-transfected CMV-Renilla activity.

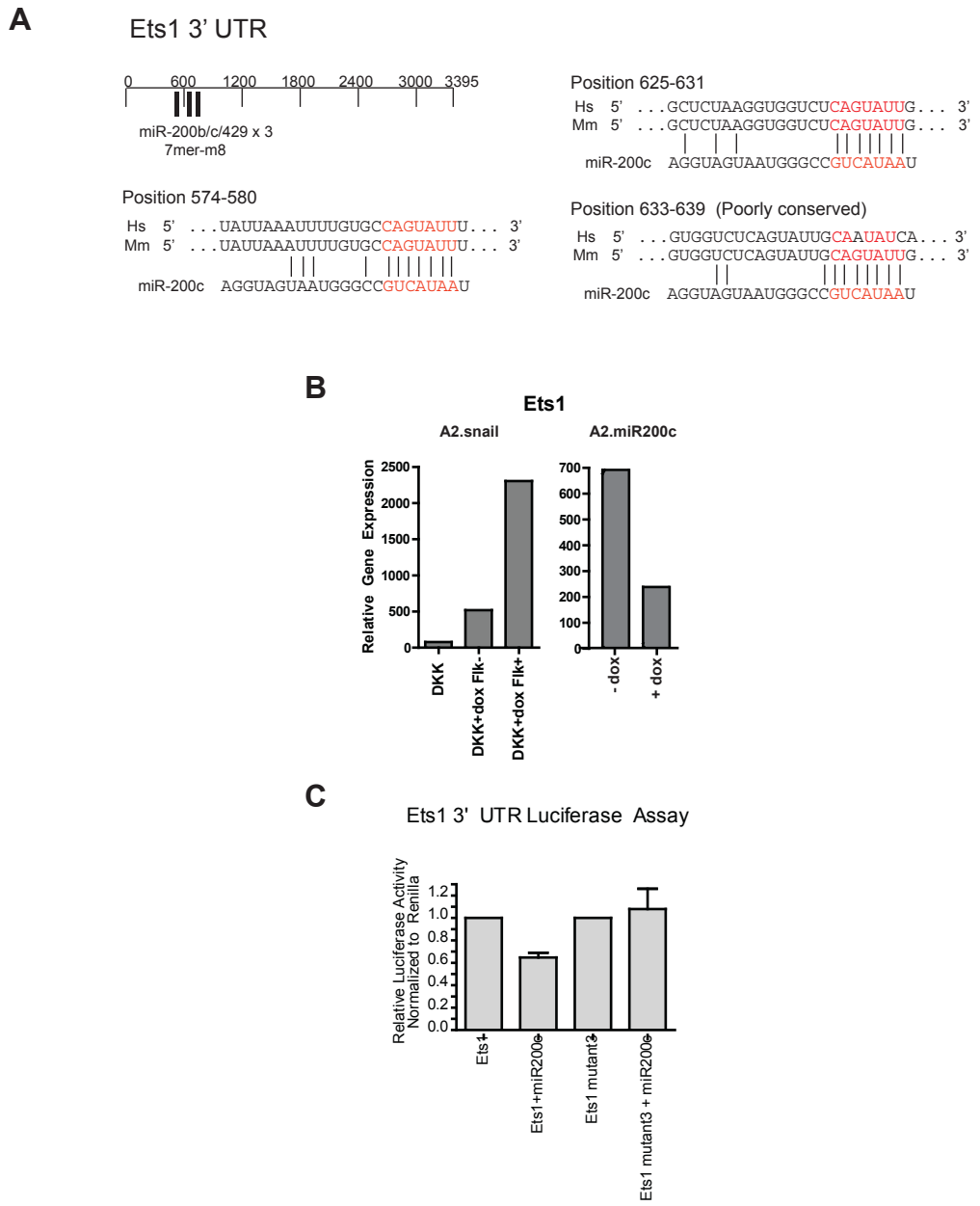

Figure 47: Snail directly targets the 3' UTR of Ets1. (A) Diagram of predicted miR-200c target sites in the 3' UTR of Ets1. (B) Relative expression of Ets in *A2.Snail* sorted populations from Fig. 41 as well as in day 5 *A2.miR200c* cells induced or not induced to express miR-200c/141 by doxycycline from day 2. (C) Relative luciferase activity of 293T cells transfected with a CMV-luciferase-Ets1 3'UTR construct, with or without addition of a miR-200c mimic, as well as 293T cells transfected with a CMV-luciferase-Ets1 MUTATED 3' UTR construct, with or without addition of a miR-200c mimic. Data was normalized to co-transfected CMV-Renilla activity.

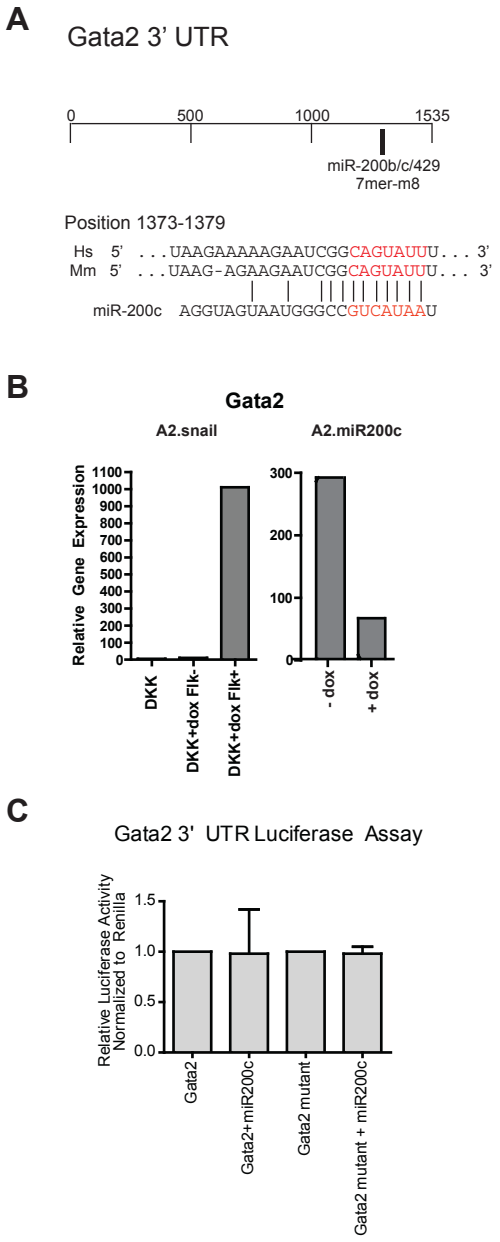

Figure 48: Snail does not directly target the 3' UTR of Gata2. (A) Diagram of predicted miR-200c target sites in the 3' UTR of Gata2. (B) Relative expression of Gata2 in *A2.Snail* sorted populations from Fig. 41 as well as in day 5 *A2.miR200c* cells induced or not induced to express miR-200c/141 by doxycycline from day 2. (C) Relative luciferase activity of 293T cells transfected with a CMV-luciferase-Gata2 3'UTR construct, with or without addition of a miR-200c mimic, as well as 293T cells transfected with a CMV-luciferase-Gata2 MUTATED 3' UTR construct, with or without addition of a miR-200c mimic. Data was normalized to co-transfected CMV-Renilla activity.

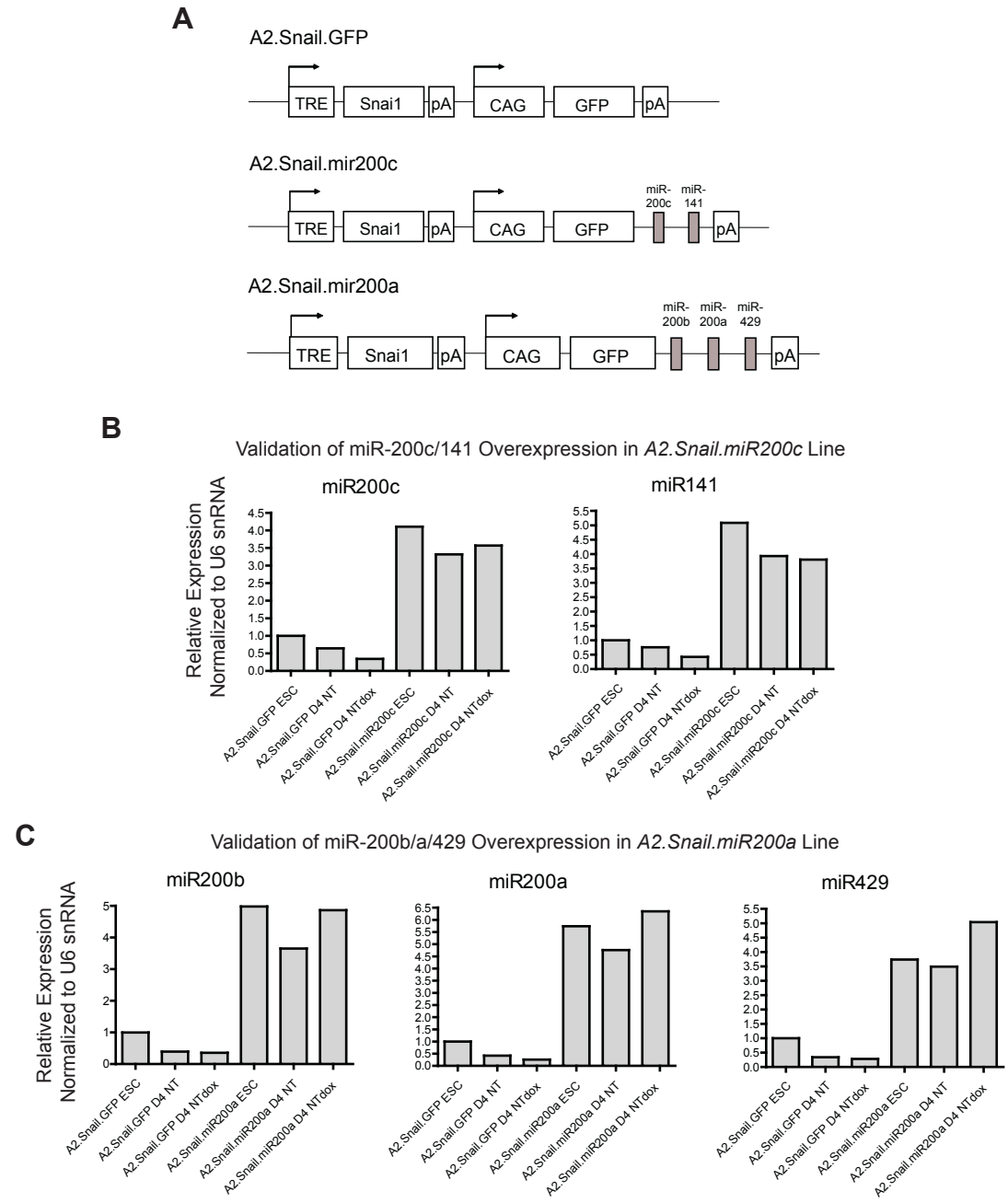

Figure 49: Generation of *A2.Snail.GFP*, *A2.Snail.miR200a*, and *A2.Snail.miR200c* ES cell lines. (A) Diagram of cell lines generated with inducible Snail expression with or without constitutive expression of miR-200c/141 or miR200b/a/429. (B) Validation of miR-200c/141 overexpression in the *A2.Snail.miR200c* line. RNA was harvested from ES cells as well as day 4 NT and NT+dox cultures of *A2.Snail.GFP* and *A2.Snail.CAG.miR200c* lines. Taqman miRNA assays were performed to detect miR-200c and miR-141 levels normalized to U6 snRNA. (C) Validation of miR-200b/a/429 overexpression in the *A2.Snail.miR200a* line. See (B) for setup.

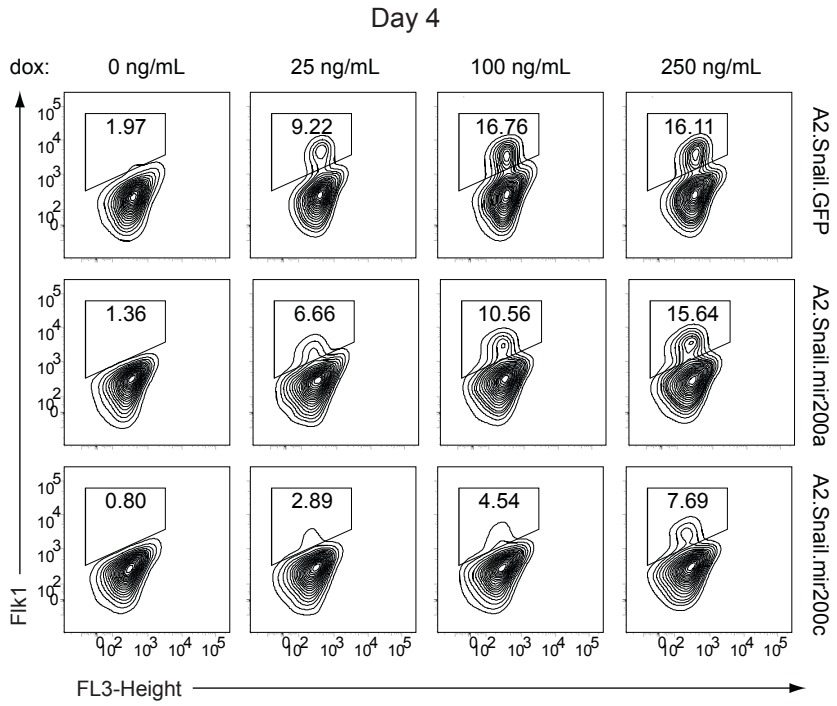

Figure 50: Snail requires the down-regulation of the miR-200 family to efficiently generate Flk1+ cells. *A2.Snail.GFP* (top), *A2.Snail.miR200a* (middle), and *A2.Snail.miR200c* (bottom) ES cells were differentiated with or without various concentrations of doxycycline induction on day 2. FACS analysis was performed for Flk1 expression on day 4. Shown are gated live cells.

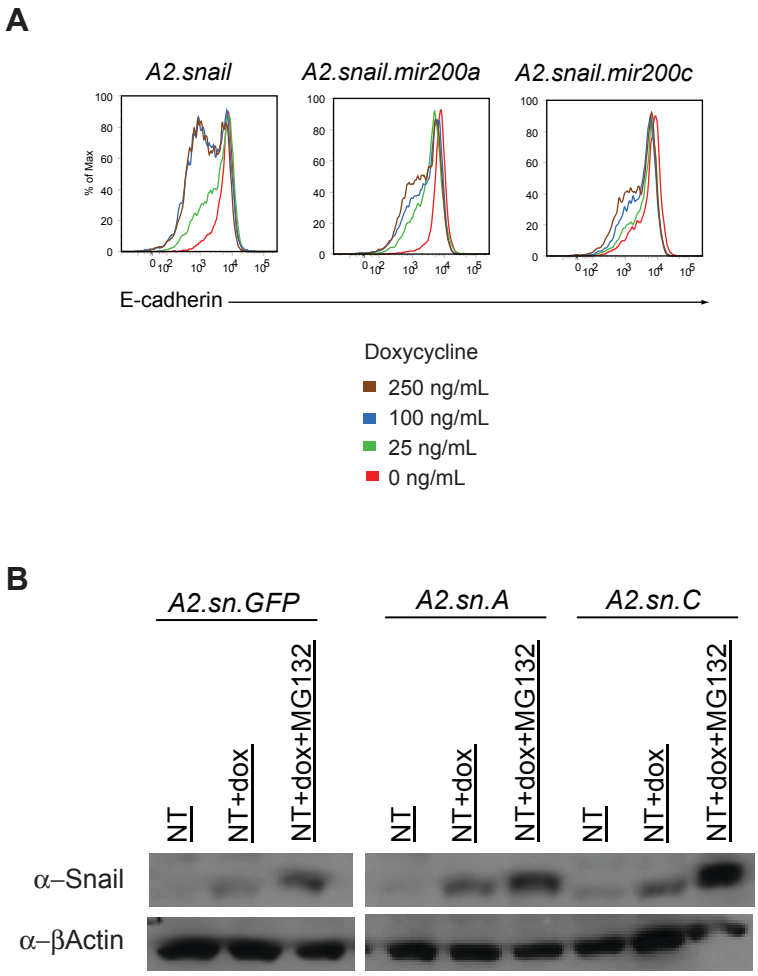

Figure 51: Snail requires the down-regulation of the miR-200 family to efficiently down-regulate E-cadherin. (A) *A2.Snail.GFP, A2.Snail.miR200a*, and *A2.Snail.miR200c* ES cells were differentiated with or without various concentrations of doxycycline induction on day 2 (See Fig. 50). FACS analysis was performed for E-cadherin expression on day 4. Shown are gated live cells. (B) Western blot examining Snail and β-actin expression in the indicated differentiating ES cell lines on day 3, 24 hours after doxycycline induction on day 2.

CHAPTER 7

Discussion

Snail and the miR-200 Family in Gastrulation

Snail has been associated with E-cadherin repression during gastrulation, but its downstream pathways and association with fate determination have not been well-characterized. In this study we have uncovered a role for Snail in promoting EMT and mesoderm differentiation within a specific timeframe of ES cell differentiation corresponding to the early epiblast. During this time, Snail alters the expression of a number of miRNAs, including the miR-200 family. Further, we have demonstrated that the miR-200 family functions conversely to Snail to inhibit EMT and germ layer fate commitment in differentiating ES cells, and acts to maintain cells in an EpiSC-like stage. We show that progression past this stage occurs through the down-regulation of the miR-200 family caused by Snail or by removal of Activin, inducing EMT and skewing cell fates toward mesoderm or neuroectoderm, respectively. Together our data illustrate how Snail and the miR-200 family act in opposition to regulate EMT and exit from the epiblast state towards germ layer fate commitment.

Recent studies have reached different conclusions about whether miR-200 promotes (Wellner et al., 2009) or attenuates differentiation (Lin et al., 2009). While our gene chip analysis supports many of the indicated targets described in both reports, including Cadherin 11 (Lin et al., 2009), Neuropilin 1 (Lin et al., 2009), and Bmi1 (Wellner et al., 2009), we do not see miR-200c/141 down-regulation of Sox2 (Wellner et al., 2009) (which is actually induced in our system). By using stable, inducible

expression of the miR-200 family, a global transcriptional analysis, flow cytometry, and EpiSC culturing, we support the interpretation that the miR-200 family stalls ES cell differentiation at a specific point in differentiation, the EpiSC stage.

Our demonstration that Snail biases fate determination builds on earlier studies of its role in the mouse embryo. Previously, it was found that Snail-deficient embryos die before E8.5 and arrest at the onset of gastrulation (Carver et al., 2001). In Snail-deficient embryos, cells of the primitive streak fail to down-regulate E-cadherin or migrate, and mesoderm formation is diminished as demonstrated by low expression of Brachyury. Interestingly, the epiblast and neuroectoderm marker *Otx2* fails to be restricted to the anterior segment in Snail-deficient embryos. Together with our findings, these data suggest that Snail plays a more active role in promoting differentiation and germ layer fate induction than previously considered. Given the expression of miR-200 in the early mouse embryo (Landgraf et al., 2007), including its restriction to non-mesoderm fates in the chick embryo (Darnell et al., 2006), it is possible Snail may also repress miR-200 in the early embryo to allow progression and differentiation of cells from the epiblast to early mesoderm.

In addition to mesoderm defects, the conditional deletion of Snail under control of Meox2-Cre demonstrated failures in establishment of left-right asymmetry (Murray and Gridley, 2006). In this conditional Snail deletion, left-right axis formation is disrupted and Nodal expression is no longer restricted to the left lateral plate mesoderm, perhaps suggesting that redundant mechanisms between Snail's restriction of Nodal in axis formation and Snail's restriction of Activin/Nodal in the maintenance of the epiblast. Snail and the miR-200 family both interact and influence multiple components of the

TGF-beta signaling pathway (Burk et al., 2008; Lin et al., 2009; Vincent et al., 2009). Thus, these factors could conceivably interact in a manner to antagonize one another's actions by opposing influences in the same signaling pathways, but this aspect of the molecular mechanism will require further study.

The basis for the molecular antagonism between Snail and Activin signaling is not yet characterized, but previous studies have shown that another EMT transcription factor, Zeb2/SIP1, can antagonize Activin-Nodal signaling through its direct interaction with the MH2 domain of activated SMAD proteins (Verschueren et al., 1999). Furthermore, Zeb2/SIP1 can promote neuroectoderm while inhibiting Activin-induced mesendoderm induction in human ES cells (Chng et al., 2010). Although the effect of Zeb2 on EMT in differentiating ES cells was not examined, Zeb2 was identified in a screen of transcription factors that were induced upon the inhibition of Activin signaling. Since we find that inhibiting Activin signaling in differentiating ES cell induces EMT, we would hypothesize that Zeb2 may be responsible for the miR-200 repression mediating the EMT observed during later neuroectoderm differentiation, explaining why Zeb2-deficient mice display defects in cranial neural crest migration along with specification of neuroectoderm. Our data suggest a model in which Snail acts in concert with Activin to promote mesoderm differentiation and migration, whereas Zeb2 functions in the absence of Activin to promote neuroectoderm differentiation and delamination of neural crest (Fig. 7B). Both Snail and Zeb2 induction of EMT appear to oppose Activin-induced maintenance of miR-200 and thereby promote progression past the epiblast state.

The relationship between Snail expression and miR-200 family members has recently been suggested (Burk et al., 2008; Vetter et al., 2010), but not been examined in

depth. One study indicated that over-expression of Snail in HCT116 cells could repress transcription from the regulatory regions of miR-200c and miR-141 (Burk et al., 2008). A second study examined microRNAs regulated by Snail in MCF7 breast cancer cells and identified a number of microRNAs that were strongly induced by Snail (Vetter et al., 2010). This study also noted that miR-200 family members were repressed by Snail, but did not further examine the consequences of this repression functionally. Our study illustrates the first functional antagonism between Snail and the miR-200 family and its consequential effects on EMT in a system relevant for gastrulation.

Snail and Vasculogenesis

Studies in several tumor models suggest that *Snail* and the miR-200 family of microRNAs have roles in EMT as well as "stemness"(Mani et al., 2008; Wellner et al., 2009). Here, we show that the miR-200 family also has a role in vasculogenesis by directly repressing key transcripts such as Flk1 and Ets1. An important finding in this study is the characterization of cells which form endothelium in response to *Snail* expression. *Snail*'s dependence on FGF signaling to induce formation of such cells, and the $Gata6^{+}Nanog^{lo}$ transcriptional profile of the cells in which *Snail* acts, suggests that the $Flk1^{+}$ endothelial cells arise from a subset of differentiating ES cells biased towards primitive endoderm.

These findings have implications for the phenotypes observed in Snail-deficient embryos, particularly in Meox2-Cre/$Snail^{loxp/loxp}$ mice. Our studies would suggest that Snail is important for the cell-autonomous generation of endothelial cells in these embryos. While they did appear to have limited PECAM+ endothelial progenitors, these

progenitors appeared to be very sparse and failed to form a normal vascular network. The yolk sac was not examined in these mice, which would have been useful for further establishing a role for Snail in extraembryonic vascular development. Because we would hypothesize that some of the yolk sac vasculature could arise from primitive endoderm, Meox2-Cre may not be sufficient for deletion of Snail in these cells.

Like primitive endoderm and its derivatives, cancer stem cells seem uniquely poised to promote endothelial differentiation due to their shared expression of pro-vasculogenic factors such as VEGF(Bao et al., 2006; Damert et al., 2002), FGFRs(Fillmore et al., 2010; Yamanaka et al., 2010), IGFs(Dallas et al., 2009), and β-catenin(Malanchi et al., 2008) (Figure 52). In addition to sharing similar expression patterns, the FGF-dependence and appearance of cancer stem cells at the invasive borders of tumors are very reminiscent of the specification of primitive endoderm on the border of differentiating ES cell embryoid bodies. Based on our studies, we propose that the heterogeneity found in ES cell cultures can serve as a model for the known heterogeneity demonstrated within tumors themselves, particularly in the context of cancer stem cells and early endothelial progenitors (Figure 53).

In conclusion, we propose that *Snail* and miR-200c link EMT and vasculogenesis in a subset of ES cells that resemble primitive endoderm and cancer stem cells. The promotion of endothelial progenitors depends on FGF signaling as well as *Snail*'s down-regulation of the miR-200 family, which directly target Flk1 and Ets1. Understanding the mechanism behind *Snail*'s dual functions may be important in future studies and therapeutics aimed at limiting tumor vasculogenesis.

	Snail-induced Flk1+ Cell	Cancer stem-like cells
Induced by Snail/EMT	Yes	Yes
FGF-dependence	Yes	Yes
Bmi1	↑	↑
C-myc	↑	↑
CD44	↑	↑
CD24	↓	lo
CD34	↑	↑
CD133	↑	↑
Epcam	⇓	↑
CD105	↑	↑

Figure 52: Similarities between Snail-induced Flk1+ cells and cancer stem cells. Table demonstrating similarities and differences between Snail-induced Flk1+ cells (likely from primitive endoderm) and cancer stem cells.

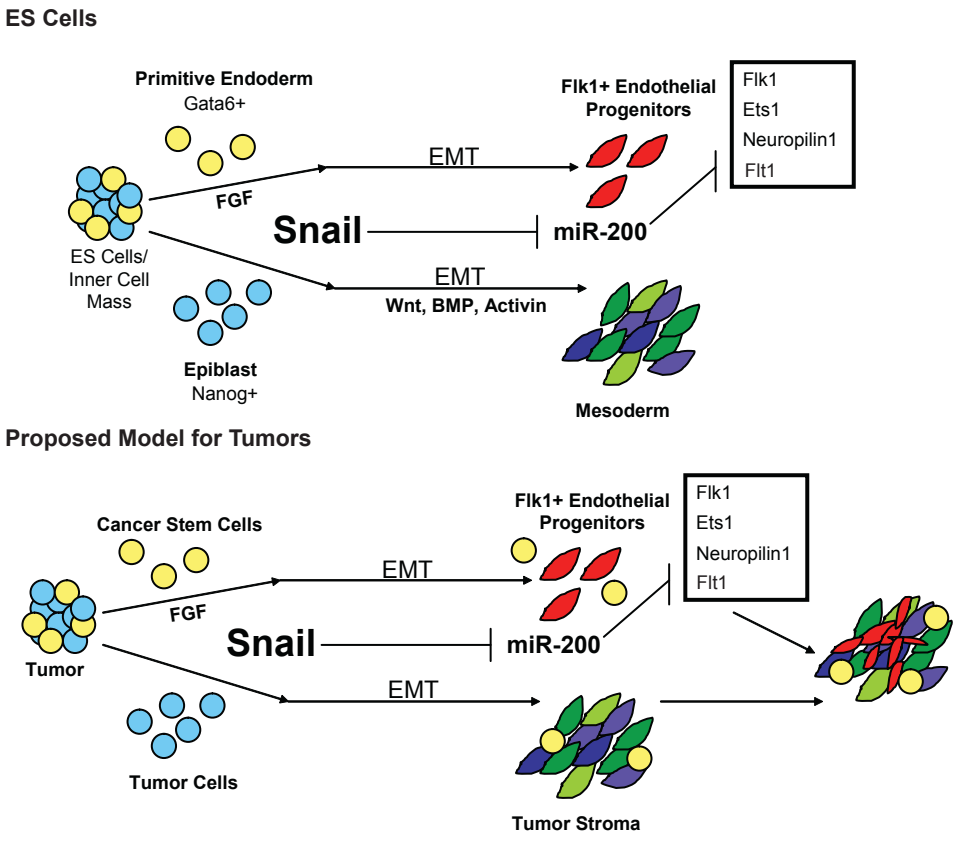

Figure 53: Proposed model of Snail in ES cell and tumor vasculogenesis. Proposed model: In differentiating ES cells, Snail promotes Flk1+ endothelial progenitors in a cell-intrinsic manner in a subset of primitive endoderm-like cells. This process requires the down-regulation of the miR-200 family which directly target Flk1 and Ets1, as well as Neuropilin 1 and Flt1. We propose a similar model in tumors where Snail may cell-autonomously direct cancer stem cells towards a Flk1+ endothelial fate in a manner dependent on miR-200 down-regulation. Recent findings of endothelial differentiation in glioblastoma cancer stem cells where Snail is known to be expressed, support this hypothesis.

REFERENCES

Bao, S., Wu, Q., Sathornsumetee, S., Hao, Y., Li, Z., Hjelmeland, A. B., Shi, Q., McLendon, R. E., Bigner, D. D., and Rich, J. N. (2006). Stem cell-like glioma cells promote tumor angiogenesis through vascular endothelial growth factor. *Cancer Research* **66**, 7843-7848.

Barrallo-Gimeno, A. and Nieto, M. A. (2005). The Snail genes as inducers of cell movement and survival: implications in development and cancer. *Development* **132**, 3151-3161.

Bolos, V., Peinado, H., Perez-Moreno, M. A., Fraga, M. F., Esteller, M., and Cano, A. (2003). The transcription factor Slug represses E-cadherin expression and induces epithelial to mesenchymal transitions: a comparison with Snail and E47 repressors. *Journal of Cell Science* **116**, 499-511.

Boutet, A., De Frutos, C. A., Maxwell, P. H., Mayol, M. J., Romero, J., and Nieto, M. A. (2006). Snail activation disrupts tissue homeostasis and induces fibrosis in the adult kidney. *EMBO J* **25**, 5603-5613.

Bracken, C. P., Gregory, P. A., Kolesnikoff, N., Bert, A. G., Wang, J., Shannon, M. F., and Goodall, G. J. (2008). A double-negative feedback loop between ZEB1-SIP1 and the microRNA-200 family regulates epithelial-mesenchymal transition. *Cancer Research* **68**, 7846-7854.

Brennan, J., Lu, C. C., Norris, D. P., Rodriguez, T. A., Beddington, R. S. P., and Robertson, E. J. (2001). Nodal signalling in the epiblast patterns the early mouse embryo. *Nature* **411**, 965-969.

Brons, I. G., Smithers, L. E., Trotter, M. W., Rugg-Gunn, P., Sun, B., Chuva de Sousa Lopes SM, Howlett, S. K., Clarkson, A., Ahrlund-Richter, L., Pedersen, R. A. et al. (2007). Derivation of pluripotent epiblast stem cells from mammalian embryos. *Nature* **448**, 191-195.

Burk, U., Schubert, J., Wellner, U., Schmalhofer, O., Vincan, E., Spaderna, S., and Brabletz, T. (2008). A reciprocal repression between ZEB1 and members of the miR-200 family promotes EMT and invasion in cancer cells. *EMBO Rep.* **9**, 582-589.

Camus, A., Perea-Gomez, A., Moreau, A., and Collignon, J. (2006). Absence of Nodal signaling promotes precocious neural differentiation in the mouse embryo. *Dev.Biol* **295**, 743-755.

Cano, A., Perez-Moreno, M. A., Rodrigo, I., Locascio, A., Blanco, M. J., del Barrio, M. G., Portillo, F., and Nieto, M. A. (2000). The transcription factor snail

controls epithelial-mesenchymal transitions by repressing E-cadherin expression. *Nat Cell Biol* **2**, 76-83.

Carver, E. A., Jiang, R. L., Lan, Y., Oram, K. F., and Gridley, T. (2001). The mouse snail gene encodes a key regulator of the epithelial-mesenchymal transition. *Molecular and Cellular Biology* **21**, 8184-8188.

Chambers, S. M., Fasano, C. A., Papapetrou, E. P., Tomishima, M., Sadelain, M., and Studer, L. (2009). Highly efficient neural conversion of human ES and iPS cells by dual inhibition of SMAD signaling. *Nat Biotechnol.* **27**, 275-280.

Chan, Y. C., Khanna, S., Roy, S., and Sen, C. K. (2011). miR-200b Targets Ets-1 and Is Down-regulated by Hypoxia to Induce Angiogenic Response of Endothelial Cells. *J Biol Chem.* **286**, 2047-2056.

Chazaud, C., Yamanaka, Y., Pawson, T., and Rossant, J. (2006). Early lineage segregation between epiblast and primitive endoderm in mouse blastocysts through the Grb2-MAPK pathway. *Dev.Cell* **10**, 615-624.

Chen, T., Yuan, D., Wei, B., Jiang, J., Kang, J., Ling, K., Gu, Y., Li, J., Xiao, L., and Pei, G. (2010). E-cadherin-mediated cell-cell contact is critical for induced pluripotent stem cell generation. *Stem Cells* **28**, 1315-1325.

Chenoweth, J. G. and Tesar, P. J. (2010). Isolation and maintenance of mouse epiblast stem cells. *Methods Mol Biol* **636**, 25-44.

Chng, Z., Teo, A., Pedersen, R. A., and Vallier, L. (2010). SIP1 Mediates Cell-Fate Decisions between Neuroectoderm and Mesendoderm in Human Pluripotent Stem Cells. *Cell Stem Cell* **6**, 59-70.

Choi, K., Kennedy, M., Kazarov, A., Papadimitriou, J. C., and Keller, G. (1998). A common precursor for hematopoietic and endothelial cells. *Development* **125**, 725-732.

Ciruna, B. and Rossant, J. (2001). FGF signaling regulates mesoderm cell fate specification and morphogenetic movement at the primitive streak. *Dev.Cell* **1**, 37-49.

Comijn, J., Berx, G., Vermassen, P., Verschueren, K., van Grunsven, L., Bruyneel, E., Mareel, M., Huylebroeck, D., and Van Roy, F. (2001). The two-handed E box binding zinc finger protein SIP1 downregulates E-cadherin and induces invasion. *Mol Cell* **7**, 1267-1278.

Dallas, N. A., Xia, L., Fan, F., Gray, M. J., Gaur, P., van Buren, G., Samuel, S., Kim, M. P., Lim, S. J., and Ellis, L. M. (2009). Chemoresistant colorectal cancer cells, the cancer stem cell phenotype, and increased sensitivity to insulin-like growth factor-I receptor inhibition. *Cancer Research* **69**, 1951-1957.

Damert, A., Miquerol, L., Gertsenstein, M., Risau, W., and Nagy, A. (2002). Insufficient VEGFA activity in yolk sac endoderm compromises haematopoietic and endothelial differentiation. *Development* **129**, 1881-1892.

Darnell, D. K., Kaur, S., Stanislaw, S., Konieczka, J. H., Yatskievych, T. A., and Antin, P. B. (2006). MicroRNA expression during chick embryo development. *Dev.Dyn.* **235**, 3156-3165.

Doetschman, T. C., Eistetter, H., Katz, M., Schmidt, W., and Kemler, R. (1985). The in vitro development of blastocyst-derived embryonic stem cell lines: formation of visceral yolk sac, blood islands and myocardium. *J Embryol.Exp.Morphol.* **87**, 27-45.

Eastham, A. M., Spencer, H., Soncin, F., Ritson, S., Merry, C. L., Stern, P. L., and Ward, C. M. (2007). Epithelial-mesenchymal transition events during human embryonic stem cell differentiation. *Cancer Research* **67**, 11254-11262.

Eger, A., Aigner, K., Sonderegger, S., Dampier, B., Oehler, S., Schreiber, M., Berx, G., Cano, A., Beug, H., and Foisner, R. (2005). DeltaEF1 is a transcriptional repressor of E-cadherin and regulates epithelial plasticity in breast cancer cells. *Oncogene* **24**, 2375-2385.

Evans, M. J. and Kaufman, M. H. (1981). Establishment in culture of pluripotential cells from mouse embryos. *Nature* **292**, 154-156.

Fillmore, C. M., Gupta, P. B., Rudnick, J. A., Caballero, S., Keller, P. J., Lander, E. S., and Kuperwasser, C. (2010). Estrogen expands breast cancer stem-like cells through paracrine FGF/Tbx3 signaling. *Proc.Natl.Acad.Sci U.S A*

Gadue, P., Huber, T. L., Nostro, M. C., Kattman, S., and Keller, G. M. (2005). Germ layer induction from embryonic stem cells. *Exp.Hematol.* **33**, 955-964.

Gibbons, D. L., Lin, W., Creighton, C. J., Rizvi, Z. H., Gregory, P. A., Goodall, G. J., Thilaganathan, N., Du, L., Zhang, Y., Pertsemlidis, A. et al. (2009). Contextual extracellular cues promote tumor cell EMT and metastasis by regulating miR-200 family expression. *Genes & Development* **23**, 2140-2151.

Greenburg, G. and Hay, E. D. (1982). Epithelia suspended in collagen gels can lose polarity and express characteristics of migrating mesenchymal cells. *J Cell Biol* **95**, 333-339.

Gregory, P. A., Bert, A. G., Paterson, E. L., Barry, S. C., Tsykin, A., Farshid, G., Vadas, M. A., Khew-Goodall, Y., and Goodall, G. J. (2008). The miR-200 family and miR-205 regulate epithelial to mesenchymal transition by targeting ZEB1 and SIP1. *Nat Cell Biol* **10**, 593-601.

Grimes, H. L., Chan, T. O., Zweidler-McKay, P. A., Tong, B., and Tsichlis, P. N. (1996). The Gfi-1 proto-oncoprotein contains a novel transcriptional repressor

domain, SNAG, and inhibits G1 arrest induced by interleukin-2 withdrawal. *Mol Cell Biol* **16**, 6263-6272.

Herranz, N., Pasini, D., Diaz, V. M., Franci, C., Gutierrez, A., Dave, N., Escriva, M., Hernandez-Munoz, I., Di Croce, L., Helin, K. et al. (2008). Polycomb complex 2 is required for E-cadherin repression by the Snail1 transcription factor. *Mol Cell Biol* **28**, 4772-4781.

Huelsken, J., Vogel, R., Brinkmann, V., Erdmann, B., Birchmeier, C., and Birchmeier, W. (2000). Requirement for beta-catenin in anterior-posterior axis formation in mice. *J Cell Biol.* **148**, 567-578.

Iacovino, M., Hernandez, C., Xu, Z., Bajwa, G., Prather, M., and Kyba, M. (2009). A conserved role for Hox paralog group 4 in regulation of hematopoietic progenitors. *Stem Cells Dev.* **18**, 783-792.

Ikenouchi, J., Matsuda, M., Furuse, M., and Tsukita, S. (2003). Regulation of tight junctions during the epithelium-mesenchyme transition: direct repression of the gene expression of claudins/occludin by Snail. *Journal of Cell Science* **116**, 1959-1967.

Kelly, O. G., Pinson, K. I., and Skarnes, W. C. (2004). The Wnt co-receptors Lrp5 and Lrp6 are essential for gastrulation in mice. *Development* **131**, 2803-2815.

Korpal, M., Lee, E. S., Hu, G., and Kang, Y. (2008). The miR-200 family inhibits epithelial-mesenchymal transition and cancer cell migration by direct targeting of E-cadherin transcriptional repressors ZEB1 and ZEB2. *J Biol Chem.* **283**, 14910-14914.

Kramer, J., Hegert, C., Guan, K., Wobus, A. M., Muller, P. K., and Rohwedel, J. (2000). Embryonic stem cell-derived chondrogenic differentiation in vitro: activation by BMP-2 and BMP-4. *Mechanisms of Development* **92**, 193-205.

Landgraf, P., Rusu, M., Sheridan, R., Sewer, A., Iovino, N., Aravin, A., Pfeffer, S., Rice, A., Kamphorst, A. O., Landthaler, M. et al. (2007). A mammalian microRNA expression atlas based on small RNA library sequencing. *Cell* **129**, 1401-1414.

Langer, E. M., Feng, Y., Zhaoyuan, H., Rauscher, F. J., III, Kroll, K. L., and Longmore, G. D. (2008). Ajuba LIM proteins are snail/slug corepressors required for neural crest development in Xenopus. *Dev.Cell* **14**, 424-436.

Lee, D., Park, C., Lee, H., Lugus, J. J., Kim, S. H., Arentson, E., Chung, Y. S., Gomez, G., Kyba, M., Lin, S. et al. (2008). ER71 acts downstream of BMP, Notch, and Wnt signaling in blood and vessel progenitor specification. *Cell Stem Cell* **2**, 497-507.

Li, C. and Wong, W. H. (2001a). Model-based analysis of oligonucleotide arrays: expression index computation and outlier detection. *Proc.Natl.Acad.Sci U.S.A* **98**, 31-36.

Li, C. and Wong, W. H. (2001b). Model-based analysis of oligonucleotide arrays: model validation, design issues and standard error application. *Genome Biol.* **2**, R32.1-R32.11.

Li, R., Liang, J., Ni, S., Zhou, T., Qing, X., Li, H., He, W., Chen, J., Li, F., Zhuang, Q. et al. (2010). A mesenchymal-to-epithelial transition initiates and is required for the nuclear reprogramming of mouse fibroblasts. *Cell Stem Cell* **7**, 51-63.

Lillie, F. R. (1908). The Development of the Chick.

Lin, C. H., Jackson, A. L., Guo, J., Linsley, P. S., and Eisenman, R. N. (2009). Myc-regulated microRNAs attenuate embryonic stem cell differentiation. *EMBO J* **28**, 3157-3170.

Lindsley, R. C., Gill, J. G., Kyba, M., Murphy, T. L., and Murphy, K. M. (2006). Canonical Wnt signaling is required for development of embryonic stem cell-derived mesoderm. *Development* **133**, 3787-3796.

Lindsley, R. C., Gill, J. G., Murphy, T. L., Langer, E. M., Cai, M., Mashayekhi, M., Wang, W., Niwa, N., Nerbonne, J. M., Kyba, M. et al. (2008). Mesp1 coordinately regulates cardiovascular fate restriction and epithelial-mesenchymal transition in differentiating ESCs. *Cell Stem Cell* **3**, 55-68.

Liu, P., Wakamiya, M., Shea, M. J., Albrecht, U., Behringer, R. R., and Bradley, A. (1999). Requirement for Wnt3 in vertebrate axis formation. *Nat Genet* **22**, 361-365.

Lomeli, H., Starling, C., and Gridley, T. (2009). Epiblast-specific Snai1 deletion results in embryonic lethality due to multiple vascular defects. *BMC Res Notes* **2**, 22.

Lugus, J. J., Chung, Y. S., Mills, J. C., Kim, S. I., Grass, J., Kyba, M., Doherty, J. M., Bresnick, E. H., and Choi, K. (2007). GATA2 functions at multiple steps in hemangioblast development and differentiation. *Development* **134**, 393-405.

Lumelsky, N., Blondel, O., Laeng, P., Velasco, I., Ravin, R., and McKay, R. (2001). Differentiation of Embryonic Stem Cells to Insulin-Secreting Structures Similar to Pancreatic Islets. *Science* **292**, 1389-1394.

Malanchi, I., Peinado, H., Kassen, D., Hussenet, T., Metzger, D., Chambon, P., Huber, M., Hohl, D., Cano, A., Birchmeier, W. et al. (2008). Cutaneous cancer stem cell maintenance is dependent on beta-catenin signalling. *Nature* **452**, 650-653.

Mani, S. A., Guo, W., Liao, M. J., Eaton, E. N., Ayyanan, A., Zhou, A. Y., Brooks, M., Reinhard, F., Zhang, C. C., Shipitsin, M. et al. (2008). The epithelial-mesenchymal transition generates cells with properties of stem cells. *Cell* **133**, 704-715.

Martin, G. R. (1981). Isolation of a pluripotent cell line from early mouse embryos cultured in medium conditioned by teratocarcinoma stem cells. *Proc.Natl.Acad.Sci U.S.A* **78**, 7634-7638.

Mesnard, D., Guzman-Ayala, M., and Constam, D. B. (2006). Nodal specifies embryonic visceral endoderm and sustains pluripotent cells in the epiblast before overt axial patterning. *Development* **133**, 2497-2505.

Murray, S. A. and Gridley, T. (2006). Snail family genes are required for left-right asymmetry determination, but not neural crest formation, in mice. *Proc.Natl.Acad.Sci U.S A* **103**, 10300-10304.

Nambu, J. R., Franks, R. G., Hu, S., and Crews, S. T. (1990). The single-minded gene of Drosophila is required for the expression of genes important for the development of CNS midline cells. *Cell* **63**, 63-75.

Nieto, M. A., Bennett, M. F., Sargent, M. G., and Wilkinson, D. G. (1992). Cloning and developmental expression of Sna, a murine homologue of the Drosophila snail gene. *Development* **116**, 227-237.

Niwa, H., Ogawa, K., Shimosato, D., and Adachi, K. (2009). A parallel circuit of LIF signalling pathways maintains pluripotency of mouse ES cells. *Nature* **460**, 118-122.

Olmeda, D., Jorda, M., Peinado, H., Fabra, A., and Cano, A. (2007). Snail silencing effectively suppresses tumour growth and invasiveness. *Oncogene* **26**, 1862-1874.

Olmeda, D., Montes, A., Moreno-Bueno, G., Flores, J. M., Portillo, F., and Cano, A. (2008). Snai1 and Snai2 collaborate on tumor growth and metastasis properties of mouse skin carcinoma cell lines. *Oncogene* **27**, 4690-4701.

Olson, P., Lu, J., Zhang, H., Shai, A., Chun, M. G., Wang, Y., Libutti, S. K., Nakakura, E. K., Golub, T. R., and Hanahan, D. (2009). MicroRNA dynamics in the stages of tumorigenesis correlate with hallmark capabilities of cancer. *Genes & Development* **23**, 2152-2165.

Park, S. M., Gaur, A. B., Lengyel, E., and Peter, M. E. (2008). The miR-200 family determines the epithelial phenotype of cancer cells by targeting the E-cadherin repressors ZEB1 and ZEB2. *Genes & Development* **22**, 894-907.

Parker, B. S., Argani, P., Cook, B. P., Liangfeng, H., Chartrand, S. D., Zhang, M., Saha, S., Bardelli, A., Jiang, Y., St Martin, T. B. et al. (2004). Alterations in

vascular gene expression in invasive breast carcinoma. *Cancer Research* **64**, 7857-7866.

Peinado, H., Ballestar, E., Esteller, M., and Cano, A. (2004a). Snail mediates E-cadherin repression by the recruitment of the Sin3A/histone deacetylase 1 (HDAC1)/HDAC2 complex. *Mol Cell Biol* **24**, 306-319.

Peinado, H., Del Carmen Iglesias-de la Cruz, Olmeda, D., Csiszar, K., Fong, K. S., Vega, S., Nieto, M. A., Cano, A., and Portillo, F. (2005). A molecular role for lysyl oxidase-like 2 enzyme in snail regulation and tumor progression. *EMBO J* **24**, 3446-3458.

Peinado, H., Marin, F., Cubillo, E., Stark, H. J., Fusenig, N., Nieto, M. A., and Cano, A. (2004b). Snail and E47 repressors of E-cadherin induce distinct invasive and angiogenic properties in vivo. *Journal of Cell Science* **117**, 2827-2839.

Peinado, H., Olmeda, D., and Cano, A. (2007). Snail, Zeb and bHLH factors in tumour progression: an alliance against the epithelial phenotype? *Nat Rev Cancer* **7**, 415-428.

Peiro, S., Escriva, M., Puig, I., Barbera, M. J., Dave, N., Herranz, N., Larriba, M. J., Takkunen, M., Franci, C., Munoz, A. et al. (2006). Snail1 transcriptional repressor binds to its own promoter and controls its expression. *Nucleic Acids Res* **34**, 2077-2084.

Ricci-Vitiani, L., Pallini, R., Biffoni, M., Todaro, M., Invernici, G., Cenci, T., Maira, G., Parati, E. A., Stassi, G., Larocca, L. M. et al. (2010). Tumour vascularization via endothelial differentiation of glioblastoma stem-like cells. *Nature* **468**, 824-828.

Roybal, J. D., Zang, Y., Ahn, Y. H., Yang, Y., Gibbons, D. L., Baird, B. N., Alvarez, C., Thilaganathan, N., Liu, D. D., Saintigny, P. et al. (2011). miR-200 Inhibits Lung Adenocarcinoma Cell Invasion and Metastasis by Targeting Flt1/VEGFR1. *Mol Cancer Res* **9**, 25-35.

Samavarchi-Tehrani, P., Golipour, A., David, L., Sung, H. K., Beyer, T. A., Datti, A., Woltjen, K., Nagy, A., and Wrana, J. L. (2010). Functional genomics reveals a BMP-driven mesenchymal-to-epithelial transition in the initiation of somatic cell reprogramming. *Cell Stem Cell* **7**, 64-77.

Sato, N., Meijer, L., Skaltsounis, L., Greengard, P., and Brivanlou, A. H. (2004). Maintenance of pluripotency in human and mouse embryonic stem cells through activation of Wnt signaling by a pharmacological GSK-3-specific inhibitor. *Nat Med.* **10**, 55-63.

Schwock, J., Bradley, G., Ho, J. C., Perez-Ordonez, B., Hedley, D. W., Irish, J. C., and Geddie, W. R. (2010). SNAI1 expression and the mesenchymal phenotype:

an immunohistochemical study performed on 46 cases of oral squamous cell carcinoma. *BMC Clin.Pathol* **10**, 1.

Singh, A. M., Hamazaki, T., Hankowski, K. E., and Terada, N. (2007). A heterogeneous expression pattern for Nanog in embryonic stem cells. *Stem Cells* **25**, 2534-2542.

Smith, A. G., Heath, J. K., Donaldson, D. D., Wong, G. G., Moreau, J., Stahl, M., and Rogers, D. (1988). Inhibition of pluripotential embryonic stem cell differentiation by purified polypeptides. *Nature* **336**, 688-690.

Smith, D. E., Franco, d. A., and Gridley, T. (1992). Isolation of Sna, a mouse gene homologous to the Drosophila genes snail and escargot: its expression pattern suggests multiple roles during postimplantation development. *Development* **116**, 1033-1039.

Stoker, M. and Perryman, M. (1985). An epithelial scatter factor released by embryo fibroblasts. *Journal of Cell Science* **77**, 209-223.

Sumi, T., Tsuneyoshi, N., Nakatsuji, N., and Suemori, H. (2008). Defining early lineage specification of human embryonic stem cells by the orchestrated balance of canonical Wnt/beta-catenin, Activin/Nodal and BMP signaling. *Development* **135**, 2969-2979.

Sun, L., Tran, N., Liang, C., Tang, F., Rice, A., Schreck, R., Waltz, K., Shawver, L. K., McMahon, G., and Tang, C. (1999). Design, synthesis, and evaluations of substituted 3-[(3- or 4-carboxyethylpyrrol-2-yl)methylidenyl]indolin-2-ones as inhibitors of VEGF, FGF, and PDGF receptor tyrosine kinases. *J Med.Chem.* **42**, 5120-5130.

Tam, P. P. and Loebel, D. A. (2007). Gene function in mouse embryogenesis: get set for gastrulation. *Nat Rev Genet* **8**, 368-381.

Tesar, P. J., Chenoweth, J. G., Brook, F. A., Davies, T. J., Evans, E. P., Mack, D. L., Gardner, R. L., and McKay, R. D. (2007). New cell lines from mouse epiblast share defining features with human embryonic stem cells. *Nature* **448**, 196-199.

Thiery, J. P., Acloque, H., Huang, R. Y., and Nieto, M. A. (2009). Epithelial-mesenchymal transitions in development and disease. *Cell* **139**, 871-890.

Tropepe, V., Hitoshi, S., Sirard, C., Mak, T. W., Rossant, J., and van der, K. D. (2001). Direct neural fate specification from embryonic stem cells: a primitive mammalian neural stem cell stage acquired through a default mechanism. *Neuron* **30**, 65-78.

Vega, S., Morales, A. V., Ocana, O. H., Valdes, F., Fabregat, I., and Nieto, M. A. (2004). Snail blocks the cell cycle and confers resistance to cell death. *Genes & Development* **18**, 1131-1143.

Veltmaat, J. M., Orelio, C. C., Ward-Van Oostwaard, D., Van Rooijen, M. A., Mummery, C. L., and Defize, L. H. (2000). Snail is an immediate early target gene of parathyroid hormone related peptide signaling in parietal endoderm formation. *Int.J Dev.Biol* **44**, 297-307.

Verschueren, K., Remacle, J. E., Collart, C., Kraft, H., Baker, B. S., Tylzanowski, P., Nelles, L., Wuytens, G., Su, M. T., Bodmer, R. et al. (1999). SIP1, a novel zinc finger/homeodomain repressor, interacts with Smad proteins and binds to 5'-CACCT sequences in candidate target genes. *J Biol Chem.* **274**, 20489-20498.

Vetter, G., Saumet, A., Moes, M., Vallar, L., Le Bechec, A., Laurini, C., Sabbah, M., Arar, K., Theillet, C., Lecellier, C. H. et al. (2010). miR-661 expression in SNAI1-induced epithelial to mesenchymal transition contributes to breast cancer cell invasion by targeting Nectin-1 and StarD10 messengers. *Oncogene* **29**, 4436-4448.

Vincent, T., Neve, E. P., Johnson, J. R., Kukalev, A., Rojo, F., Albanell, J., Pietras, K., Virtanen, I., Philipson, L., Leopold, P. L. et al. (2009). A SNAIL1-SMAD3/4 transcriptional repressor complex promotes TGF-beta mediated epithelial-mesenchymal transition. *Nat Cell Biol* **11**, 943-950.

Wanami, L. S., Chen, H. Y., Peiro, S., Garcia, d. H., and Bachelder, R. E. (2008). Vascular endothelial growth factor-A stimulates Snail expression in breast tumor cells: implications for tumor progression. *Exp.Cell Res* **314**, 2448-2453.

Wang, R., Chadalavada, K., Wilshire, J., Kowalik, U., Hovinga, K. E., Geber, A., Fligelman, B., Leversha, M., Brennan, C., and Tabar, V. (2010). Glioblastoma stem-like cells give rise to tumour endothelium. *Nature* **468**, 829-833.

Wei, G., Srinivasan, R., Cantemir-Stone, C. Z., Sharma, S. M., Santhanam, R., Weinstein, M., Muthusamy, N., Man, A. K., Oshima, R. G., Leone, G. et al. (2009). Ets1 and Ets2 are required for endothelial cell survival during embryonic angiogenesis. *Blood* **114**, 1123-1130.

Wellner, U., Schubert, J., Burk, U. C., Schmalhofer, O., Zhu, F., Sonntag, A., Waldvogel, B., Vannier, C., Darling, D., zur, H. A. et al. (2009). The EMT-activator ZEB1 promotes tumorigenicity by repressing stemness-inhibiting microRNAs. *Nat Cell Biol* **11**, 1487-1495.

Whiteman, E. L., Liu, C. J., Fearon, E. R., and Margolis, B. (2008). The transcription factor snail represses Crumbs3 expression and disrupts apico-basal polarity complexes. *Oncogene* **27**, 3875-3879.

Winnier, G., Blessing, M., Labosky, P. A., and Hogan, B. L. (1995). Bone morphogenetic protein-4 is required for mesoderm formation and patterning in the mouse. *Genes & Development* **9**, 2105-2116.

Xu, R. H., Sampsell-Barron, T. L., Gu, F., Root, S., Peck, R. M., Pan, G., Yu, J., Antosiewicz-Bourget, J., Tian, S., Stewart, R. et al. (2008). NANOG is a direct target of TGFbeta/activin-mediated SMAD signaling in human ESCs. *Cell Stem Cell* **3**, 196-206.

Yamanaka, Y., Lanner, F., and Rossant, J. (2010). FGF signal-dependent segregation of primitive endoderm and epiblast in the mouse blastocyst. *Development* **137**, 715-724.

Yamashita, S., Miyagi, C., Fukada, T., Kagara, N., Che, Y. S., and Hirano, T. (2004). Zinc transporter LIVI controls epithelial-mesenchymal transition in zebrafish gastrula organizer. *Nature* **429**, 298-302.

Yanagawa, J., Walser, T. C., Zhu, L. X., Hong, L., Fishbein, M. C., Mah, V., Chia, D., Goodglick, L., Elashoff, D. A., Luo, J. et al. (2009). Snail promotes CXCR2 ligand-dependent tumor progression in non-small cell lung carcinoma. *Clin.Cancer Res* **15**, 6820-6829.

Yang, J., Mani, S. A., Donaher, J. L., Ramaswamy, S., Itzykson, R. A., Come, C., Savagner, P., Gitelman, I., Richardson, A., and Weinberg, R. A. (2004). Twist, a master regulator of morphogenesis, plays an essential role in tumor metastasis. *Cell* **117**, 927-939.

Yang, Z., Rayala, S., Nguyen, D., Vadlamudi, R. K., Chen, S., and Kumar, R. (2005). Pak1 phosphorylation of snail, a master regulator of epithelial-to-mesenchyme transition, modulates snail's subcellular localization and functions. *Cancer Research* **65**, 3179-3184.

Ying, Q. L., Nichols, J., Chambers, I., and Smith, A. (2003). BMP induction of Id proteins suppresses differentiation and sustains embryonic stem cell self-renewal in collaboration with STAT3. *Cell* **115**, 281-292.

Yook, J. I., Li, X. Y., Ota, I., Fearon, E. R., and Weiss, S. J. (2005). Wnt-dependent regulation of the E-cadherin repressor snail. *J Biol Chem.* **280**, 11740-11748.

Zhang, K., Li, L., Huang, C., Shen, C., Tan, F., Xia, C., Liu, P., Rossant, J., and Jing, N. (2010). Distinct functions of BMP4 during different stages of mouse ES cell neural commitment. *Development* **137**, 2095-2105.

Zidar, N., Gale, N., Kojc, N., Volavsek, M., Cardesa, A., Alos, L., Hofler, H., Blechschmidt, K., and Becker, K. F. (2008). Cadherin-catenin complex and transcription factor Snail-1 in spindle cell carcinoma of the head and neck. *Virchows Arch.* **453**, 267-274.